European Journal of Immunology

HIGHLIGHTS

Guidelines for DC preparation and flow cytometry analysis of mouse nonlymphoid tissues

Hans Christian Probst[1,2,#,*], *Patrizia Stoitzner*[3,#,*], *Lukas Amon*[4], *Ronald A. Backer*[2,5], *Anna Brand*[5], *Jianzhou Chen*[6], *Björn E. Clausen*[2,5,#], *Sophie Dieckmann*[3], *Diana Dudziak*[4,7,8,9,#], *Lukas Heger*[4], *Katrin Hodapp*[1,2], *Florian Hornsteiner*[3], *Avi-Hai Hovav*[10], *Lukas Jacobi*[4], *Xingqi Ji*[11,12], *Nadine Kamenjarin*[1,2], *Katharina Lahl*[13,14], *Imran Lahmar*[6], *Jelena Lakus*[5], *Christian H. K. Lehmann*[4,7], *Daniela Ortner*[3], *Marion Picard*[6], *Maria Paula Roberti*[6,15,16], *Lukas Rossnagel*[4], *Yasmin Saba*[10], *Carmen Schalla*[17,18], *Andreas Schlitzer*[19,#], *Barbara U. Schraml*[11,12,#], *Kristian Schütze*[1,2], *Anna Seichter*[4], *Kristin Seré*[17,18,#], *Athanasios Seretis*[20], *Sieghart Sopper*[21,22], *Helen Strandt*[3], *Martina M. Sykora*[21,22], *Hannah Theobald*[19], *Christoph H. Tripp*[3] *and Laurence Zitvogel*[6]

[1] Institute of Immunology, University Medical Center Mainz, Mainz, Germany
[2] Research Center for Immunotherapy (FZI), University Medical Center of the Johannes Gutenberg-University, Mainz, Germany
[3] Department of Dermatology, Venereology and Allergology, Medical University of Innsbruck, Innsbruck, Austria
[4] Laboratory of Dendritic Cell Biology, Department of Dermatology, University Hospital Erlangen, Hartmannstraße 14, D-91052 Erlangen, Germany
[5] Institute for Molecular Medicine, Paul Klein Center for Immune Intervention, University Medical Center of the Johannes Gutenberg-University, Mainz, Germany
[6] Gustave Roussy Cancer Campus (GRCC), U1015 INSERM, University Paris Saclay, Villejuif, France
[7] Medical Immunology Campus Erlangen (MICE), D-91054 Erlangen, Germany
[8] Deutsches Zentrum Immuntherapie (DZI), Germany
[9] Friedrich-Alexander University (FAU), Erlangen-Nürnberg, Germany
[10] Institute of Biomedical and Oral Research, Faculty of Dental Medicine, Hebrew University, Jerusalem, Israel
[11] Walter-Brendel-Centre of Experimental Medicine, University Hospital, LMU Munich, 82152 Planegg-Martinsried, Germany
[12] Institute for Cardiovascular Physiology and Pathophysiology, Biomedical Center, Faculty of Medicine, LMU Munich, 82152 Planegg-Martinsried, Germany
[13] Section for Experimental and Translational Immunology, Institute for Health Technology, Technical University of Denmark (DTU), Kongens Lyngby 2800, Denmark
[14] Immunology Section, Lund University, Lund 221 84, Sweden
[15] Department of Medical Oncology, National Center for Tumor Diseases (NCT), Heidelberg University Hospital (UKHD), Heidelberg, Germany
[16] Clinical Cooperation Unit Applied Tumor Immunity, German Cancer Research Center (DKFZ), Heidelberg, Germany
[17] Institute for Biomedical Engineering, Department of Cell Biology, RWTH Aachen University Medical School, Aachen, Germany
[18] Helmholtz Institute for Biomedical Engineering, RWTH Aachen University, Aachen, Germany
[19] Quantitative Systems Biology, Life and Medical Sciences (LIMES) Institute, University of Bonn, Germany
[20] Institute for Biomedical Aging Research, University of Innsbruck, Innsbruck, Austria
[21] Internal Medicine V, Hematology and Oncology, Medical University of Innsbruck, Innsbruck, Austria
[22] Tyrolean Cancer Research Center, Innsbruck, Austria

*Correspondence: Dr. Hans Christian Probst and Prof. Patrizia Stoitzner
e-mail: hcprobst@uni-mainz.de; patrizia.stoitzner@i-med.ac.at

[#] Section lead authors

This article is part of the Dendritic Cell Guidelines article series, which provides a collection of state-of-the-art protocols for the preparation, phenotype analysis by flow cytometry, generation, fluorescence microscopy and functional characterization of mouse and human dendritic cells (DC) from lymphoid organs and various nonlymphoid tissues. DC are sentinels of the immune system present in almost every mammalian organ. Since they represent a rare cell population, DC need to be extracted from organs with protocols that are specifically developed for each tissue. This article provides detailed protocols for the preparation of single-cell suspensions from various mouse nonlymphoid tissues, including skin, intestine, lung, kidney, mammary glands, oral mucosa and transplantable tumors. Furthermore, our guidelines include comprehensive protocols for multiplex flow cytometry analysis of DC subsets and feature top tricks for their proper discrimination from other myeloid cells. With this collection, we provide guidelines for in-depth analysis of DC subsets that will advance our understanding of their respective roles in healthy and diseased tissues. While all protocols were written by experienced scientists who routinely use them in their work, this article was also peer-reviewed by leading experts and approved by all coauthors, making it an essential resource for basic and clinical DC immunologists.

Keywords: Dendritic cells · Discrimination of dendritic cell subsets · Mouse nonlymphoid tissue · Multiplex flow cytometry analysis · Tissue digestion protocols

Contents

1 Isolation of DC from mouse nonlymphoid tissues

1.1 Preparation of single-cell suspensions from mouse skin

1.1.1 *Introduction*

The skin, as an epithelial surface, is continuously exposed to the environment and has the task of defending the body against invading pathogens. In addition to the mechanical barrier function and chemical protection mechanisms of the skin, a dense network of cutaneous immune cells provides immune surveillance. For this purpose, various immune cell populations reside in skin tissue. Each population fulfills its unique function while acting in close collaboration within the tissue as well as the systemic network.

The skin is structured in two compartments: the epidermis and the dermis (Fig. 1A). The outermost layer, the epidermis, is separated from the subjacent dermis by the basement membrane. The deepest part of the dermis is the hypodermis, which is mainly composed of adipocytes [1]. In general, skin tissue can be traversed by hair follicles, sebaceous glands, nerves, blood and lymphatic vessels. Keratinocytes are the most abundant cell type in the epidermis. Keratinocytes are arranged in four strata in progressive stages of differentiation. The outermost stratum of stratified keratinocytes prevents water loss from the body [2]. Together with keratinocytes, melanocytes, Langerhans cells (LC) [3], tissue-resident memory T cells and, in mice, γδ T cells [4] are lodged in this layer. Similar to keratinocytes in the epidermis, the structural cells of the dermis are fibroblasts. Different populations of myeloid and lymphoid immune cell populations are also located in the dermis. In contrast to the epidermis, the dermal mononuclear cell network is more heterogenous, comprising different subsets of dendritic cells (DC) and macrophages [5]. As DC migrate to skin-draining lymph nodes to induce immune responses or to mediate tolerance [6], information from both immunological compartments is of value when studying DC [7]. Furthermore, the dermal layer can contain innate lymphoid cells, NK cells, CD8 and CD4 T cells, B cells, granulocytes, mast cells and monocytes. Immune cells can also traffic through the tissue, which results in highly dynamic changes in the composition of cell populations in the dermis, especially during inflammation [8].

The skin, as a tissue made up of tightly connected cells that are rich in collagen fibers, has to be enzymatically digested to obtain a single-cell suspension. This suspension can then be used for many downstream applications, such as flow cytometry analysis. In the following, we provide a detailed protocol for skin tissue dissociation to generate single-cell suspensions from the skin of mouse ear pinnae. The protocol can be applied analogously to body skin

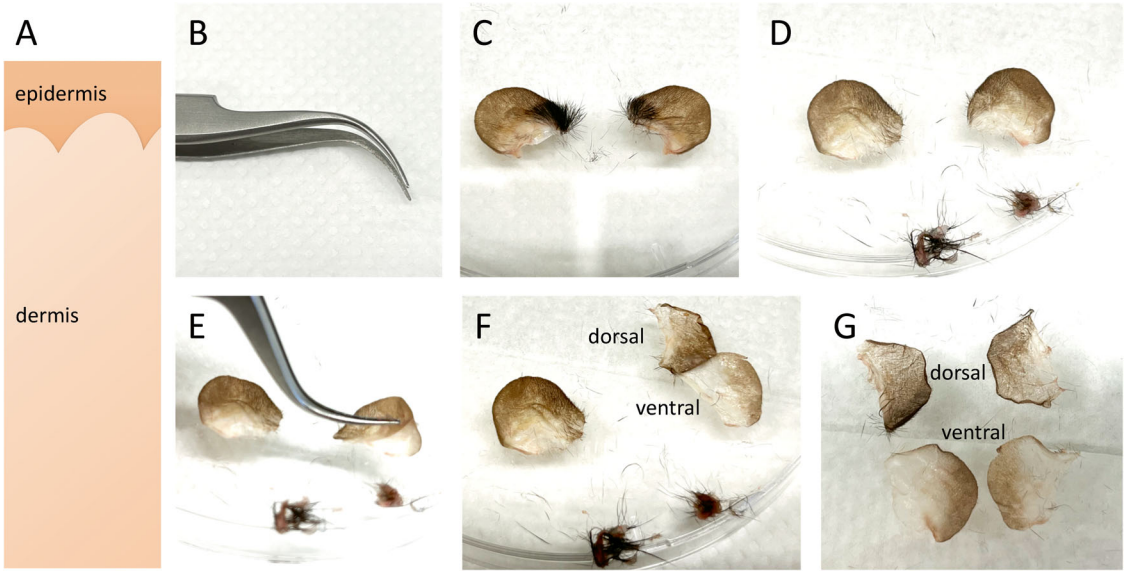

Figure 1. The skin layers and preparation steps of mouse ear skin prior to enzymatic tissue digestion. (A) Schematic picture of the two skin layers. (B) Tissue is prepared by using curved forceps. (C) Ears are cut off at the base along the fur line. (D) Excessive hair is removed from the ears. (E) Starting at one edge of the ear, the dorsal and ventral halves are separated. (F) After separation, each ear is split into a dorsal and a ventral half. (G) Dorsal and ventral ear halves are used to dissociate tissue using enzymatic digestion.

Table 1. Reagents, enzymes, chemicals and solutions

Reagent	Manufacturer	Ordering Number
Enzymes		
Collagenase IV	Worthington	LS0004186
Deoxyribonuclease I (DNase I)	Roche	11284932001
Dispase® II	Roche	04942078001
Liberase™	Roche	5401119001
Chemicals & Solutions		
Roswell Park Memorial Institute (RPMI) 1640 Medium	Fisher Scientific	11530586
Dulbecco's Phosphate Buffered Saline (PBS) without calcium and magnesium	Sigma	D8537
BSA (Albumin bovine Fraction V)	Serva	11930
0.5 M Ethylenediaminetetraacetic (EDTA)solution	Sigma	03690
Gibco™ RPMI 1640 Medium (RPMI-1640)	Fisher Scientific	11530586
1 M HEPES	Fisher Scientific	15630056

samples if fat tissue and hair have been removed beforehand. Our description includes instructions for analyzing either the whole skin tissue (1.1.3.3.1) or the epidermal and dermal layers separately (1.1.3.3.2).

1.1.2 *Materials*

1.1.2.1 Reagents. A complete list of reagents is provided in Table 1.

1.1.2.1 Equipment. The necessary equipment is listed in Table 2.

1.1.3 *Step-by-step sample preparation*

1.1.3.1 Preparation of stocks and solutions.

FACS buffer

PBS supplemented with 0.5% BSA (v/v) and 2 mM EDTA.

Dispase II

Dissolve the lyophilized Dispase II enzyme in HEPES-buffered saline (50 mM HEPES/KOH pH 7.4, 150 mM NaCl) to obtain a stock solution of 10 mg/mL. Store aliquots at −20°C and avoid freeze–thaw cycles. Use sterile solutions and aseptic techniques.

DNase I

Dissolve Deoxyribonuclease I (DNase I) in phosphate buffered saline (PBS) to reach a final concentration of 1 mg/mL. Store in aliquots at −20°C and avoid freeze–thaw cycles. Use sterile solutions and aseptic techniques.

Table 2. Necessary equipment

Equipment	Company	Purpose
Centrifuge Hereaus Multifuge 3 L	Thermo Scientfic	Centrifugation of 50 mL tubes, 15 mL tubes and U-bottom plates
Heatable tube shaker "Thermoshaker TS-100"	Peqlab	Heating and shaking tissue during enzymatic digestion
Incubator 37°C	Sanyo	Dispase II digestion step
Laminar flow MSC-advantage	Thermo	Performance of all aseptic procedures
Curved Forceps (#11271-30) Dumoxel®	FST by Dumont	Specialized surgical forceps being used to separate dorsal from ventral halves of the ear skin
Small Scissors (14060-10)	FST by Dumont	Super fine scissors to cut ear tissue in small pieces
Petri dish 60 × 15 mm (#628161)	Greiner bio-one	Surface is used to separate dorsal from ventral halves
6-well plates (#657102)	Greiner bio-one	digestion of skin tissue using Dispase II
50 mL tubes (#62.547.254)	Sarstedt	Centrifugation of cell suspensions through cell strainer, mixing digesting mix
15 mL tubes (#188271-N)	Greiner bio-one	Centrifugation of cell suspensions, mixing digesting mix
2 mL Eppendorf tubes (#72.691)	Sarstedt	Cutting tissue into pieces, incubation of tissue with digesting mix on heatable tube shaker
Serological pipettes (#606180)	Greiner bio-one	Pipetting
70 μm filter for 50 mL tubes (#542070)	Greiner bio-one	Isolation of single cells from tissue

Liberase™

Dissolve the lyophilized Liberase™ in 1× RPMI Medium without FCS or any other supplements to obtain a stock solution of 5 mg/mL. Store in aliquots at −20°C, and avoid freeze–thaw cycles. Use sterile solutions and aseptic techniques.

1.1.3.2 Harvesting mouse ear skin.

1. Euthanize mice;
2. Cut off ears at the base just above the fur line;
3. If necessary, store samples in 2 mL Eppendorf tubes on ice or 4°C until further processing.

1.1.3.3 Generation of single-cell suspensions from mouse ear skin.

1.1.3.3.1 Preparation of a whole tissue single-cell suspension.

1. Put ears on the surface of a sterile Petri dish (Fig. 1C);
2. Remove excessive hair from the tissue by running the forceps across the tissue (Fig. 1D);
3. Use curved forceps (Fig. 1B) to split each ear into dorsal and ventral halves (Fig. 1E–G);
4. Preheat tube shaker to 37°C;
5. Prepare digesting solution starting with the RPMI-Medium, place 200 μl of media without enzymes in each 2 mL Eppendorf tube, and then add the required enzymes to the remaining volume of media as indicated in Table 3;
6. Add skin tissue (two whole ears maximum per tube), store on ice;
7. Use fine scissors to cut the tissue into very small pieces until a pulpy mass is obtained;
8. Add 1.8 mL of digesting solution;
9. Vortex the tubes and put them into a tube shaker (37°C, 900 rpm, 90 min);
10. Add 40 μl of 0.5 M EDTA to each tube;
11. Vortex and incubate for an additional 10 min (37°C, 900 rpm);
12. Put a 70 μm strainer on top of a 50 mL tube;
13. Equilibrate the strainer by adding 5 mL of FACS buffer;
14. Vortex the tissue suspension and pour each sample onto an equilibrated strainer;
15. Rinse each strainer with 5 mL FACS buffer;
16. Centrifuge the 50 mL tube with the attached strainer at 468 × g and 4°C for 5 min;
17. Remove the strainer and supernatant (starting with the fatty layer and bubbles on the surface);
18. Use cell pellets for further analysis. If necessary, store cells resuspended in FACS buffer at 4°C.

1.1.3.3.2 Preparation of single-cell suspensions of epidermis and dermis separately. To isolate DC from the epidermis separate from DC from the dermis, different digestion solutions are used for the isolation of cells from the respective layer. For optimal yields of LC, Liberase is used, whereas Collagenase digestion mix is applied to the dermal tissue to obtain high yields of dermal DC.

1. Put ears on the surface of a sterile Petri dish (Fig. 1C);
2. Remove excessive hair from the tissue by running the forceps across the tissue (Fig. 1D);
3. Use curved forceps (Fig. 1B) to split each ear into its dorsal and ventral halves (Fig. 1E–G);
4. Add 4 mL of PBS to each well of a 6-well plate;

Table 3. Preparation of digestion solution for whole tissue

	Stock concentration	Working concentration	Dilution	Volume per 2 mL-Tube
RPMI-Medium	1×	1×	–	1780 μl (200 μl for cutting the tissue, the remaining volume for digesting solution)
Collagenase IV	Lyophilized powder	800 U/mL	Batch specific	–
Dispase II	10 mg/mL	1 mg/mL	1:10	200 μl
DNase I	1 mg/mL	10 μg/mL	1:100	20 μl

Table 4. Preparation of digestion solution for the separation of the epidermis from the dermis

	Stock concentration	Working concentration	Dilution	Volume per well
PBS	1×	1×	–	2765 μl
Dispase II	10 mg/mL	2 mg/mL	1:5	700 μl
DNase I	1 mg/mL	10 μg/mL	1:100	35 μl

Table 5. Preparation of digestion solution for the epidermis

	Stock concentration	Working concentration	Dilution	Volume per 2 mL-Tube
RPMI-Medium	1×	1×	–	1900 μl (200 μl for cutting the tissue, rest of the volume for digest solution)
Liberase™	5 mg/mL	200 μg/mL	1:25	80 μl
DNase I	1 mg/mL	10 μg/mL	1:100	20 μl

5. Put ears (up to two ears per well) with the epidermal part facing up and the dermal part facing down; thus, only the dermal part is exposed to the digesting solution;
6. Remove PBS with caution (ears should lay completely flat on the bottom of each well);
7. Add 3–3.5 mL Dispase II solution (2.5 mg/mL in PBS + 10 μg/mL DNase I) into each well, thereby ensuring that the solution does not come into contact with the epidermal part; this information is summarized in Table 4;
8. Incubate at 4°C overnight (approximately 16 h) or 45 min at 37°C;
9. Using forceps, take the ear halves out of the solution and put them on a sterile Petri dish;
10. Use the forceps to run across the tissue and peel the quite thin and almost transparent layer of epidermal cells (facing up); the remaining layer underneath is the dermal part;
11. Place the epidermal and dermal parts of the tissue in two separate 2 mL tubes and store on ice or at 4°C until further processing;
12. Preheat tube shaker to 37°C;
13. Prepare the digestion solution for the epidermal layer as indicated in Table 5;
14. Prepare the digestion solution for the dermal layer as indicated in Table 6;
15. Place 200 μl of RPMI Medium in a 2mL Eppendorf tube and add epidermis or dermis tissue (tissue of two ears maximum per tube), store on ice;
16. Use fine scissors to cut the tissue into very small pieces until a pulpy mass is obtained;
17. Add 1.8 mL of the respective digestion solution;
18. Vortex the tubes and place them into a tube shaker (37°C, 900 rpm, 90 min);
19. Add 40 μl of 0.5 M EDTA to each tube;
20. Vortex and incubate for an additional 10 min (37°C, 900 rpm);
21. Put a 70 μm strainer on top of a 50 mL tube;
22. Equilibrate the strainer by adding 5 mL of FACS buffer;
23. Vortex the tissue suspension and pour each sample onto an equilibrated strainer;
24. Rinse each strainer with 5 mL FACS buffer;
25. Centrifuge the 50 mL tube with the attached strainer at 468 × g and 4°C for 5 min;
26. Remove the strainer and supernatant (starting with the fatty layer and bubbles on the surface);
27. Use cell pellets for further analysis. If necessary, store cells resuspended in FACS buffer at 4°C.

1.1.4 *Data analysis*

Examples of flow cytometry data analysis of cutaneous DC subsets using the described single-cell preparation are covered in detail in the section 2.1 "**Flow cytometry analysis of DC subsets in mouse skin**".

Table 6. Preparation of digestion solution for the dermis

	Stock concentration	Working concentration	Dilution	Volume per 2 mL-Tube
RPMI-Medium	1×	1×	–	1980 μl (200 μl for cutting the tissue, rest of the volume for digest solution)
Collagenase IV	Lyophilized powder	800 U/mL	Batch specific	–
DNase I	1 mg/mL	10 μg/mL	1:100	20 μl

1.1.5 *Pitfalls*

Problem: Studying rare cell populations
Potential solutions:
When aiming for fluorescence-activated cell sorting or single-cell RNA sequencing and/or if rare cell populations are studied, DC should be enriched by using, e.g., magnetic cell sorting with anti-CD11c or anti-MHC-class-II microbeads or density gradient centrifugation.

Problem: Low cellular yields
Potential solutions:
Either cut tissue into smaller pieces (perhaps also scissors are no longer sharp enough) and/or increase enzyme concentrations or incubation times (note: an increase in enzymatic activity can lead to the loss of epitopes).

Problem: Loss of surface markers due to enzymatic digestion
Potential solutions:
Contaminating proteinases from collagenases or dispase can lead to the loss of some surface markers, in particular CD11c and CD103. Furthermore, lineage markers such as CD4, CD8 and CD19, can be affected. The optimal digestion duration and enzyme concentration should be carefully chosen, and different batches of enzymes should be tested.

Problem: Studying LC in particular
Potential solutions:
Protocols using liberase instead of collagenase IV result in higher LC yields and are advisable if a quantitative isolation of LC from whole skin digests is desired [9, 10].

1.1.6 *Top tricks*

- If higher numbers of cutaneous cells are necessary for downstream analysis or if the ear skin cannot be used, body skin samples can also be processed this protocol. Make sure that any adipose or subcutaneous tissue is removed. To remove hair from the body skin, hair-removal crème is suggested.
- For each area of skin, a specific draining lymph node exists, where primary immune responses develop. In the case of studying immune responses in skin, migratory cells in the skin-draining lymph nodes would also be worth analyzing.

1.2 Preparation of single-cell suspensions from mouse intestinal tract

1.2.1 *Introduction*

In the following, we will provide a detailed protocol for preparing single-cell suspensions from various tissues of the intestinal tract, including cells from the intestinal epithelium and lamina propria of the small intestine and colon, as well as cells from mesenteric lymph nodes and Peyer's patches within one workflow (Fig. 2).

In general, the intestinal wall is composed of four different layers comprising the mucosa, the submucosa, the muscularis propria and the serosa. The mucosa forms the borderline to the environment, since it is in direct contact with the intestinal lumen. The mucosa itself can be separated into three different layers

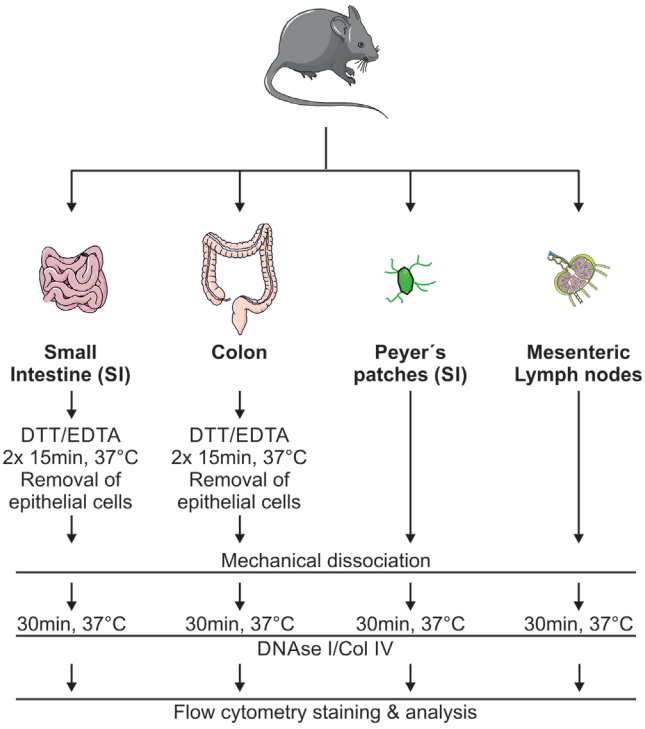

Figure 2. Schematic overview of the generation of single-cell suspensions from the intestinal tract. Illustrations are provided and adapted from Servier Medical Art (smart.servier.com), and these illustrations are licensed under the Creative Commons Attribution 3.0 Unported license (creativecommons.org/licenses/by/3.0/).

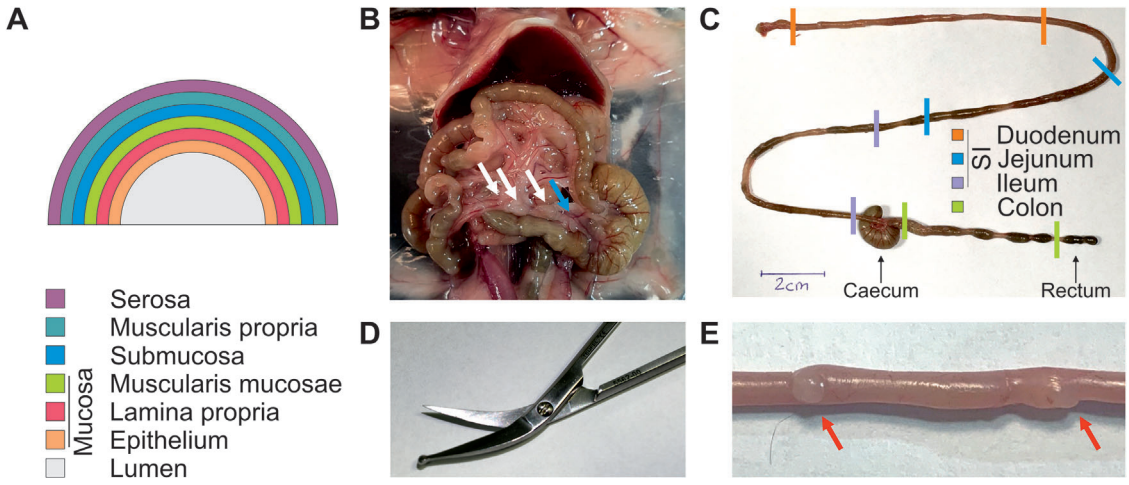

Figure 3. Architecture of the mouse intestinal tract. (**A**) Schematic cross-section of the intestinal wall; (**B**) Location of the major draining mesenteric lymph nodes (MLN) after opening the abdominal wall of a C57BL/6 mouse. Starting from the cecum with a colon draining MLN, mesenteric lymph nodes line up as a string; Blue and white arrows indicate colon and small intestine (SI) draining mesenteric lymph nodes, respectively; (**C**) Partitioning of the intestine from stomach to rectum. In general, the intestine consists of the small intestine, including the duodenum, jejunum and ileum, and the large intestine, including the cecum, colon and rectum. The duodenum, jejunum and ileum each roughly represent one-third of the small intestine. Bold, colored lines indicate suggested cutting sites to avoid overlap of the different intestinal sections during analysis. For the analysis of total SI, cut at the first and last indicated cutting site of duodenum and ileum, respectively; (**D**) Ball head scissors utilized to perform longitudinal cuts of intestinal tissue to allow for access of the digestion buffer; (**E**) Red arrows indicate examples for Peyer's patches located in the SI.

comprising the epithelium, representing a single layer of epithelial cells directly facing the intestinal lumen. The lamina propria mainly consists of connective tissue and lymphoid structures and the muscularis mucosae, which are formed by smooth muscle cells [11, 12]. Immune cells that are termed intraepithelial lymphocytes (IEL) and lamina propria cells (LPC) populate the epithelium and the lamina propria, respectively. A schematic representation of the intestinal wall architecture is shown in Fig. 3A.

While the general architecture of the intestinal wall is maintained along the intestinal tract, the intestine can be separated into compartments that are characterized by a distinct role during the food digestion processes and therefore display a particular crypt cell morphology and a distinct immune cell composition. From stomach to rectum, the intestine can be distinguished into the small intestine and the large intestine [11, 12]. The small intestine is composed of the duodenum, jejunum and ileum, each representing approximately one-third of the small intestine (Fig. 3C). On the other hand, the large intestine consists of the cecum, colon and rectum. While specialized lymphoid structures called Peyer's patches are located in all segments of the small intestine, the large intestine is devoid of Peyer's patches. In addition to Peyer's patches, mesenteric lymph nodes (MLN) act as harbors for immune cells and particle drainage of the intestinal tract. Houston et al. and others demonstrated that certain MLN serve as destinations for migratory cells of either the small intestine or the colon, enabling the analysis of the respective draining tissue in relation to single intestinal sections [13]. In the following, we provide a detailed protocol for the generation of single-cell suspensions from the small intestine and its Peyer's patches, the colon and the associated MLN for use in several downstream applications.

1.2.2 *Materials*

1.2.2.1 Reagents. A complete list of reagents is provided in Table 7.

1.2.2.2 Equipment. The necessary equipment is listed in Table 8.

1.2.3 *Step-by-step sample preparation*

1.2.3.1 Preparation of stocks and solutions.

Calcium chloride ($CaCl_2$) and magnesium sulfate ($MgSO_4$) stock solutions

Prepare 1 M stock solutions of $CaCl_2$ and $MgSO_4$ by dissolving salts in double-distilled H_2O. Sterile filter both stock solutions via a 0.22 μm filter membrane. Use aseptic techniques. Store stock solutions at room temperature.

DNAse I

Dissolve Deoxyribonuclease I (DNAse I) in Hank's balanced salt solution (HBSS) to reach a final concentration of 4200 U/mL. Sterile filter the solution through a sterile 0.22 μm membrane. Store in aliquots at −20°C and avoid freeze-thaw cycles. Use sterile solutions and aseptic techniques.

Collagenase IV / Collagenase D

Dissolve Collagenase IV (Col IV) in HBSS containing 3 mM $CaCl_2$ to reach a final concentration of 1500 U/mL. Sterile filter the solution through a sterile 0.22 μm membrane. Store in

Table 7. Reagents, enzymes, chemicals and solutions

Reagent	Manufacturer	Ordering Number
Enzymes		
Collagenase IV	Worthington	LS0004186
Deoxyribonuclease I (DNAse I)	Worthington	LS002139
Chemicals & Solutions		
Hank's Balanced Salt Solution (HBSS) without calcium and magnesium	Sigma	H6648
Dulbecco's Phosphate Buffered Saline (PBS) without calcium and magnesium	Sigma	D8537
Calcium chloride ($CaCl_2$)	Roth	HN04.3
Ditihiothreitol (DTT)	Roth	6908.1
Ethylenediaminetetraacetic acid (EDTA)	Invitrogen	15575-038
Magnesium sulfate ($MgSO_4$)	Roth	0261.1
Sodium chloride (NaCl)	Roth	3957.1
Trypan blue	Sigma	T6146
Fetal Bovine Serum (FCS)	Sigma	F7524

aliquots at −20°C and avoid freeze-thaw cycles. Use sterile solutions and aseptic techniques.

FCS

Quickly thaw FCS at 37°C in a water bath. Once completely thawed, incubate for 15 min at 42°C in the water bath to destroy complement activity. Directly filter the warm FCS through a sterile 0.22 μm membrane (Corning #431118) into a sterile storage bottle (Corning #430518) and aliquot into 50 mL portions. Use aseptic techniques during the whole procedure. Aliquots of FCS should be stored at −20°C. Avoid freeze-thaw cycles.

FACS buffer

Add 2% FCS (v/v) to phosphate buffered saline solution (PBS).

Table 8. Necessary equipment

Equipment	Company	Purpose
Centrifuge "Allegra X-15R"	Beckman-Coulter	Centrifugation of 50 mL tubes, 15 mL tubes and V-bottom plates
Shaker "Multitron"	INFORS HT	Shaker & incubator for IEL and LPC digestions
Incubator "HERAEUS BBD6220"	Thermo Scientific	Cabinet style incubator with 5% CO_2 and 96% relative humidity for the lymphoid tissue digestion
Neubauer chamber 0.100 mm; 0.0025 mm^2	Superior Marienfeld	Cell counting
Corning storage bottle (#430518) and 0.22 μM sterile filter (#431118)	Corning	Sterile filtration and storage of solutions
Sterile bench "Mars Safety Class 2"	Scanlaf	Performance of all aseptic procedures
Ball head scissor (#5562-00)	Teufel	Specialized surgical scissor for performing longitudinal cuts in intestinal tissue
6-well plates (#140675)	Thermo Scientific	Storage of organs, digestion of lymphoid tissues
96-well V-bottom plate (651 180)	Greiner bio-one	Sample preparation for flow cytometry
Pestles (#309658)	BD	Passage of organ material via 100 μm filters
50 mL tubes (#352070)	Falcon	Centrifugation of cell suspensions; Digestion of intestinal tissues
15 mL tubes (#188271)	Greiner bio-one	Centrifugation of cell suspensions
Serological pipettes (#606180)	Greiner bio-one	Pipetting
100 μm filter for 50 mL tubes (#542000)	Greiner bio-one	Isolation of single cells from tissues
70 μm filters for 50 mL tubes (#542070)	Greiner bio-one	Generation of single cell suspensions from intestinal tissues by passive filtration
40 μm filters for 50 mL tubes (#542040)	Greiner bio-one	Generation of single cell suspensions from lymphoid tissues by passive filtration

Digestion buffer for the isolation of intraepithelial lymphocytes (IEL buffer)

Per analyzed intestinal section, prepare 10 mL of IEL buffer (3x concentration). Therefore, add 15% FCS (v/v), 3 mM DTT and 15 mM EDTA to PBS and pre-warm at 37°C before use. For long-term storage, keep IEL buffer at 4°C.

Hank's balanced salt solution for the preparation of lamina propria cell (LPC) buffer and lymphoid tissue buffer (LT buffer)

Prepare a Hank's balanced salt solution (HBSS) stock by adding 2% FCS (v/v), 2 mM $CaCl_2$, and 2 mM $MgSO_4$. The stock solution was stored at 4°C.

Digestion buffer for the isolation of lamina propria cells (LPC buffer)

Per analyzed intestinal section, take 5 mL of the prepared HBSS stock and add 500 μl Collagenase IV and 100 μl DNAse I. Pre-warm before use to 37°C in the water bath allowing for optimal enzyme activity.

Digestion buffer for the isolation of cells from mesenteric lymph nodes and Peyer's patches (lymphoid tissue buffer (LT buffer))

To digest mesenteric lymph nodes (MLN) and Peyer's patches, add 50 μl Collagenase IV and 50 μl DNAse I per 1 mL of HBSS stock solution containing 2% FCS (v/v), 2 mM $CaCl_2$ and 2 mM $MgSO_4$. Pre-warm before use to 37°C in the water bath. Digest colon- or small intestine draining MLN and Peyer's patches isolated from one individual mouse in 2 mL of LT buffer.

Trypan blue

Create a 0.9% (w/v) NaCl solution by dissolving NaCl in double-distilled H_2O. Dissolve 0.36% (w/v) Trypan blue powder in 0.9% NaCl solution. Sterile filter the solution via a 0.22 μm membrane and store at room temperature.

1.2.3.2 Harvesting tissues of the intestinal tract.

1. Euthanize mice;
2. Carefully open the skin on the ventral side to expose the abdominal wall;
3. Open the abdominal wall;
4. Preparate the mesenteric lymph nodes (MLN) before removal of the intestine. For the analysis of individual MLN, start with the isolation of the MLN close to the cecum (colon-draining MLN). After identification of the colon-draining MLN, other MLN line up as a string. With increasing distance to the colon-draining MLN, these MLN are responsible for drainage from the small intestine (Fig. 3B). Completely remove fatty tissue;
5. Store the tissues covered in a drop of PBS in a 6-well plate on ice;
6. Cut the intestine at the anterior end close to the stomach and at the posterior end close to the rectum;
7. Put intestines into a 6-well plate containing PBS to keep the tissue wet and avoid ruptures until all intestines are prepared;
8. Store intestines in a 6-well plate on ice until further processing;
9. Separate the colon (part from cecum to rectum) and the small intestine (section between stomach and cecum);
10. Carefully remove all fatty tissue;
11. Cut out Peyer's patches present in the small intestine (not present in the colon), put them into a 6-well plate and cover the tissue with a drop of PBS; Examples for Peyer's patches are depicted in Fig. 3E;
12. Store Peyer's patches in a 6-well plate on ice until further processing;
13. Carefully squeeze out luminal content with a closed tweezer of every intestinal section; alternatively, the intestinal lumen can be rinsed with FACS buffer (PBS+2% FCS) using oral gavage needles for rats;
14. Cut the intestine open in the longitudinal direction to allow for digestion buffer access to the intestinal lumen. Therefore, we recommend scissors equipped with a pin-head formed end ("ball head scissors" shown in Fig. 3D);
15. Wash the intestinal tissue with PBS in a petri dish;
16. Store each processed intestinal section in a 50 mL falcon containing 10 mL of room-temperature PBS;
17. Once all organs are harvested, tissues are ready for digestion;
18. If isolated cells are subjected to downstream assays requiring incubation at 37°C, perform all following steps under a sterile cell culture bench utilizing aseptic techniques.

1.2.3.3 Generation of single-cell suspensions from intestinal tissues.

1.2.3.3.1 Mesenteric lymph nodes and Peyer's patches.

1. Add 2 mL of prewarmed (37°C) LT buffer per well to MLN or Peyer's patches;
2. Mince the tissue completely with tweezers to increase digestion buffer access;
3. Digest tissue for 30 min at 37°C in an incubator supplying a 5% CO_2 atmosphere;
4. Pipette the cell suspension on a 100 μm filter and rinse the well with FACS buffer;
5. Carefully grind the tissue with a pestle while avoiding pressure;
6. Rinse the filter and pestle with FACS buffer; keep the total volume below 15 mL;
7. Directly filter passively through a 40 μm filter;
8. Rinse the filter with FACS buffer. Keep the total volume below 15 mL;
9. Directly transfer the cell suspension to a 15 mL tube to minimize pellet surface and therefore cell-loss during the washing steps;
10. Centrifuge the samples at 700 × g for 5 min at 4°C;

Table 9. Expected cellular yields in single-cell suspensions of organs from the intestinal tract

Tissue	Live cells	Expected cDC
Small Intestine MLN	0.7×10^6 to 3.0×10^6 per MLN	7,000–30,000 per MLN
Small Intestine Peyer's patches	1.4×10^6 to 3.6×10^6 per mouse	2,000–8,000 per mouse
Small Intestine IEL	6.5×10^6 to 20×10^6 per mouse	0–200 per mouse
Small Intestine LPC	7.1×10^6 to 10.0×10^6 per mouse	5,000–20,000 per mouse
Colon MLN	0.8×10^6 to 3.0×10^6 per MLN	8,000–30,000 per MLN
Colon IEL	2×10^6 to 3×10^6 per mouse	0–200 per mouse
Colon LPC	4.0×10^6 to 6.5×10^6 to per mouse	3,000–6,000 per mouse

11. If a fat layer is present after centrifugation, remove it using a serological pipette before proceeding to decanting the supernatant. Decant the supernatant and remove most of the liquid by putting the tube upside down onto a paper towel for 2–5 min. If single cell suspensions are generated under aseptic conditions, do not use paper towels. Instead, decant the supernatant and briefly centrifuge cells again for 1 min at 700 × g at 4°C. Carefully take off the remaining supernatant utilizing a Gilson pipette and filter tips;
12. Resuspend the pellet in 1 mL of FACS buffer using a Gilson pipette;
13. Top up to 8–10 mL with FACS buffer;
14. Mix the sample by vortexing;
15. Centrifuge the samples at 700 × g for 5 min at 4°C;
16. Discard supernatant;
17. Repeat the steps 10–16 two times (equaling three washings steps in total). To determine cell number, count an aliquot of cells utilizing trypan blue directly before the last centrifugation (expected yields for C57BL/6 mice can be found in Table 9);
18. After the last centrifugation, resuspend each sample containing all cells resulting from the preparation of either all small intestine-draining MLN or Peyer's patches or colon draining MLN from one mouse in 100 μl FACS buffer and transfer to a 96-well V-bottom plate for antibody staining;
19. If your cell count strongly differs from the expected cellular yields (>factor 1.5), scale the volume of antibody cocktails up and down accordingly; do not stain in less than 35 μl; Store the sample containing plate at 4°C or on ice until all tissues are processed for flow cytometry staining;
20. Alternatively, single-cell suspensions can be used for the direct generation of RNA, the creation of cell lysates for Western blots, enrichment and cell sorting or for singularization procedures allowing for RNA single-cell sequencing.

1.2.3.3.2 Intraepithelial Lymphocyte (IEL) and Lamina Propria Cell (LPC) isolation from intestinal sections.

1. Add 5 mL of 3 concentrated IEL buffer per isolated intestinal section that is stored in 10 mL of PBS (sample resulting from the preparation described in section 1.2.3.2 "Harvesting tissues of the intestinal tract" step 18);
2. Swirl to facilitate mixing;
3. Incubate samples at 37°C for 15 min while shaking at 230 rpm (Shaker "Multitron");
4. Pour the supernatant containing the intraepithelial lymphocyte (IEL) fraction via a 100 μm filter;
5. Repeat the digestion by adding 10 mL of PBS and 5 mL of 3 concentrated IEL buffer;
6. In the meantime, centrifuge IEL that were filtered via the 100 μm strainer at 700 × g for 5 min at 4°C to remove the IEL buffer and resuspend the pellet in 5 mL of FACS buffer; keep the samples on ice;
7. After another 15 min of digestion in IEL buffer, the supernatant containing the remaining IEL was filtered via the same 100 μm strainer;
8. After washing, pool with the respective IEL fraction of the first digestion round;
9. Centrifuge IEL at 700 × g for 5 min at 4°C and resuspend in 5 mL;
10. The purification protocol for the IEL fraction continues at point **20**;
11. Wash the remaining intestinal tissue two times in 10 mL PBS to completely remove the EDTA included in the IEL buffer, since EDTA would block collagenase IV and DNAse I activity during digestion with the LPC buffer;
12. Prepare fresh tubes containing 5 mL prewarmed LPC buffer;
13. Cut the intestine into small pieces in the cap of the digestion tube utilizing scissors (the smaller the resulting fragments are, the higher the cellular yields owing to increased digestion buffer access);
14. Place a 50 mL cap on the 50 mL falcon;
15. Mix and ensure that every tissue fragment is allocated to the digestion buffer;
16. Perform the digestion for the isolation of LPC for 30 min at 37°C while shaking at 230 rpm;
17. After 30 min of digestion, pour the tissue onto a fresh 100 μm filter;
18. Carefully triturate the tissue utilizing a pestle (do not apply pressure to avoid passage of unwanted tissue fragments via the filter);
19. Rinse the digestion tube, filter and pestle with FACS buffer;
20. After this step, the purification procedure for IEL and LPC occurs analogously;
21. Centrifuge the samples at 700 × g for 5 min at 4°C;
22. If a fat layer is seen after centrifugation, remove it using a serological pipette before proceeding to decanting the

supernatant. Decant the supernatant and remove most of the liquid by putting the tube upside down onto a paper towel for 2–5 min. If single cell suspensions are generated under aseptic conditions, do not use paper towels. Instead, decant the supernatant and briefly centrifuge cells again for 1 min at 700 × g at 4°C. Carefully take off the remaining supernatant utilizing a Gilson pipette;

23. Resuspend the cell pellet in 1 mL of FACS buffer, top up to 5 mL and vortex the sample;
24. Passively filter via a 70 μm cell strainer;
25. Rinse tube and strainer with 5 mL of FACS buffer;
26. Directly transfer the filtrate into a 15 mL tube to minimize cell loss during centrifugation;
27. Centrifuge the samples at 700 × g for 5 min at 4°C;
28. Carefully decant the supernatant and remove most of the liquid by putting the tube upside down onto a paper towel. Keep the tube constantly upside down during this procedure. If single-cell suspensions are generated under aseptic conditions, do not use paper towels. Instead, decant the supernatant and briefly centrifuge the cells again for 1 min at 700 × g at 4°C. Carefully take off the remaining supernatant utilizing a Gilson pipette;
29. Resuspend in 1 mL of FACS buffer, top up to 8–10 mL and vortex the sample;
30. Centrifuge the samples at 700 × g for 5 min at 4°C;
31. Repeat steps 28–30 two times (3 washing steps in total);
32. Determine the cell count utilizing a Neubauer chamber and trypan blue to distinguish alive and dead cells;
33. Resuspend the cell pellet after the last centrifugation in 100 μl of FACS buffer and transfer to a 96-well V-bottom plate;
34. If your cell count strongly differs from the expected cellular yields that are shown in Table 9 (>factor 1.5), scale the volume of antibody cocktails up and down accordingly; Do not stain in less than 35 μl;
35. Alternatively, single-cell suspensions can be used for the direct generation of RNA, the creation of cell lysates for Western blots, enrichment and cell sorting procedures or for singularization procedures allowing for RNA single-cell sequencing.

1.2.4 *Data analysis*

Examples of flow cytometry data analysis of intestinal DC subsets using the described single-cell preparation are covered in detail in Section 2.2 "**Flow cytometry analysis of DC subsets in mouse intestinal tissue**".

1.2.5 *Pitfalls*

Problem: Low cell viability in IEL and LPC samples
Potential solutions:

A major factor that can negatively influence the viability of cells during the preparation of single-cell suspensions from the intestinal tract is the overall time needed for preparation. Thus, it is of utmost importance to work quickly and efficiently. To achieve optimal results and to limit strong variations in cell viability, adjust the amount of prepared tissues to the experimenter's speed. Ensure that intestinal tissue stays wet during the whole preparation procedure to avoid unnecessary tissue ruptures.

Directly after digestion with IEL buffer and isolation of the IEL containing supernatant, wash the IEL fraction, while the digestion is repeated.

Intestinal tissues contain very sensitive epithelial cells. To avoid a high ratio of dead cells, do not shorten the amount or volumes of the suggested washing steps. Except for tissue digestions at 37°C, keep samples and buffers on ice during the whole procedure. Use pre-cooled centrifuges and centrifuge inlays.

If flow cytometry is employed as analysis technique, perform data acquisition directly after finishing the above procedure. If storage of samples overnight is necessary, fix the samples. If samples are fixed, do not use DAPI during sample acquisition.

Problem: Low cellular yields
Potential solutions:

Fat covering intestinal tissues and MLN needs to be completely removed before starting the digestion procedures to avoid cell loss. MLN and the covering fat can look very similar. To ensure that MLN are isolated instead of fat, place the isolated tissue in PBS. MLN will settle down, while fat will stay at the surface.

Ensure that enzymes and digestion buffers are prewarmed to 37°C before usage.

MLN have a durable capsular tissue. To efficiently isolate cells from MLN, the capsule has to be broken up mechanically to allow for access of digestion buffer and the release of cells. To ensure capsule ruptures, increase the time of mincing with tweezers.

To allow for optimal digestion buffer access, ensure that the complete intestine is cut open longitudinally before performing digestion. Employ a tube size that allows for proper mixing by shaking while performing digestions. Ensure that tubes are not placed in a shaker vertically but display an inclination angle of approximately 45 degrees. For the isolation of LPC and cells from MLN and Peyer's patches, the output of cells is tremendously increased if the digested fragments are cut or minced into smaller fragments.

During washing steps (independent of the tissue), ensure that no fat layer has formed on top of the pellet. Any fat layer must be removed by careful pipetting before decanting the supernatant.

1.2.6 *Top tricks*

- By utilizing photoinducible mice, Houston et al. showed that individual MLN are responsible for the drainage of migratory immune cells, in particular DC, from either the small intestine

or the colon (for detailed information on the location of MLN and the associated cellular drainage, please refer to [13, 14]).
- The small intestine and its respective Peyer's patches can be further subdivided into three different compartments, including the duodenum, jejunum and ileum (listed in the direction stomach to cecum) [11]. Today, it is assumed that the different sections serve distinct immunological functions. Since each of these sections (as indicated in Fig. 3) roughly represents one-third of the small intestine, the immune cell compartment of these specialized sections can be analyzed by pooling cells derived from the sections of three individual mice. We recommend leaving spacers left and right to where the border of the individual sections is assumed to ensure the analysis of single sections without contamination of cells located in neighboring sections (see Fig. 3C).

1.3 Preparation of single-cell suspensions from mouse lung

1.3.1 *Introduction*

The lung is constantly exposed to the environment and hence to a wide range of pathogens, such as viruses and bacteria. Therefore, the lung harbors a dense network of antigen-presenting cells (APC), including specialized dendritic cell (DC) and macrophage subsets, which fulfill an essential sentinel function and orchestrate appropriate immune responses toward incoming pathogens and other immunological threats. On the other hand, DC and macrophages also regulate inflammation by several direct and indirect tolerogenic mechanisms. These include the promotion of regulatory T cells (Treg), the induction of T-cell anergy, and the secretion of regulatory cytokines such as IL-10 [15]. When DC sensitize T cells against harmless Ag instead of inducing Tregs, inappropriate detrimental immune reactions, such as allergic asthma, can occur. Pulmonary DC comprise three main classes: plasmacytoid DC (pDC), conventional DC (cDC) and monocyte-derived DC (moDC), all of which express CD11c and MHC class II (MHC-II). The pDC can be identified as $CD11c^{low}$ Siglec-H^+ $B220^+$ PDCA-1^+ cells, produce significant amounts of type I IFN during viral infections [16], and induce tolerance to inhaled innocuous Ag [17]. cDC can be further divided into $CD103^+$ $XCR1^+$ cDC1 and $CD11b^+$ $CD172\alpha^+$ cDC2 subsets [18]. Pulmonary cDC locally control innate immune responses *in situ* and upon Ag recognition migrate to the lung-draining mediastinal lymph nodes. Both cDC1 and cDC2 sample antigens, but while cDC1 are particularly good in inducing Th1 polarization and in cross-presenting viral Ags to $CD8^+$ T cells, cDC2 primarily prime $CD4^+$ T cells against bacterial Ags and trigger Th2 responses during allergic reactions [19]. In addition, upon inflammation, monocytes migrate into the lung tissue where they differentiate into inflammatory moDC, which can be identified by the expression of CD11b, MAR-1 and CD64 [20]. The moDC produce type-I IFN, thereby helping to limit viral replication, and they locally interact with T effector cells and can reactivate $CD8^+$ memory T cells [18]. Notably, there are also bona fide inflammatory cDC2 that can acquire expression of the Fc receptor CD64, which can be distinguished from inflammatory moDC by expression of CD26 [21].

Next to DC, several macrophage subsets reside in the lung. Among these, the best characterized population is alveolar macrophages, which are identified by typical macrophage markers (e.g., CD64, MerTK) in combination with SiglecF and high expression of CD11c [22]. These alveolar macrophages are located in the alveolar lumen and play a pivotal role in maintaining lung homeostasis by clearing apoptotic cells and cell debris and in regulating pulmonary immune responses [23]. The remaining pulmonary macrophage subsets are all collectively referred to as interstitial macrophages and represent a heterogeneous population of cells, consisting of at least two distinct populations [24–26]. These interstitial macrophages can be identified by the expression of typical macrophage markers (e.g., CD64 and MerTK) and CD11b.

In the following, we provide a detailed protocol for the isolation of DC and macrophages from the lung for use in several downstream applications.

1.3.2 *Materials*

1.3.2.1 Reagents. A complete list of reagents is provided in Table 10.

1.3.2.2 Equipment. The necessary equipment is listed in Table 11.

1.3.3 *Step-by-step sample preparation*

1.3.3.1 Preparation of stocks and solutions.

DNase I

Dissolve Deoxyribonuclease I (DNAse I) in PBS to reach a final concentration of 500 U/mL. Prepare aliquots, store dissolved DNase I at −20°C and avoid repeated freeze-thaw cycles. Use sterile solutions and aseptic techniques.

Collagenase IV

Dissolve Collagenase IV in PBS to reach a concentration of 10,000 U/mL. Prepare aliquots, store dissolved Collagenase IV at −20°C and avoid repeated freeze-thaw cycles. Use sterile solutions and aseptic techniques.

FCS

Thaw FCS at 37°C in a water bath and once completely thawed, incubate at 56°C for 30 min in the water bath. Directly filter the warm FCS through a sterile 0.45 μm filter and prepare aliquots. Store heat-inactivated FCS at −20°C and avoid repeated freeze-thaw cycles. Use aseptic techniques during the whole procedure.

Table 10. Reagents, enzymes, chemicals and solutions

Reagent	Manufacturer	Ordering Number
Enzymes		
Collagenase Type 4	Worthington	LS0004186
Deoxyribonuclease I (DNAse I)	Roche	10104159001
Chemicals & Solutions		
Roswell Park Memorial Institute (RPMI) 1640 Medium	Thermo Fisher Scientific Inc.	11530586
Dulbecco's Phosphate Buffered Saline (PBS) without calcium and magnesium	Sigma	D8537
Fetal Bovine Serum (FCS)	Sigma	F7524
Ethylendiamintetraacetat (EDTA, (0.5 M))	Sigma	E5134-500G
Gibco Trypan Blue Solution, 0.4%	Thermo Fisher Scientific Inc.	11538886
Ethylenediaminetetraacetic acid disodium salt dihydrate	Sigma	E5134-1KG
Sodium hydroxide ≥98%, p.a., ISO, in pellets	Carlroth	6771.1

FACS buffer

Add 2% FCS (v/v) and 2 mM EDTA to 500 mL of PBS.

Digestion solution

Per mouse, prepare 2 mL of digestion solution consisting of 200 U/mL Collagenase IV and 0.5 U/mL DNAse I in RPMI medium.

10× ACK lysis buffer

Dissolve 186.2 g EDTA (ethylenediaminetetraacetic acid disodium salt dihydrate) in 800 mL H_2O and add 20 g NaOH pellets. Adjust the pH to 8 and add H_2O to 1000 mL. Store at room temperature and remember to dilute the buffer to 1-fold concentration before use.

1.3.3.2 Step-by-step sample preparation of mouse lung macrophages/DC.

1. Euthanize mice using CO_2;
2. Immobilize the animal on a pad by pinning down the paws. Spray the animal with 70% ethanol;
3. Cut the skin above the abdomen, open further toward the chin and expose the abdominal cavity;
4. Open the abdominal cavity by cutting the ribs using a pair of blunt-tip scissors;
5. Pull the ribs away;
6. Dissect out the lung. Note that the right lung consists of four lobes, while the left lung has only one lobe;

Table 11. Necessary equipment

Equipment	Company	Purpose
Sharp tissue scissors HSB 088-14 (51754511)	Hammacher	Cut open the abdominal cavity and the ribs
Fine small tissue scissors HSB 390-10 (51807020)	Hammacher	Dissection of the lung, cut up the tissue in 2 mL Eppendorf tube
Forceps	Hammacher	Take out lung lobes, separate trachea and fat from tissue
2 mL Eppendorf tube	Thermo Fisher Scientific Inc.	Digestion of lung tissue
Thermo Shaker	Laboratory Technology	Shaker and incubator for tissue digestion
50 mL tube	Greiner bio-one	Collect and centrifuge cell suspension
70 μm cell strainer	Greiner bio-one	Generation of single cell suspension
Injekt-F 1 mL Disposable Fine Dosage Syringe, 9166017 V	B. Braun	Mesh tissue through cell strainer
Centrifuge "Z 446 K"	Hermle LaborTechnik	Centrifugation of 50 mL tube
Pipette tips	Brand	Pipetting
PipetMan (P10-P1,000)	Gilson	Pipetting
PipetBoy	Fisher scientific	Pipetting
Serological pipettes (1–25 mL)	Gilson	Pipetting
Neubauer chamber 0.100 mm; 0.0025 mm^2	Superior Marienfeld	Cell counting
0.45 μm Filtropur V50	Sarstedt	filter FCS

7. Carefully cut off the trachea and remove any fat attached to the lung;
8. Harvest the lung into a 2 mL microcentrifuge tube containing 300 μl digestion solution;
9. Mince the lung into small pieces in the tube using scissors;
10. Add 700 μl digestion solution;
11. Incubate the sample for 30 min at 37°C on a thermoshaker at 800 rpm;
12. Take the tube from the shaker and add an additional 1 mL of digestion solution;
13. Quickly vortex the sample;
14. Incubate the sample for another 30 min at 37°C on a thermoshaker at 800 rpm;
15. Take the tube from the shaker and place it on ice for 2 min;
16. Add 40 μl of 500 mM EDTA and incubate on ice for 2 min;
17. Prepare a 70 μm cell strainer on a 50 mL tube by moistening it with 1 mL FACS buffer;
18. Apply the lung cell suspension onto the cell strainer and use the syringe plunger to mesh the tissue through the strainer;
19. Wash the remaining cells from the strainer by adding 9 mL FACS buffer;
20. Centrifuge the cells at 380 × g for 7 min at 4°C;
21. Lyse erythrocytes by resuspending the cell pellet in 1× ACK lysis buffer at room temperature for 2 min;
22. Stop the lysis by adding excess FACS buffer;
23. Centrifuge the cells at 380 × g for 7 min at 4°C;
24. Resuspend the cell pellet in 2 mL FACS buffer. If necessary, remove clumps by filtering the suspension through a 70 μm cell strainer;
25. Determine the cell count using a Neubauer chamber and trypan blue.

1.3.4 *Data analysis*

Examples of flow cytometry data analysis of pulmonary myeloid cells with a focus on DC subsets using the obtained single-cell suspension are covered in detail in Section 2.3 "**Flow cytometry analysis of DC subsets in mouse lung**".

1.3.5 *Pitfalls*

- Cervical dislocation should be avoided, as it can lead to bleeding into the lung and bias its immune cell composition.
- To avoid bloody abdominal cavity during organ harvest, quickly take out both lung and heart with one cut and isolate the lung on a moistened tissue.
- To maximize cell yield, always control if clumps or fat can be found in the sample and remove them as soon as possible by careful pipetting. Also, try to keep the cell suspension in the same tube, and only change it if necessary. You may lose cells with each transfer.

1.3.6 *Top tricks*

- If you also want to isolate the lung draining mediastinal lymph nodes, first identify and isolate the nodes and remove the lung afterwards.
- Always use the same method for euthanasia as it affects the pH that can lead to a change in cell composition.
- Avoid pipetting too much up and down as this will stress the cells. Moreover, mechanical shear forces can result in phenotypic DC maturation.
- Note that mice are not perfused, as the cells of interest (DC and macrophages) are located within the tissue and are rarely part of the vascular leukocytes. Perfuse the mice if you want to analyze cells like tissue-resident monocytes or T cells to exclude any circulating cells from your preparation. Insert a needle in the left atrium before removing the lung and perfusing with PBS until the lung turns white. With this, you can reduce the number of vascular leukocytes. If perfusion is performed remember that still many intravascular leukocytes are present. Consider to intravenously inject anti-CD45 to stain and identify vascular leukocytes. In this way you can distinguish vascular and pulmonary leukocytes during flow cytometry.
- To remove or separately analyze alveolar cells, collect the bronchoalveolar lavage fluid (BALF) before harvesting the lung. Therefore, make a small incision in the trachea and pass a tube in the trachea. Fill the lung via the tube with up to 1 mL ice cold PBS. Watch the lung bloat and do not overinflate. Collect approximately 1 mL of BALF. Repeat this procedure three times. Of note, usually the BALF is only analyzed from inflamed lungs, i.e., after viral infection or in asthma models.
- When working with inflamed lungs, carefully pipetting the lung tissue up and down with a Pasteur pipette instead of meshing it through a strainer may help to reduce cell death. To this end, the smaller the pieces of lung tissue are cut, the better the digestion will work.

1.4 Preparation of single-cell suspensions from mouse oral mucosal tissues

1.4.1 *Introduction*

The oral mucosa consists of distinct immunological niches, including the gingiva, which is the tissue surrounding the teeth, the buccal mucosa, and the tongue. As a barrier tissue, the oral mucosa is covered with a stratified epithelium whose major function is to protect the internal tissues from invading pathogens [27]. Based on the anatomical location and structure, the oral mucosa can be separated into three main categories: the lining mucosa, the masticatory mucosa, and the specialized mucosa. The buccal mucosa at the sides of the cheeks belongs to the lining mucosa, which represents the largest part of the oral tissue. The epithelium covering the lining mucosa is nonkeratinized and thus allows direct interaction with environmental antigens. The

masticatory mucosa, including the gingiva, is covered with a partially keratinized epithelium and is thereby protected from mechanical forces such as chewing. The gingiva is located close to the palate and the nasal-associated lymphoid tissue (NALT) [28]. The specialized tissue of the tongue, typically described as a muscular organ, is covered by an epithelium containing lingual papillae and taste buds [29].

The oral mucosa consists of two main layers, the epithelium and the lamina propria, the underlying connective tissue. In some regions of the oral mucosa, a layer of loose connective tissue, the so-called submucosa, lies beneath the lamina propria. In areas such as the gingiva and hard palate, the lamina propria is directly attached to the periosteum of the underlying bone [30]. The various oral mucosal tissues comprise a complex network of immune cells that regulate both immunity against invading pathogens and tolerance to harmless foreign antigens and commensal bacteria. This balance ensures the maintenance of oral immune homeostasis, and its breakdown leads to dysbiosis resulting in periodontal inflammation [31]. Therefore, it is important to understand how the different cell types of the oral mucosal immune system maintain homeostasis. One cell type that is crucial in maintaining homeostasis is dendritic cells (DC). They can be distinguished into different subpopulations that are very heterogenous in their phenotype and immune regulatory function. In oral mucosal tissues, DC comprise different Langerhans cell (LC) subsets located in the epithelium and cDC1 and cDC2 in the lamina propria. While the LC has been shown to play an important protective immunoregulatory role in a model of inflammation-induced alveolar bone resorption, the exact functional specialization of the different LC and DC subpopulations is not yet known [32]. Similar to anatomical differences, the cellular composition of the oral mucosal tissues also differs, which requires the individual analysis of each tissue. Here, we provide a detailed protocol for isolating the different parts from the mouse oral cavity (Figs 4 and 5). In addition, we describe how to prepare the tissues to obtain single-cell suspensions for further flow cytometry analysis.

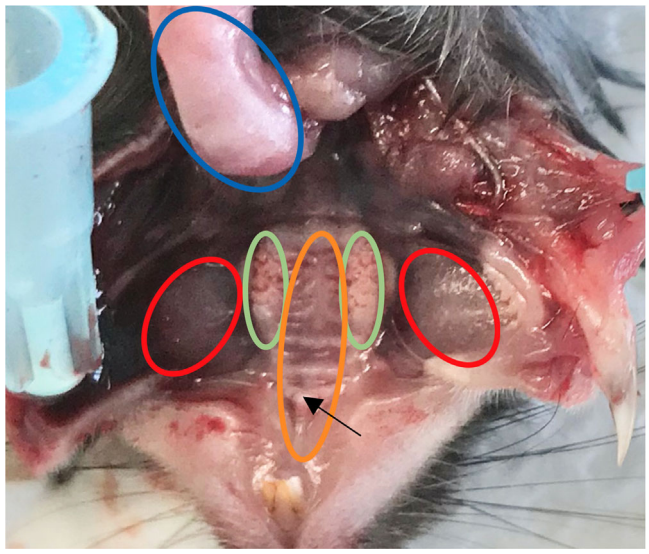

Figure 4. Mouse oral mucosal tissues. View of the mouse oral cavity after cutting between the lower incisors showing the anatomical location of the different oral tissues. The tongue (blue circle) is part of the specialized mucosa containing taste buds, while the gingiva (green circles), part of the masticatory mucosa, surrounds the teeth. Next to the gingiva, the hard palate (orange circle) that includes the underlying NALT (indicated by the black arrow) can be found. The buccal mucosa (red circles) belonging to the lining mucosa is located on the side of the cheeks.

Table 12. Reagents, enzymes, chemicals and solutions

Reagent	Manufacturer	Ordering Number
Enzymes		
Collagenase Type 2	Life Technologies (Gibco)	17101-015
Deoxyribonuclease I (DNase I)	Roche	10104159001
Dispase II	Roche	04942078001
Chemicals & Solutions		
Dulbecco's Phosphate Buffered Saline (PBS) without calcium and magnesium	Sigma	D8537
Fetal Bovine Serum (FCS)	Sigma	F7524
Ethylendiamintetraacetat (EDTA, (0,5 M))	Sigma	E5134-500G

1.4.2 *Materials*

1.4.2.1 Reagents. A complete list of reagents is provided in Table 12.

1.4.2.2 Equipment. The necessary equipment is listed in Table 13.

1.4.3 *Step-by-step sample preparation*

1.4.3.1 Preparation of buffer and digestion mix.

FCS

Quickly thaw FCS at 37°C in a water bath. Once completely thawed, incubate for 60 min at 56°C in the water bath to destroy complement activity. Aliquot the FCS into 50 mL portions and store at −20°C. Avoid freeze-thaw cycles. Use aseptic techniques during the whole procedure.

FACS buffer

Add 2% FCS (v/v) to 500 mL of PBS.

Digestion mix

Prepare 1 mL digestion mix per sample;

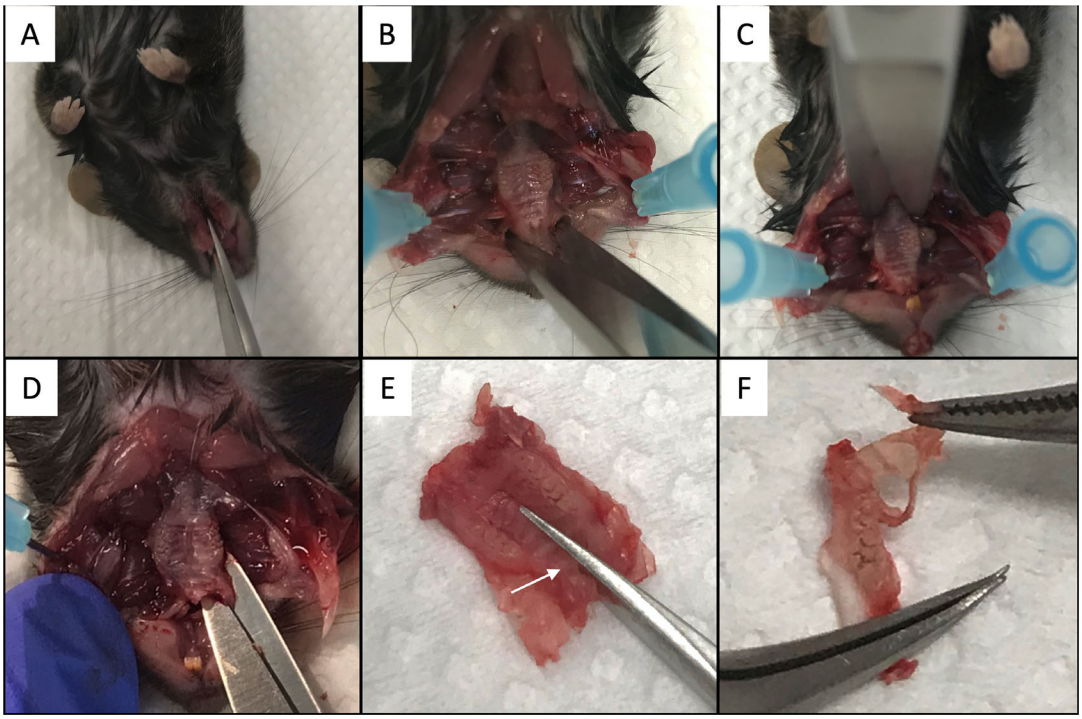

Figure 5. Isolation of mouse oral mucosal tissues. After cutting between the lower incisors (A), the mouse should be immobilized with needles on each side of the jaw to access the oral cavity. The tongue and the buccal mucosa can be cut out using fine scissors. Incisions through the soft and hard tissue behind the upper incisors (B) and behind the third molar (C) detach the palate from the underlying tissue. Pulling down the mandible allows cutting parallel to the palate through the nasal cavity on both sides (D). After cutting the palate in the middle and removing the NALT (white arrow) (E), the gingival tissue can be detached from both parts of the maxilla (F).

Add 2 mg/mL collagenase II and 1 mg/mL DNase I to FACS buffer.

Dispase II solution (if separation of epithelium and lamina propria is required)

Prepare 1 mL Dispase II solution per sample;

Add 2 mg/mL Dispase II to FACS buffer.

1.4.3.2 Isolation of mucosal tissues from the mouse oral cavity.

1. Euthanize mice;
2. Using sharp tissue scissors, cut between the lower incisors to separate both sides of the mandible;
3. Immobilize each side of the mandible with needles on a pad to access the oral cavity;

Table 13. Necessary Equipment

Equipment	Company	Purpose
Sharp tissue scissors	Hammacher HSB 088-14 (51754511)	Cutting between the lower incisors and the palate
Fine small tissue scissors	Hammacher HSB 390-10 (51807020)	Isolation of the buccal tissue; Cutting up the tissues in 1.5 mL Eppendorf tubes
Surgical splinter forceps	Hammacher HSC 553-11	Separation of the gingival tissue from the teeth
24-well plate	Thermo Fisher Scientific Inc.	Storage of oral tissues
1.5 mL Eppendorf tubes	SARSTEDT AG & Co. KG	Digestion of oral tissues
50 mL tubes	Greiner bio-one	Centrifugation of cell suspensions
70 μm filters for 50 mL tubes	Greiner bio-one	Generation of single-cell suspensions from oral tissues
Centrifuge Z 446 K	HERMLE Labortechnik GmbH	Centrifugation of 50 mL tubes and V-bottom plates
Thermoshaker	Laboratory Technology Buddeberg	Shaker & incubator for tissue digestion
CASY Model TT	Roche Diagnostics	Cell counting
96-well V-bottom plate	Greiner bio-one	Sample preparation for flow cytometry

4. Cut out the tongue (Fig. 4, blue circle) and remove the muscle from the tissue;
5. Store the tongue in a 24-well plate with 1 mL FACS buffer on ice;
6. Use fine scissors to cut out both sides of the buccal mucosa (Fig. 4, red circles) and place them in a 24-well plate with 1 mL FACS buffer on ice;
7. Sharp scissors were used to cut through the soft and hard tissue behind the upper incisors (Fig. 5B);
8. Make an incision posterior to the third molar through the soft and hard tissue (Fig. 5C);
9. Pull down the mandible to access the nasal cavity;
10. To dissect the tissue away from the nasal cavity, use sharp scissors and cut parallel to the palate with one blade in the nasal cavity and the other blade on the side of the molars (Fig. 5D);
11. Repeat step 10 on the other side;
12. Cut out the palatal and the maxillary bone;
13. Cut the palate in the middle (Fig. 5E) and detach the gingival tissue from both parts of the maxilla (Fig. 5F);
14. Using fine scissors, carefully and precisely remove the tissue belonging to the palate and the NALT from the gingiva;
15. Place and store the tissue in 1 mL FACS buffer in a 24-well plate on ice.

1.4.3.3 Preparation of single-cell suspensions from oral mucosal tissues.

1. Transfer the tissues to 1.5 mL Eppendorf tubes and add 200 μl of digestion mix;
2. Cut the tissues into very small pieces using fine scissors (clean the scissors between the samples to avoid cross-contamination);
3. Add 800 μl of digestion mix per sample;
4. Incubate the samples for 20 min on a thermoshaker at 37°C with shaking at 1200 rpm;
5. Add 20 μl of 0.5 M EDTA per sample (final concentration of 10 mM) and incubated for another 10 min at 37°C on a thermoshaker;
6. Pipette the samples up and down several times and pass them through 70 μm cell strainers into 50 mL tubes;
7. Wash the 1.5 mL Eppendorf tubes with 1 mL FACS buffer, vortex, and add it to the cell strainers;
8. Wash the cell strainers with 10 mL FACS buffer;
9. Centrifuge the cells for 5 min at 350 × *g* at 4°C;
10. Discard the supernatant;
11. Resuspend the cells in 500 μl FACS buffer;
12. Count the cells and keep them on ice for further analysis.

1.4.4 *Data analysis*

Examples of flow cytometry analysis of oral LC and DC subsets using the described single-cell preparation are discussed in detail in Section 2.4 "**Flow cytometry analysis of DC subsets in mouse oral mucosa**".

1.4.5 *Pitfalls*

- To analyze subpopulations of rare cell types such as DC, we recommend pooling oral tissues from 2–3 mice per sample.
- Mixing male and female mice should be avoided, as males harbor lower numbers of LC in the oral tissues than females.
- To increase the viability of the cells, keep the samples on ice.
- Sharp scissors are helpful to isolate the tissue.
- Treatment with Dispase II to separate the epithelium and lamina propria can affect the expression of surface markers such as CD103.
- Ensure that all pieces of epithelium are peeled away from the lamina propria to avoid overlapping during the analysis.

1.4.6 *Top tricks*

- It is critical to carefully and precisely remove the NALT, which is located close to the gingiva of the maxilla, to avoid contamination from this leukocyte-rich lymphoid tissue.
- It is also possible to mince the tissue with a scalpel in a petri dish. By cutting the tissue directly in the digestion mix, one can avoid losing cells while transferring them to a tube after cutting.
- Although this has not been necessary for oral mucosal tissues, 2 mM EDTA can be added to the FACS buffer after tissue digestion to avoid cell aggregates and clogging of the FACS instrument.
- The epithelium and lamina propria can be analyzed separately from each other and can be separated prior to collagenase/DNAse digestion. Therefore, incubate the tissues in a Dispase II solution at 37°C:

  - gingiva: 35 min
  - buccal mucosa: 60 min
  - tongue: 70 min

- The epithelium can be detached from the underlying lamina propria under a dissecting microscope (Fig. 6), and both parts can be processed as described in 1.4.3.3.

1.5 Preparation of single-cell suspensions from mouse kidney

1.5.1 *Introduction*

Kidneys remove toxic waste products from the blood and excrete them into the urine. Additionally, they critically control various physiological processes, such as blood ionic composition, pH, osmolarity, and hematopoiesis. Anatomically, the kidney can be divided into two major regions, the cortex and the medulla. The

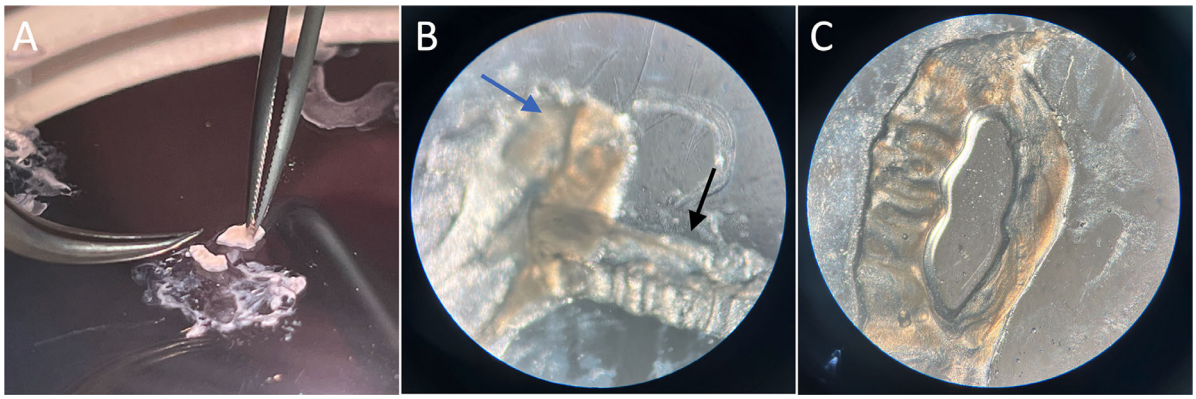

Figure 6. Separation of the epithelium and lamina propria of the gingiva. After incubation with Dispase II solution for 35 min, the epithelium can be detached from the underlying lamina propria using fine forceps (A). Under a dissecting microscope, it is possible to distinguish between the epithelium (black arrow) and the lamina propria (blue arrow) (B). Depiction of the gingival epithelium (C).

cortex extends from the renal capsule to the renal pyramids and contains the major kidney filtration units called glomeruli. In the medulla, the tubules generate a countercurrent system with a high osmotic gradient that concentrates the filtrate [33–36]. Kidney injury, even if temporary, can lead to excess fibrosis, subjecting patients to an increased risk of chronic disease. Despite improved diagnostic techniques that allow for early detection of kidney damage, terminal kidney failure is rocketing worldwide, and few therapies exist to attenuate kidney damage or expedite the healing process. If kidney function cannot sufficiently be recovered, treatment necessitates renal replacement therapy in the form of dialysis or, if possible, a kidney transplant. However, renal replacement therapy is not an efficient solution, as it is time intensive and costly and leaves patients at increased risk of morbidity/mortality [33–36].

Immune mechanisms are centrally involved in the progression of kidney disease and as such provide attractive targets for designing therapeutic strategies to treat kidney disease and failure [33–36]. Mononuclear phagocytes, including macrophages, monocytes and DC, form an intricate network throughout the entire kidney interstitium. While the specific functions of mononuclear phagocyte subsets in kidney pathology remain poorly characterized when compared to other organs, studies in rodents indicate that kidney mononuclear phagocytes can promote but also dampen inflammation and the resulting kidney damage [33–36]. This highlights the need for a better understanding of the specific functions of macrophages, monocytes and DC in kidney pathology. Here, we describe a detailed protocol for the generation of single immune cell suspensions from mouse kidneys for downstream analyses, such as flow cytometry.

1.5.2 *Materials*

1.5.2.1 Reagents. A complete list of reagents and equipment is provided in Tables 14 and 15, respectively.

1.5.3 *Step-by-step sample preparation*

1.5.3.1 Preparation of stocks and solutions.

Collagenase stock solution (10,000 U/mL stock)

Dissolve Collagenase IV (Col IV) in cell culture grade water to reach a final concentration of 10,000 U/mL. Sterile filter the solution through a 0.22 μm membrane and prepare aliquots in Eppendorf tubes. Aliquots can be stored at −20°C for several months. While repeated freeze–thaw cycles should be avoided, we have achieved consistent results after up to 3 freeze thaw cycles.

DNase I stock solution (20 mg/mL stock)

Dissolve DNase I in cell culture water to reach a final concentration of 20 mg/mL. Sterile filter the solution through a sterile 0.22 μm membrane and prepare aliquots in Eppendorf tubes. Aliquots can be stored at −20°C for several months. While repeated freeze–thaw cycles should be avoided, we have achieved consistent results after up to 3 freeze thaw cycles.

Table 14. Reagents, enzymes, chemicals and solutions

Reagent	Manufacturer	Order number
Collagenase IV	Worthington	LS0004189
Deoxyribonuclease I (DNase I)	Roche	11284932001
Hank's Balanced Salt Solution (HBSS) without calcium and magnesium	Sigma	H9394-500ML
Dulbecco's Phosphate Buffered Saline (PBS) without calcium and magnesium	Sigma	D8537-500ML
RPMI	Gibco	31870-074
Fetal Bovine Serum (FCS)	Sigma	F7524
Percoll	Cytiva	17089101

Table 15. Necessary equipment

Equipment	Manufacturer	Steps
Centrifuge 'MULTIFUGE X3R'	Thermo Fisher	Centrifugation steps
Thermo shaker 'INNOVA44'	New Brunswick Scientific	Kidney digestion
Bend head scissors '14059-11' and forceps '11000-12, 11271-30, 11231-20'	F.S.T	Dissection
Bijou vials '129A'	Thermo Fisher	Tissue harvest and digestion
1.2 mL individual reaction tubes 'E1710-0000'	Starlab	To store kidney immune cells suspension
15 mL centrifuge tubes 'ML10535'	Moonlabplastics	Centrifugation
50 mL centrifuge tubes '227261'	Greiner Bio-one	Centrifugation
96well v-bottom plate '277143'	Thermo Fisher	To stain cells suspension with antibody for FACS
23G needle '300800'	BD Microlance	Perfusion
20 mL injector '4606205 V'	B.BRAUN	Perfusion
Serological pipettes of various sizes	Sigma	Pipetting solutions
100μm strainer '43-50070-51'	pluriSelect	Filter digestion suspension
Pasteur pipettes 'PP88SA'	COPAN	Immune cell collection from Percoll

Digestion solution

Prepare a 2× Master mix of Col IV and DNase I in RPMI without FCS and without other additives. A total of 1 mL of 2× master mix is required for each kidney (total digestion volume is 2 mL). For the 2× master mix, a 1:25 dilution of the collagenase stock solution and make a 1:50 dilution of the DNase I stock solution to reach a concentration of 400 U/mL Col IV and 0.4 mg/mL DNase I in the required volume of RPMI.

FACS buffer

PBS containing 1% FCS, 2.5 mM EDTA, and 0.02% sodium azide. No sodium azide must be added when cells are prepared for functional studies, as sodium azide interferes with membrane mobility and will lead to cell death. Sodium azide can be beneficial for the staining intensity of some surface markers, as it interferes with endocytosis.

10% sodium azide stock solution

Prepare a mass:volume 1:10 stock of sodium azide by dissolving the required amount of sodium azide in deionized water.

Isotonic Percoll solution

Adjust the osmolarity of Percoll by adding one part 10x phosphate buffered saline to 9 parts Percoll. This is the 100% Percoll stock. This stock should be kept sterile, as Percoll can easily be contaminated.

Percoll density layers

Prepare 70% Percoll solution by adding 30 mL HBSS phenol red to 70 mL isotonic Percoll solution. For the 37% Percoll layer add 63 mL PBS to 37 mL isotonic Percoll solution. For the 30% Percoll, use HBSS phenol red to reach the desired dilution. Note that a lower volume of the 30% layer is needed, and therefore, the amount of stock solution can be adjusted accordingly.

1.5.3.2 Harvesting kidneys and preparation of single-cell suspensions. Before organ harvest:

- Prepare one Bijou vial with 1 mL RPMI medium (no additives) for each sample. **TIP**: The technique here is described for the harvest of one kidney. However, both kidneys can be harvested to increase cell yield if needed, for instance, for functional analyses.
- Thaw Col IV and DNase I.

1. Perfuse mice immediately after euthanizing them with PBS (using a 26G needle) to eliminate vascular blood content. It is possible that the efficacy of perfusion is improved by adding EDTA or using PBS at room temperature or 37°C. This should be empirically determined. The optimal perfusion site for the kidney is the inferior vena cava, although the whole animal can be perfused if needed. The kidney color will change to yellow ochre upon perfusion;
2. Isolate the kidney and carefully remove the kidney capsule by tugging on the thin layer of tissue surrounding the organ. Place the kidney in a Bijou vial containing 1 mL RPMI and keep on ice until further processing;
3. Use dissection scissors to cut the kidneys into small pieces (the smaller the better);
4. Prepare a 2× Master Mix of Col IV and DNase I in complete RPMI without additives. Add 1 mL of the 2× Master Mix to all samples to reach a final concentration of 200 U/mL Col IV and 0.2 mg/mL DNAse I. A total volume of 2 mL digestion mix can be used for the digestion of one or two kidneys;
5. Incubate at 37°C for 1 hour while shaking at 200–250 rpm in a bacterial shaker;
6. During the incubation time, prepare a 50 mL conical tube with a 100 μm cell strainer for each sample;
7. After 1 hour, the tissue should be sufficiently digested so it can be pipetted up and down using a P1000 pipette and 1 mL filter pipette tips. This step varies slightly depending

on how well the tissue was minced before digestion. **TIP**: If tissue pieces cannot be further broken down by pipetting, consider increasing the digestion time by another 15 min. Then, repeat pipetting;

8. Transfer digested solution to a 100 μm strainer placed on top of a 50 mL conical tube, and use the plunger of a syringe to pass the kidney through the strainer. Wash strainer 2× with 5 mL ice-cold FACS buffer. Fill up the conical tube with FACS buffer;
9. Centrifuge cells at 400 × *g* (ca. 1350 rpm at Rmax) for 5 min at 4°C;
10. A large brown pellet should be visible. Discard the supernatant by decantation. Decant liquid slowly into a waste container and catch the last drops by carefully touching the angled conical tube onto a paper towel. **TIP**: Never place the tube upright and then slant it again, as this will loosen the pellet and lead to cell loss;
11. Drag the bottom of the conical tube carefully over a rough surface such as an Eppendorf rack to loosen the pellet;
12. Resuspend the cells in 4 mL of the 70% Percoll solution and transfer into a 15 mL conical tube. Overlay the cells with 4 mL of 37% Percoll followed by 1 mL of 30% Percoll (Fig. 7). **TIP**: to pour a sharp interface between the layers use a 5 mL serological pipette and place it directly on top of the 70% layer before slowly releasing the liquid (Fig. 7). This will use surface tension to help keep the solutions from mixing;
13. Centrifuge the samples at 900 × g (ca. 2000 rpm at Rmax) for 30 min at room temperature without break/deceleration. Note that this will take some time because no breaking mechanism is active;
14. Remove the 30% top layer using a plastic disposable Pasteur pipette and discard. Then collect the cells at the 70%–37% interface by carefully inserting a fresh plastic Pasteur pipette through the 37% layer until it reaches the 70%–37% interface. Collect cells by slowly releasing pressure from the fingers and sucking liquid into the Pasteur pipette while moving the pipette along the interface. Transfer the contents of the pipette to a new 15 mL conical tube and top up with FACS buffer;
15. Centrifuge the cells and discard the supernatant as above. The cell pellet is now smaller and will stick to the bottom of the tube better so that the liquid can be removed more easily. Resuspend the cell pellet in 0.5–1 mL FACS buffer for further analyses;
16. Count the cells for downstream analysis if necessary. Because kidneys contain many autofluorescent nonimmune cells, it is recommended to count cells via flow cytometry. Leukocytes should be identified based on a live/dead marker in combination with an anti-CD45 antibody and a leukocyte scatter gate. For adult male mice, the leukocyte cell count is on average 120,000 cells/kidney; for adult female mice, it is on average 80,000 cells/kidney. Alternatively, cell numbers can be assessed retrospectively by adding counting beads prior to acquisition of the sample using flow cytometry. For the latter case, we suggest using approximately 1/5th of the total volume of the recovered single cell suspension from two kidneys or approximately half of the total volume of the recovered single cell suspension from one kidney for one FACS staining. This number of cells allows for flow cytometry visualization of most leukocyte populations in steady-state kidneys.

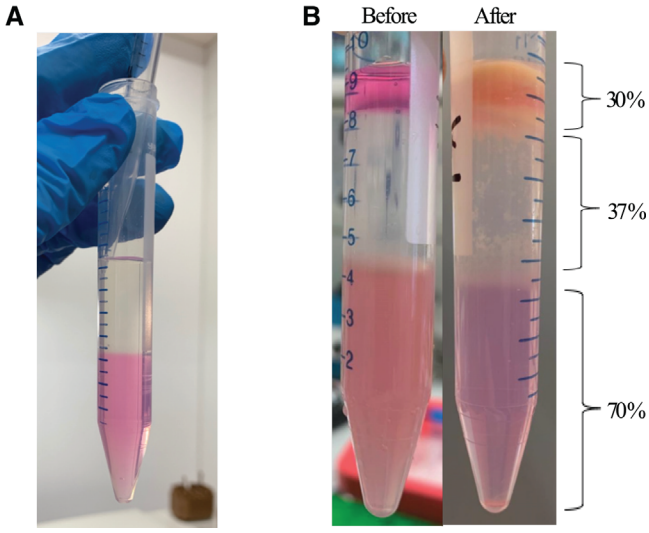

Figure 7. Percoll gradient procedure. (A) Layering the Percoll gradient. The 37% Percoll was overlaid on the top of the 70% Percoll layer by directly placing the tip of the 5 mL serological pipette onto the surface of the 70% Percoll layer (containing the cell suspension). The 37% Percoll solution was slowly released while holding the pipette steady on the surface of the layer (i.e., the pipette tip moves up with the liquid). This method uses surface tension to avoid mixing of the layers. Repeat for the 30% layer. (B) Percoll solution before and after centrifugation. Note the amount of debris that rises to the 30% layer and the cell suspension at the 70–37% interface. The 30% layer containing the debris was removed before harvesting the cells at the 70–37% interface.

1.5.4 *Data analysis*

Examples of flow cytometry analysis of DC subsets in the mouse kidney using the described single-cell preparation are discussed in detail in Section 2.5 "**Flow cytometry analysis of DC subsets in mouse kidney**".

1.5.5 *Pitfalls*

Incomplete perfusion (blood spots visible in kidneys after perfusion)

Perfusion should be performed immediately after euthanizing mice, as clotting of blood can affect perfusion efficiency. Perfusion can be repeated if not all blood can be removed in the first attempt. Perfusion serves to remove cells that are located in the bloodstream and not the interstitium. A separation of blood cells from those located in the interstitium can alternatively be

achieved by injecting a fluorescently labeled anti-CD45 antibody intravenously 2 min before harvesting the organ. This will label blood leukocytes but not those in the interstitium.

Incomplete tissue digestion – tissue still contains unbreakable clumps after digestion

- Consider increasing the digestion time by another 15 min. Then repeat pipetting.
- Cut kidneys into smaller pieces before digestion.
- Try prewarming the enzymatic digestion mix containing collagenase/DNAse immediately before adding to the tissue. This will help the mix reach the optimal 37°C.

The interfaces between the Percoll layers are not sharp

- Prewarm Percoll to room temperature before pouring the gradient.
- To generate a sharp interface between the layers use a 5 mL serological pipette and place it directly on top of underlying layer before slowly releasing the liquid. This will use the surface tension to help keep the solutions from mixing (Fig. 7).

Poor cell recovery

- Check digestion efficiency.
- Cell loss can occur during washing, for instance, when decanting the supernatant if the flipping speed is too slow and the cells in the bottom of the conical tube will become dislodged and be dumped out. This should be visible when performing steps 10 and 15 above. While a liquid suction vacuum pump can in principle be used as an alternative to decantation, we find this is not practical, as the cell pellet before Percoll gradient enrichment is very fragile, and a large volume of liquid must be removed.

Many nonleukocytes in FACS analysis

- Isolating leukocytes from kidneys generates a large amount of debris from structural cells of the kidney, evident as small, autofluorescent debris in FACS analysis. While it is impossible to fully remove these cells, debris can be reduced by removing the 30% Percoll layer before collecting cells at the 70–37% interface. Importantly, when collecting cells at the 70–37% interface, try to only collect cells from the interface without sucking up too much additional volume of the 37% Percoll layer, as this layer will also contain some debris.

1.5.6 *Top tricks*

- The kidney cortex and medulla contain distinct subsets of immune cells; therefore, analyses of single-cell suspensions from the cortex and medulla may be desirable [33, 37]. In this case, kidneys can be cut longitudinally, and medullary tissue can be separated from cortical tissue using a dissection microscope [37]. When perfusion is not used and tissue-resident immune cells are to be distinguished from blood-bourne immune cells by intravenous injection of a fluorescently labeled anti-CD45 antibody, the fluorophore used should be chosen compatible with downstream staining applications.

1.6 Preparation of single-cell suspensions from mouse mammary glands

1.6.1 *Introduction*

The mammary gland is a secretory organ composed of a network of ducts that secrete milk proteins during lactation. The mammary gland develops in phases, starting during embryogenesis when a rudimentary ductal tree is formed [38]. At puberty, ducts start to elongate and bifurcate, giving rise to a highly branched ductal network that fills up the whole fat pad they reside in. Pregnancy and lactation represent another phase of major remodeling and expansion, as alveolar structures develop at the end of the ducts that produce and secrete milk proteins. When lactation ends, the mammary gland reverts to its prepregnancy state via a process called involution, which is accompanied by massive cell death. This amazing remodeling capacity makes the mammary gland a very dynamic organ.

The ducts of the mammary gland are lined by an epithelial bilayer, with an inner layer of luminal and an outer layer of basal epithelial cells (Fig. 8A). The luminal cells consist of hormone receptor-positive and hormone receptor-negative cells and differentiate during pregnancy into milk-producing lobuloalveolar structures. The basal cells are contractile myoepithelial cells. The ducts are embedded in fat pads, which further contain fibroblasts, adipocytes and vascular cells and are generally referred to as stroma. In addition, various immune cells are present in the mammary gland stroma, including innate immune cells such as macrophages, eosinophils and mast cells, as well as B and T lymphocytes. Importantly, the interaction between immune cells and epithelial cells is essential for mammary gland development and function and occurs via the production of growth factors and cytokines [39, 40]. As such, immune cells contribute to the various phases of tissue remodeling in the mammary gland. Several studies have reported the presence of classical dendritic cells (cDC) in the mammary gland [41–43]. However, the composition, phenotype and function of DC subsets at the various phases of tissue remodeling are poorly understood.

This protocol describes the digestion of the mouse mammary gland in two steps. In the first step, the stromal tissue is homogenized, releasing most immune cells. In a second step, the remaining ducts are digested into single cells. cDC1 and cDC2 are enriched in the stromal fraction, whereas the ductal fraction contains many epithelial cells and epithelium-associated ductal macrophages. Mice have 5 pairs of mammary glands, numbered mammary gland 1 (MG1) to MG5, with MG1 closest to the head. For the analysis, mostly MG4 and MG3 are used (Fig. 8B). They

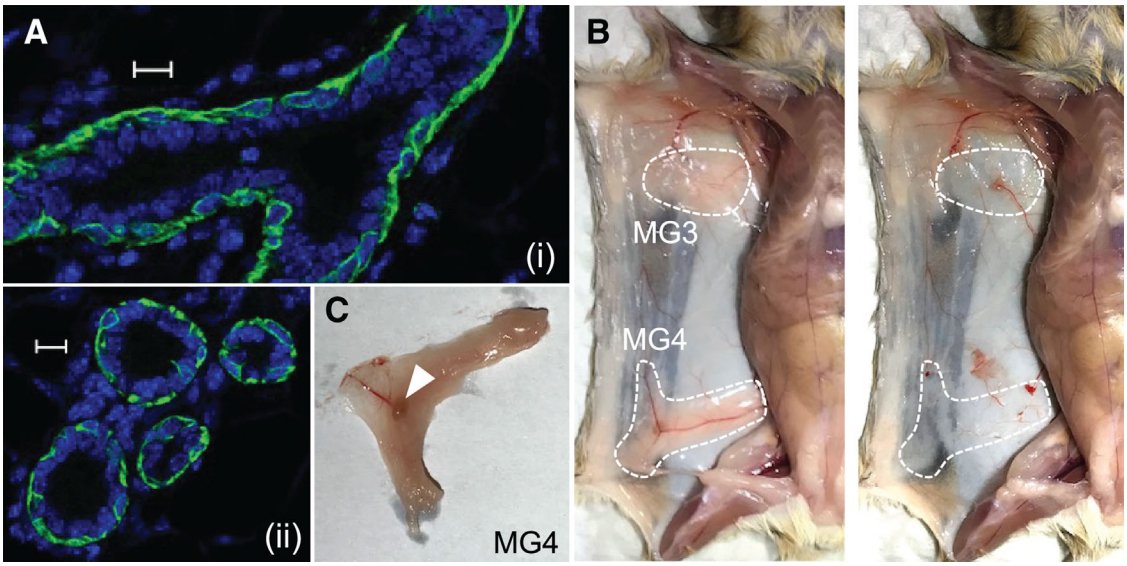

Figure 8. Structure, location, and dissection of mouse mammary glands. (A) MG consists of a network of ducts, which are lined by an epithelial bilayer, as shown by confocal imaging. Three-micrometer sections of formalin-fixed, paraffin-embedded MG4 were stained with DAPI (blue) and α smooth muscle actin (aSMA, green). aSMA is expressed by basal myoepithelial cells, not by the luminal epithelium, as shown in longitudinal (i) and cross sections (ii). Scale bars represent 10 μm. (B) Mammary glands are embedded in fat pads, which allows localization of the glands. Mammary gland numbers 3 and 4 (MG3 and MG4) are indicated, and left and right images are taken before and after dissection, respectively. (C) Dissected MG4 with inguinal lymph nodes (arrowhead). If the tissue is digested for flow cytometry, the lymph node should be removed.

can be easily dissected and remain intact when opening the skin, which is particularly important when tissue is prepared for histological purposes (Fig. 8C). For flow cytometry, tissue is digested and homogenized, and thus parts of other MGs could be included as well.

1.6.2 *Materials*

1.6.2.1 Reagents. A complete list of reagents is provided in Table 16.

1.6.2.2 Equipment. The necessary equipment is listed in Table 17.

1.6.3 *Step-by-step sample preparation*

1.6.3.1 Preparation of stocks and solutions.

Calcium chloride ($CaCl_2$) stock solution

Prepare a 1 M stock solution of $CaCl_2$ by dissolving salts in double-distilled H_2O. Optionally, sterile filter the stock solution via a 0.22 μm filter membrane and store at room temperature.

DNase I

Dissolve Deoxyribonuclease I (DNase I) in HBSS to reach a final concentration of 2000 Units/mL. Avoid vortexing. Optionally, sterile filter the solution through an 0.22 μm membrane. Prepare aliquots and store at −20°C. Right before use, thaw one aliquot on ice. Avoid freeze-thaw cycles.

Collagenase IV

Dissolve Collagenase NB 4G (Col IV) in HBSS to reach a final concentration of 34 Units/mL. Optionally, sterile filter the solution through an 0.22 μm membrane. Prepare aliquots and store at −20°C. Right before use, thaw one aliquot on ice. Avoid freeze-thaw cycles.

Table 16. Reagents, enzymes, chemicals and solutions*

Reagent	Manufacturer	Ordering Number
Enzymes		
Collagenase NB 4G Proved Grade	Nordmark Biochemicals	S1746502
Deoxyribonuclease I (DNase I)	Worthington	LS006330
Chemicals & Solutions		
Hank's Balanced Salt Solution, with $CaCl_2$ and $MgCl_2$ (HBSS)	Gibco	14025-050
Dulbecco's Phosphate Buffered Saline (PBS), no calcium, no magnesium	Sigma	D8537
Calcium chloride ($CaCl_2$)	Roth	HN04.3
Bovine Serum Albumin (BSA)	Sigma	A8806
Fetal Bovine Serum (FBS)	Gibco	10270106
UltraPure 0.5 M EDTA, pH 8.0	Thermo Scientific	15575020

* Reagents can be purchased from other vendors.

Table 17. Necessary equipment*

Equipment	Company	Purpose
Centrifuge "Heraeus megafuge 16 series"	Thermo Scientific	Centrifugation of 15 mL tubes
Thermomixer type C	Eppendorf	Shaking and mixing of 2 mL reaction tubes during tissue digestion
Microcentrifuge Eppendorf 5424	Eppendorf	Centrifugation of 2 mL reaction tubes
Microscope "Primovert Series", with Axiocam 208 color camera	Zeiss	Observation of cells and acquisition of images
Surgical scissors (#14101-14)	Fine Science Tools	Surgical scissor for cutting skin
Forceps (#11051-10)	Fine Science Tools	Dissecting mammary gland
Disposable scalpel No 22, with blade	Feather	Dissecting mammary gland
Fine sharp scissors (#14060-11)	Fine Science Tools	Mincing mammary gland tissue
SafeSeal 2 mL reaction tube (#72.695.500)	Sarstedt	Digestion of tissue
Falcon 15 mL Conical Centrifuge Tubes	Fisher Scientific	Centrifugation of cell suspensions
Falcon 50 mL Conical Centrifuge Tubes	Fisher Scientific	Centrifugation of cell suspensions
PipetteBoy	Integra	Pipetting
Serological pipettes 5 mL (#606180)	Greiner bio-one	Pipetting
Serological pipettes 10 mL (#607180)	Greiner bio-one	Pipetting
Micropipettes	Eppendorf	Pipetting
Pipette tips	Greiner bio-one	Pipetting
40 μm filters for 50 mL tubes (#542040)	Greiner bio-one	Filtration of cell suspensions
Microlance 3 needle 23G (#300800)	BD	Fixation of mouse paws and skin
Microlance 3 needle 20G (#301300)	BD	Tissue homogenization
Insulin syringe without needle (#9161798 V)	BBraun	Tissue homogenization
Cellstar petridish 35 × 10 mm (#627160)	Greiner bio-one	Resuspension of ducts
Whatman® Filter Unit 0.2 μm, FP 30/0.2 CA-S	GE Healthcare	Sterile filtration

* Equipment can be purchased from other vendors.

Digestion buffer

Prepare digestion buffer by adding 2 mM $CaCl_2$ and 2% (w/v) BSA to HBSS. Optionally, sterile filter the solution through a 0.22 μm membrane. Store at 4°C.

Digestion solution

Freshly prepare digestion solution by diluting DNase I and Collagenase NB 4G 1:100 in digestion buffer. Pre-warm to 37°C right before use.

Staining buffer

Prepare PBS containing 0.5% FBS (v/v) and 2.5 mM EDTA.

1.6.3.2 Harvesting mammary glands.

1. Euthanize mouse;
2. Fix the paws with needles;
3. Spray the fur on the ventral side with 70% ethanol;
4. Open the skin on the ventral side from the abdomen to the upper thorax using surgical scissors;
5. Cut the skin alongside the four limbs until the paws using the same scissors;
6. Expose the mammary glands by detaching the skin from the abdominal wall; spread out the skin and fix it with needles (Fig. 8A);
7. To dissect mammary glands, gently lift up the end of the MG with forceps and start detaching the MG from the skin by carefully pushing a scalpel between the MG and the skin, moving the scalpel toward the body of the mouse;
8. Transfer the mammary glands into 2 mL reaction tubes, one gland per tube;

Notes:

- When MG4 is used for flow cytometry, first remove the inguinal lymph node;
- Include as little as possible connective tissue when cutting the MG from the skin.

1.6.3.3 Generation of single-cell suspensions from mammary gland tissue.

1.6.3.3.1 Stromal tissue.

1. Add 1 mL of prewarmed (37°C) digestion solution to each reaction tube;
2. Mince the tissue as fine as possible by cutting it with surgical scissors;
3. Digest the tissue at 37°C in a thermomarine for 15 min while shaking at 900 rpm;

4. Pipette the digestion mix several times up and down with a 1 mL micropipette (cut off a few mm of the tip);
5. Digest further at 37°C as in step 3 for 15 min;
6. Homogenize tissue by passing it several times through a 20G needle attached to a 1 mL syringe;
7. Transfer the suspension into a 15 mL tube containing 10 mL staining buffer, and wash the reaction tube with 1 mL staining buffer and to the 15 mL tube;
8. Centrifuge at 350 × *g* and 4°C for 6 min;
9. Start by removing the top fat layer, then remove the rest of the supernatant;
10. Resuspend the pellet in 10 mL staining buffer;
11. Centrifuge again for 6 min at 350 × *g* and 4°C;
12. Resuspend the pellet in 10 mL staining buffer;
13. Pass the suspension over a 40 μm cell strainer;
14. Store the flowthrough on ice.

General remarks:

- Digesting more glands in one tube is possible, but digestion time will increase. We digested a maximum of two mammary glands in one tube when glands were derived from younger mice. Mammary glands from older mice contain more fat, and in this case, we do not recommend digesting more than one MG per tube.

Specific remarks:

- To step 6: this should go easily, if tissue clumps remain, further digestion is needed;
- To step 7: at this point, all digested mammary glands of one mouse can be combined;
- To step 9: on top of the buffer, a large fat layer has formed and has to be removed before removing the rest of the supernatant;
- To step 11: all fat should be removed, and the supernatant should be clear; if this is not the case, additional washing steps must be included;
- To step 13: the flowthrough is enriched in cells of the MG stroma, which include DC. At this stage, ducts are mostly not digested and are retained on the cell strainer.

1.6.3.3.2 Ducts.

1. Put the cell strainer of step 13 of the previous section in a 3 cm dish;
2. Wash the ducts off the strainer with 1 mL staining buffer using a micropipette and transfer this solution with the resuspended ductal particles to a 15 mL tube;
3. Repeat this 2 more times;
4. Centrifuge at 350 × *g* and 4°C for 6 min;
5. Resuspend the pellet in 1 mL freshly prepared, prewarmed digestion solution and transfer to a 2 mL reaction tube;
6. Incubate at 37°C in a thermomarine for 30 min while shaking at 900 rpm;
7. Homogenize tissue by passing it several times through a 20G needle attached to a 1 mL syringe;
8. Filter over a 40 μm cell strainer, rinse the reaction tube with 1 mL staining buffer and pass over the cell strainer;
9. Store the flowthrough on ice.

Remarks

- To step 1: push the cell strainer quite firmly onto the dish to avoid buffer leaking through;
- To step 2: ducts are visible as floating particles in the solution and can be visualized under a microscope;
- To step 7: after homogenization, most ductal particles should have disappeared. This can be checked under a microscope: the solution should contain mostly single cells, while some small aggregates might remain. If the pieces of ductal tissue are too large, digestion should be carried out further.

1.6.4 *Data analysis*

Flow cytometry data analysis of DC subsets detected in the single-cell suspension obtained with this digestion protocol is covered in detail in Section 2.6 "**Flow cytometry analysis of DC subsets in mouse mammary glands**".

1.6.5 *Pitfalls*

Problem: Low cell viability
Potential solutions:

This digestion protocol is aimed at recovering immune cells from the mammary gland. The mammary gland contains many epithelial cells, which are rather sensitive to the tissue digestion procedure. If viable epithelial cells are needed, other means of digestion might be applied [44]. Several specific digestion protocols and solutions exist that warrant viable epithelial cells afterwards. How well these procedures generate immune cells and in particular DC is not clear and should be tested.

If too many immune cells are dead, the conditions should be adjusted. Digestion duration should not be too long, and tissue should be processed as soon as possible after dissection. Enzyme concentration and activity, mostly collagenase, also affect cell viability. With each new batch or with enzymes from different vendors, the optimal duration and collagenase concentration should be tested, as enzymatic activity might vary from batch to batch. Activity that is too low will require long digestion times, and activity that is too high affects viability.

Problem: Low cellular yields
Potential solutions:

It is important to verify whether tissue digestion is complete. This can be done by checking the digestion mix under the microscope. If too much tissue is left undigested and discarded, the cell number will drop. This protocol uses one MG per reaction tube. In theory, more mammary glands can be combined, either in a 2 mL reaction tube or in a 50 mL tube. However, the efficiency of tissue digestion will be different and should be checked very carefully.

An excessively long digestion time also has a negative effect on cell yields.

Mammary glands are fat pads, and thus, during digestion, a large amount of fat is released. It is important to remove the fat as much as possible and to wash the digest until the supernatant is completely clear. Additionally, when digestion is performed, the cells are immediately washed to remove the fat, and the whole digest is not placed on ice. This will cause the fat to solidify, which is something to avoid.

1.6.6 *Top tricks*

This protocol describes the digestion of mammary glands in two steps: first, the stromal tissue is digested, and then, the remaining ducts are digested. Although the ducts will always take longer to digest than the stroma, it is not necessary to split these two fractions, and MG can be digested in total. However, the $CD11c^{hi}$ $MHC\text{-}II^{hi}$ fraction in the mammary gland is composed of macrophages and cDC. By splitting stromal and ductal fractions, $CD11c^{hi}$ $MHC\text{-}II^{hi}$ cDC will be enriched in the stromal fraction, and $CD11c^{hi}$ $MHC\text{-}II^{hi}$ ductal macrophages will be enriched in the ductal fraction (see also "**Flow cytometry analysis of DC subsets in mouse mammary glands**").

1.7 Preparation of single-cell suspensions from transplantable mouse melanoma

1.7.1 *Introduction*

During recent decades, new treatment options for melanoma, the most aggressive type of skin cancer, have been approved. They range from specific inhibitors against constitutively active, mutated $BRAF^{V600E}$ to the application of immune checkpoint blockades to release the tumor-internal breaks against the immune system [45–47]. Nevertheless, there is still a need for new therapies and combinations thereof to overcome resistance development. A promising approach is to harness the immune system to efficiently and durably fight cancer. However, before we think of a target cell population, we need a more thorough understanding of immune cells infiltrating the tumor. To understand the melanoma immune infiltrate, many different mouse melanoma models have been developed. These models can be divided in general into humanized and nonhumanized models, which can be further subdivided into carcinogen-induced tumors, genetically engineered mouse models and transplantable tumors [48]. Transplantable or syngeneic mouse models, which are the focus of this protocol, are the most commonly used melanoma models in research [48–50]. In fact, studies that have led to major breakthroughs in oncoimmunology, such as the identification of immune checkpoint blockade, the investigation of immunogenic cell death as the main reason for the success of certain chemotherapeutics and the beneficial effect of combination therapy over monotherapies, have relied on transplantable tumor models [48].

The transplantable melanoma models in mice are established by subcutaneous injection of a histocompatible tumor cell line into the flank skin. Within days, a tumor becomes palpable and can easily be monitored. In addition, tumor growth was relatively consistent between mice injected with the same cell line. There are many cell lines used for transplantable melanoma models, namely, B16 and D4M.3A, SM1WT1, and YUMM1.7. The B16 cell line was established approximately 60 years ago from a chemically induced tumor in C57BL/6 mice [51]. Since then, a range of B16 variants have been generated, for example, the highly metastatic B16.F10 [51, 52] or the B16.OVA expressing the model antigen ovalbumin to facilitate the investigation of T-cell immunity [53]. B16 melanoma cell lines express the common melanoma antigens glycoprotein 100 (gp100) and tyrosinase-related protein 2 (TRP-2), which facilitates the investigation of immunotherapies with known tumor antigens [54, 55]. Notably, B16 cells do not have an activating BRAF mutation or a deletion of PTEN, which is in contrast to the genetic alterations observed in human melanoma [56]. However, there is the strong argument that immune therapies in B16 melanomas have the predicted efficacy as observed in the clinics, and therefore, the model is regarded as useful for preclinical studies [54]. In 2014, the Dartmouth Mouse Mutant Malignant Melanoma (D4M.3A) cell line was generated by the Constance Brinkerhoff group [57]. To generate this cell line, $Tyr::CreER;Braf^{CA};Pten^{lox/lox}$ mice were backcrossed onto C57BL/6 mice. From the tumors grown in these mice, a stable cell line was generated, which harbors the $BRAF^{V600E}$ mutation and shows a loss of the tumor suppressor PTEN, a mutation that is present in approximately 50% of human melanoma patients [58]. Due to the BRAF mutation, D4M-derived tumors are sensitive to BRAF inhibitor treatment and even develop resistance mechanisms similar to those of patients [57]. In 2013, Knight and colleagues generated the SM1WT1 cell line using an in vivo passaging protocol of the SM1 cell line in male C57BL/6 mice [59]. SM1 cells were derived from a spontaneously arising tumor in a transgenic mouse model expressing the $BRAF^{V600E}$ mutation in melanocytes, which were subsequently in vivo passaged in NSG and C57BL/6 mice [60]. In addition to the BRAF mutation, SM1 tumors harbor a CDKN2A deletion and microphtalmia-associated transcription factor (MITF) overexpression [58]. The YUMM1.7-cell line was derived from transgenic $BRAF^{V600E}Pten^{-/-}CDKN2A^{-/-}$ mice on a C57BL/6 background [61]. In this protocol section, we describe the cell culture and transplantation of the B16, D4M.3A and SM1WT1 cell lines, as these are the cell lines we mainly work with. For other models, such as the YUMM1.7-cell line, we refer to the literature.

1.7.2 *Materials*

1.7.2.1 Reagents. A complete list of reagents is provided in Table 18.

1.7.2.2 Equipment. The necessary equipment is listed in Table 19. Information on the tumor cell lines is given in Table 20.

Table 18. Reagents, enzymes, chemicals and solutions

Reagent	Manufacturer	Ordering Number
Cell culture		
Accutase cell detachment solution	Sigma–Aldrich	SCR005
Dulbecco's Modified Eagle Medium (DMEM) high glucose with 4500 mg/L glucose, L-glutamine, sodium pyruvate and sodium bicarbonate	Sigma	D6429
Iscove's Modified Dulbecco's Media (IMDM)	PAN-Biotech	P04-20150
Gentamicin	Gibco	15750045
Geneticin 418 (G418)	Genexxon	M3118.0050
Roswell Park Memorial Institute (RPMI)1640	Lonza	12-167Q
L-glutamine	Lonza	BE17-605E/U1
BioWhittaker®Pen-Strep (5000 U/mL Pen; 5000 μg/mL Strep)	Lonza	DE17-602E
Enzymes for tumor digestion		
Collagenase D	Roche Diagnostics	11088858001
Deoxyribonuclease I (DNase I)	Sigma-Aldrich	DN-25
Chemicals & Solutions		
Hank's Salt Solution (HBSS) without calcium and magnesium, without Phenol red	Pan-Biotech	L2045
Dulbecco's Phosphate Buffered Saline (PBS) without calcium and magnesium	Gibco	14190-094
BSA (Albumin bovine Fraction V)	SERVA	11930
AccuGENETM 0.5 M EDTA Solution	Lonza AccuGene	51201
Trypan blue	Sigma	T8154-100ML
FBS Supreme – South America Fetal bovine serum (FCS)	PAN-Biotech	P30-3031

1.7.3 *Step-by-step sample preparation*

1.7.3.1 Preparation of stock solutions and culture medium.

D4M.3A culture medium

DMEM was supplemented with 5% heat-inactivated FCS, 50 U/mL penicillin and 50 μg/mL streptomycin. Store at 4°C for a maximum of 3 weeks.

B16.OVA culture medium

IMDM medium was supplemented with 10% heat-inactivated FCS, 0.01% gentamicin, and 1% G418/Geneticin (for selection of transfected tumor cells). Store at 4°C for a maximum of 3 weeks.

SM1WT1 culture medium

RPMI medium was supplemented with 10% heat-inactivated FCS, 10 mM L-glutamine and 50 μg/mL gentamicin. Store at 4°C for a maximum of 3 weeks.

DNase I

To prepare the 10 mg/mL stock solution, deoxyribonuclease I (DNase I) was dissolved in 100 mL of 5 mM calcium chloride

Table 19. Necessary equipment

Equipment	Company	Purpose
Sharp fine scissors	Aesculap	For sagittal and lateral incisions to open mouse
Fine forceps	Aesculap	Hold the skin during dissection
Curved tweeers	Aesculap	Carving out tumor
Cellstar Cell culture flasks	Greiner Bio-one	For tumor cell culture
Corning storage bottle (#430518) and 0.22 μM sterile filter (#431118)	Corning	Sterile filter FCS
50 mL tubes	Greiner bio-one	Centrifugation of cell suspensions
2 mL Syringe	BD	Mesh tissue through cell strainer
100 μm filter for 50 mL tubes (#542000)	Greiner bio-one	Filter tumor cell suspension
Centrifuge Heraeus Multifuge 3 S-R	Heraeus	Centrifugation of 50 mL tubes and V-bottom plates
Incubator	Thermo Scientific	Tumor cell culture
Shaking waterbath	GFL	For tumor tissue digestion
Neubauer chamber 0.100 mm; 0.0025 mm^2	Superior Marienfeld	Cell counting with hemocytometer

Table 20. Information on mouse tumor cell lines

Name	Short description	Source
B16.OVA	Mouse melanoma cell line (pigmented)	Kind gift from Dr. Edith Lord, University of Rochester, Rochester, USA [53]
D4M.3A	Nonpigmented mouse melanoma cell line, BRAFV600E mutation and PTEN loss	Kind gift from Constance E. Brinckerhoff, Department of Biochemistry, Norris Cotton Cancer Center, Geisel School of medicine at Dartmouth, Lebanon, NH, USA [57]
SM1WT1	Mouse melanoma cell line, BRAFV600E mutation	Kind gift from Prof. Mark J. Smyth, QIMR Berghofer Medical research institute, Brisbane, Australia [59]

($CaCl_2$). Sterile filter the solution through a sterile 0.22 μm Stericup and store aliquots at −20°C.

Collagenase D

The 40 mg/mL stock solution is prepared by dissolving 500 mg collagenase D in 12.5 mL Hank's balanced salt solution (with Ca^{2+} and Mg^{2+}). Sterile filter the solution through a sterile 0.22 μm membrane and store aliquots at −20°C.

10% BSA/PBS

Dissolve 50 g of bovine serum albumin (BSA) in 500 mL PBS (can also be heated up to 40°C while stirring) and filter it through a 0.22 μm Stericup.

Würzburger Buffer

Add 50 mL of 10% BSA/PBS, 5 mL 0.5 M AccuGENE EDTA Solution, and 1 mL DNAse was added to a 500 mL bottle of PBS. Store at 4°C for several weeks.

1.7.3.2 Culture of mouse melanoma cell lines.

Thawing cells

1. Warm up 20 mL culture medium in a 50 mL tube;
2. Thaw cells for 30 sec at 37°C;
3. Pipette thawed cells into the prewarmed culture medium (see 1.7.3.1. Preparation of stocks and solutions) and wash the cryotube using 1 mL of culture medium;
4. Spin down at 485 × g for 5 min;
5. Remove the supernatant and resuspend the cell pellet in 10 mL culture medium;
6. Culture cells in 75 cm^2 flask (in 10 mL) or 175 cm^2 (in 20 mL respective medium);
7. Check the flask the next day and change medium (if there are too many dead cells).

Split cells

1. At approximately 60–80% confluency, remove medium and wash cell layer with 10 mL PBS;
2. Add Accutase to remove cells from flask:
   - for 25 cm^2 flask: 1 mL
   - for 75 cm^2 flask: 2 mL
   - for 175 cm^2 flask: 3 mL;
3. Detach cells by incubation for 3 min at 37°C;
4. Agitate flask gently and check under the microscope if cells are detached;
5. Add 10 mL of medium to stop the enzyme reaction and gently pipette the cells up and down in the flask to disrupt the cell clusters;
6. Transfer the cells into a 50 mL tube and wash the flask with another 10 mL medium;
7. Spin down at 458 × g for 5 min;
8. Remove supernatant and resuspend cell pellet in 5–10 mL culture medium depending on the cell density;
9. Count cells (maximum 5–10% dead cells);
10. Seed cells into cell culture flasks according to Table 21.

1.7.3.3 Subcutaneous injection of tumor cells.

1. 1×10^5 B16.OVA, 3×10^5 D4M.3A or 5×10^5 SM1WT1 cells were resuspended in 100 μl PBS per mouse;
2. Cells are injected subcutaneously (s.c.) into the flank skin;
3. As soon as tumors are palpable, tumor growth can be monitored using a digital caliper by measuring the shortest and longest diameters of the tumor.

Table 21. Cell density for seeding into culture flasks

Name	Area	Cell numbers (for 2–3 days of culture)
B16.OVA	75 cm^2	3×10^5
D4M.3A	25 cm^2	1×10^5
	75 cm^2	3×10^5
	175 cm^2	6×10^5
SM1WT1	75 cm^2	3×10^5

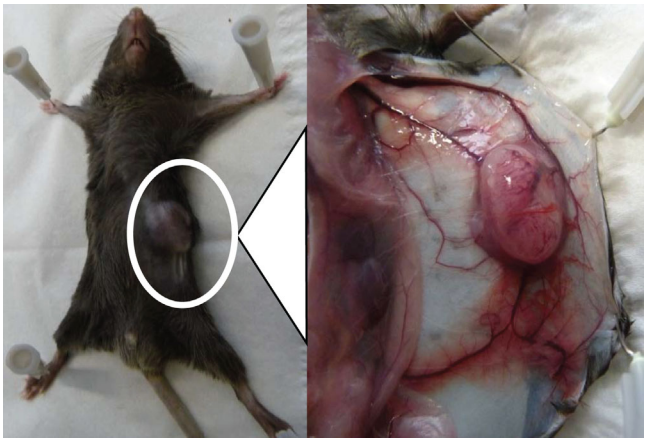

Figure 9. Dissection of a mouse bearing a transplantable melanoma. Left picture: tumor visible on the left flank (white circle). Right picture: View of the subcutaneous tumor.

1.7.3.4 Harvest tumors and preparation of single-cell suspension.

1. Euthanize mouse;
2. Spray mouse with 70% ethanol before you start dissecting tumor;
3. Open the mouse with scissors through a sagittal incision followed by lateral incisions towards the hind limbs;
4. Separate the skin from the underlying layer to reveal the subcutaneous tumors;
5. Remove the tumor with curved tweezers (Fig. 9);
6. Transfer the tumor into a small petri dish (60 × 15 mm) or a 6-well plate filled with 5 mL digestion buffer (Hanks' salt solution without Mg^{2+} and Ca^{2+} containing 2% FCS);
7. Cut the tumor into smaller pieces using scissors and curved tweezers;
8. Transfer the tumor piece suspension into a 50 mL tube;
9. Wash the petri dish with 5 mL digestion buffer → 50 mL tube containing 10 mL digestion buffer with tumor tissue;
10. Add 250 μg/mL collagenase D and 120 μg/mL DNase to the 10 mL digestion buffer with tumor tissue;
11. Incubate for 45 min at 37°C in a shaking water bath;
12. Stop digestion by adding 500 μl EDTA to a final concentration of 10 mM;
13. Cell suspension is pipetted through a 100 μm cell strainer into a 50 mL falcon tube, and the plunger of a syringe is used to press tissue through the cell strainer;
14. Wash the cell strainer with 30 mL Würzburger buffer;
15. Centrifuge the samples at 485 × g for 5 min at 4°C, and discard the supernatant;
16. Resuspend the cell pellet in 2 mL Würzburger buffer;
17. Count all cells.

1.7.4 *Data analysis*

Tumor area can be calculated by multiplying the length and the width of the tumor and is analyzed over the whole time of the experiment. An example for flow cytometry data analysis of intratumoral DC subsets using the described single-cell preparation is presented in detail in Section 2.7 "**Flow cytometry analysis of DC subsets in transplantable mouse melanoma**".

1.7.5 *Pitfalls*

Tumor cell culture

Thaw a new batch of tumor cells for every tumor cell transplantation and split the cells at least 2–3 times before transfer into mice. DO NOT let the cells grow too dense as tumor cells start to differentiate when the cell layer becomes confluent.

Tumor cell injection

Do not inject the tumor intradermally as tumors grow superficially and can ulcerate, meaning that these mice will have to be removed from the experiment. The tumor should also not be injected too deep as they can grow intraperitoneally. Check if there is bubble formation indicative of subcutaneous placement of tumor cell suspension.

Tumor digestion

Remove fat covering the tumor before starting the cutting procedures to avoid cell loss. To allow for optimal digestion ensure that the tumor is disrupted into tiny pieces. After digestion and during washing steps ensure that no fat layer has formed on the supernatant. If so, carefully reduce the supernatant below the fat layer, fill the tube again with Würzburger buffer and repeat centrifugation.

1.7.6 *Top tricks*

- Note that the immune infiltrate differs between transplantable melanoma models.
- Filter the cells a second time using a 40 μm cell strainer if the tumor digest contains cell aggregates.

2 Flow cytometry analysis of DC subsets in mouse nonlymphoid tissues

2.1 Flow cytometry analysis of DC subsets in mouse skin

2.1.1 *Introduction*

Dendritic cells (DC) are important initiators of tolerance and immunity. To ensure immune surveillance, DC act as sentinels at the frontier to the environment. For this reason, DC are lodged at high frequencies at interfaces between the body and environment, such as the skin. In general, DC subsets in healthy

Table 22. Reagents, antibodies, chemicals and solutions

	Manufacturer	Ordering Number
Dulbecco's Phosphate Buffered Saline without calcium and magnesium	Sigma	D8537
BSA (Albumin bovine Fraction V)	Serva	11930
0.5 M EDTA (Ethylenediaminetetraacetic acid solution)	Sigma	03690
anti-FcγRIIB/III (clone 2.4G2)	Biolegend	101302
anti-FcγRIV (clone 9E9)	Biolegend	149502
eFluor-780 fixable viability dye (eF780)	eBioscience	65-0865-14
Pluronic™ F68	ThermoFisher	24040032
Histofix 4%	Roth	P087.1
Precision Count Beads™	Biolegend	424902

skin comprise Langerhans cells (LC) positioned in the epidermis, dermal conventional DC and monocyte-derived cells. To gain an overview of those cells, skin tissue can be analyzed using flow cytometry. For this purpose, the mouse skin needs to be dissociated to obtain a single cell suspension, and the digestion protocol is described in detail in Section 1.1 "**Preparation of single-cell suspensions from mouse skin**".

In the following, we describe a detailed staining protocol for mouse skin tissue and guidelines for downstream data analysis of flow cytometry data. Several gating strategies have been described for flow cytometry analysis of DC subsets in healthy mouse skin. These studies focused either on the delineation of subsets of conventional DC (cDC) [62] or on the identification of monocyte-derived cells [5]. Here, we provide a novel multicolor staining panel, allowing for both the identification of cDC subsets and monocyte-derived cells using these previously published gating strategies. Furthermore, our panel allows the identification of the mononuclear phagocyte subsets in mouse skin through unsupervised clustering algorithms. To make the panel suitable for the analysis of inflamed or infected skin, several markers for inflammatory cell types, such as granulocytes, were included.

2.1.2 *Materials*

2.1.2.1 Reagents. A complete list of reagents is provided in Tables 22 and 23.

2.1.2.2 Equipment. The necessary equipment and cytometer configuration are listed in Tables 24 and 25.

2.1.3 *Step-by-step sample preparation*

2.1.3.1 Preparation of Buffers.

Live/dead dye solution

Dilute fixable viability dye 1:1000 in PBS.

FACS buffer

Supplement PBS with 0.5% BSA (v/v) and 2 mM EDTA.

Table 23. Reagents and antibodies used for flow cytometry analysis

Laser	Specificity	Fluorochrome	Clone	Manufacturer	Catalog #	Final dilution
488 nm	CD64	PerCP-eF710	X54-5/7.1	eBioscience	46-0641-82	1:500
561 nm	CD26 (DPP-4)	PE	H194-112	Biolegend	137803	1:200
	CD326 (EpCAM)	PE Dazzle	G8.8	Biolegend	118235	1:2000
	CD90.2	PE-Cy5	30-H12	Biolegend	105314	1:300
	CD19	PE-Cy5	6D5	Biolegend	115510	1:500
	NK1.1	PE-Cy5	PK136	Biolegend	108716	1:500
	CD172a (SIRP α)	PE-Cy7	P84	Biolegend	144007	1:300
637 nm	F4/80	APC	BM8	Biolegend	123115	1:500
	CD11c	APC-R700	N418	BD	565872	1:500
	Viabilty dye eF780	APC-Cy7	–	eBioscience	65-0865-14	1:1000
405 nm	SiglecF	BV480	E50-2440	BD	746668	1:500
	Ly-6C	BV570	HK1.4	Biolegend	128029	1:500
	CD11b	BV605	M1/70	BD	563015	1:500
	XCR1	BV650	ZET	Biolegend	148220	1:300
	PDCA1	BV711	927	BD	747604	1:300
	Ly-6G	BV750	1A8	BD	747072	1:500
	MHC-II (MHC class II)	BV786	M5/114	BD	742894	1:2000
355 nm	CD24	BUV395	M1/69	BD	744471	1:1000
	CCR2	BUV496	475301	BD	750043	1:250
	CD45	BUV805	30-F11	BD	748370	1:1000

Table 24. Necessary equipment

Item	Company
96-well U shape plate	Greiner Bio One
1.5 mL or 2 mL reaction tube	Eppendorf
5 mL FACS tubes	Sarstedt
15 mL or 50 mL canonical tube	Sarstedt
Serological pipettes (5 mL/10 mL/25 mL)	Greiner Bio-One
Centrifuge	Heraeus Multifuge 3 L
Incubator 37°C	Sanyo
Vibrating Platform shaker Titramax 100	Heidolph
Symphony 5 laser flow cytometer (filter setup see Table 25)	BD

Table 25. Data acquisition setup: Configuration of Symphony 5 laser flow cytometer

Laser line	Filter Longpass	Filter Bandpass	Fluorochrome
488 nm	685 LP	710/50 BP	PerCP-efl710
561 nm	570 LP	586/15 BP	PE
	600LP	610/20 BP	PE-Dazzle
	635 LP	670/30 BP	PE-Cy5
	750 LP	780/60 BP	PE-Cy7
637 nm	650 LP	670/30 BP	APC
	685 LP	730/45 BP	APC-R700
	750 LP	780/60 BP	APC-Cy7
405 nm	505 LP	525/50BP	BV480
	550 LP	586/15 BP	BV570
	595 LP	605/40 BP	BV605
	635 LP	677/20 BP	BV650
	685 LP	710/20 BP	BV711
	735 LP	750/30 BP	BV750
	750 LP	780/60 BP	BV786
355 nm		379/28 BP	BUV395
	450 LP	515/30 BP	BUV496
	690 LP	735/30 BP	BUV737
	770 LP	810/40 BP	BUV805

Staining buffer

Mix Pluronic™ F68 in a ratio 1:100 in FACS buffer. For immunofluorescent staining of cells. Pluronic™ F68 is used as a detergent within the staining buffer in order to prevent fluorescent dye interactions when applying multiparametric staining panels.

Fc-Receptor blocking solution

Dilute Anti-FcγRIIB/III 1:133 (final concentration 1:400) and anti-FcγRIV 1:133 (final concentration 1:400) in staining buffer. Blocking of Fc-Receptors before staining prevents nonspecific binding of staining antibodies via their Fc-part.

Fixation buffer

Dilute 4% Histofix 1:1 in PBS to obtain a solution of 2% Histofix.

2.1.3.2 Isolation and preparation of single-cell suspensions from mouse skin. In Section 1.1 "**Preparation of single-cell suspensions from mouse skin**", we provide a detailed protocol on how to isolate cells from whole mouse skin tissue as well as from epidermis and dermis seperately for analysis by flow cytometry.

2.1.3.3 Antibody staining of single-cell suspensions from mouse skin for flow cytometry.

1. Per staining, the cells from at least one mouse ear should be used to identify rare DC subsets. Transfer the single cell suspension of each sample into a U-shaped 96-well plate. In the following, the indicated volumes refer to one well;
2. Pellet the cells by centrifugation at 674 × *g* for 2 min at 4°C and discard the supernatant;
3. Resuspend the cells in 200 µl of PBS per well, centrifuge at 674 × *g* for 2 min at 4°C, and discard the supernatant;
4. Resuspend cells in freshly prepared 50 µl Live/Dead dye solution;
5. Incubate for 5 min at 4°C;
6. Use FACS buffer to fill each well with 200 µl to remove unbound viability dye. Centrifuge the plate at 674 × *g* for 2 min at 4°C, and discard the supernatant;
7. Resuspend the cells in 20 µl of Fc receptor blocking solution and incubate for 10–30 min at 4°C. Prepare the staining antibody mix as follows:
8. Add 20 µl of antibodies against CCR2, diluted in staining buffer to three times the final concentration indicated in Table 24;
9. Incubate for 30 min at 37°C;
10. Add 20 µl of a mix of antibodies against all surface markers (except anti CCR2, which has already been added in the previous step), diluted in staining buffer to three times the final concentrations indicated in Table 24;
11. Incubate for 30 min at 4°C;
12. Use FACS buffer to fill each well with 200 µl to remove unbound antibodies. Centrifuge the plate at 674 × *g* for 2 min at 4°C, and discard the supernatant;
13. Wash the cells two times more by adding 200 µl of FACS buffer, centrifuge the plate at 674 × *g* for 2 min at 4°C and discard the supernatant;
14. Resuspend the cells well in 100 µl fixation buffer. Keep in the dark at 4°C for 10 min;
15. Use FACS buffer to fill each well with 200 µl to remove the fixation buffer. Centrifuge the plate at 674 × *g* for 2 min at 4°C, and discard the supernatant;
16. Wash cells again by adding 200 µl of FACS buffer and centrifuging the cells at 674 × *g* for 2 min at 4°C, and discard the supernatant;
17. Resuspend cells in 120 µl of FACS buffer and keep in the dark at 4°C until analysis using a 5 laser cytometer (the suggested filter setup is shown in Table 25);
18. Optional: Add the required amount of Precision Count Beads™ (Cat# 424902 Biolegend) to count absolute num-

bers of cells within each sample. Ensure that FSC and SSC are adjusted accordingly. Counting beads are excited by a variety of lasers (405 nm, 488 nm, 562 nm, 633 nm).

2.1.4 *Data analysis*

Data acquisition was performed using a five-laser BD Symphony (excitation: 355 nm, 405 nm, 488 nm, 561 nm, 637 nm) equipped with the respective emission filter setup shown in Table 25. Using FlowJo® software Version 10.8.1, immune cell populations within the mouse skin were identified through the application of the gating strategies shown in Fig. 10. In the following, a detailed description of two published gating strategies [5, 62] is provided.

In the first step of data analysis, cell debris, doublets and dead cells (eF780$^+$) were excluded. The resulting cell population was divided into its CD45$^+$ and CD45$^-$ subsets. CD45 is utilized as a marker for bone marrow-derived cells and used to remove stromal cells such as keratinocytes and fibroblasts (CD45$^-$). From the resulting viable CD45$^+$ cell population, T cells (CD90.2$^+$), NK cells (NK1.1$^+$) and B cells (CD19$^+$) were excluded. Furthermore, neutrophils (CD11b$^+$ Ly-6G$^+$), eosinophils (CD11b$^+$ SiglecF$^+$) and plasmacytoid DC (pDC, PDCA1$^+$ Ly-6C$^+$) were excluded. Note that in healthy skin, there are very few pDC [63]. The final population of this preprocessing step was named 'no pDC'. This set can be further analyzed using two different gating strategies. The gating strategy C1 was established by Guilliams et al. and breaks down subsets of DC in general [62]. In contrast, with the help of the gating strategy C2 published by Tamoutounour, cells derived from monocytes are specified in detail [5]. For the latter strategy, one minor adaptation was undertaken to identify LC more specifically among other CD11b-positive cells.

In C1, first, macrophages (CD64$^+$ F4/80$^+$; 'Mac') were excluded based on their expression of F4/80 and CD64. The remaining F4/80$^-$ population was then further analyzed regarding differential MHC-II expression, as DC are positive for MHC-II. Among those MHC-II$^+$ cells, CD11c$^-$ CD26$^-$ cells were excluded; subsequently, cDC and LC represent the remaining set. By utilizing the markers XCR1 and CD172a/SIRP α, the unique XCR1-expressing cDC1 population (XCR1$^+$ CD172a$^-$) was identified. Among the XCR1$^-$ CD172a$^+$ cells, LC (CD24$^+$ CD26$^-$) and cDC2 (CD24$^-$ CD26$^+$) were identified based on the markers CD24 and CD26.

The gating strategy C2 focuses on monocyte-derived cell populations. In contrast to the original strategy, we exclude LC immediately after the initial gating steps (A and B). LC were excluded based on their subset-specific marker combination CD24$^+$ CD326/EpCAM$^+$ from the nonpDC population. Then, we followed the gating as described previously [5, 64]: The cells can be further resolved into myeloid (CD11b$^+$) and nonmyeloid (CD11b$^-$) cells. Among the CD11b$^+$ cells, cDC2 (Ly-6C$^-$ CD64$^-$) were identified based on the absence of the surface molecules Ly-6C and CD64. Non-cDC2 were then subdivided based on CCR2 and CD64. CCR2 is used to discriminate between two monocyte-derived cell subsets. The CCR2$^+$ compartment comprises skin-infiltrating Ly-6C^{high} monocytes and originating cells belonging to the "monocyte waterfall". After tissue entry, monocytes (P1: Ly-6C^{high} MHC-II^{low}) develop through an intermediate state (P2: Ly-6C$^+$ MHC-II$^+$) into monocyte-derived DC moDC (P3: Ly-6C^{low} to MHC-II^{high}) sharing characteristics with DC [5, 65]. However, depending on environmental stimuli, monocytes are also able to develop into tissue resident macrophages. In contrast to monocytes and moDC, tissue resident macrophages express neither CCR2 nor Ly-6C. Among the CCR2$^-$ cells, two macrophage subsets are defined based on the surface expression of MHC-II molecules: MHC-II^{low} macrophages (P4) and MHC-II^{high} macrophages (P5) [5, 65, 66].

In the previous section, subsets were identified by manual gating strategies such as C1 and C2, as shown in Fig. 10. Since an increasing number of fluorochromes have become available, multiparametric flow cytometry has become increasingly popular and requires alternative approaches for data analysis. Gating manually relies on 2D scatter plots, and the number of possible plots increases exponentially with an increasing number of parameters, which in turn makes manual gating more ambiguous and more error prone. To overcome this issue, a new visualization technique, called FlowSOM, using self-organizing maps was introduced in 2015 [67]. This algorithm was applied to the same dataset of 60,000 lineage-positive cells from the mouse skin, which was analyzed by manual gating before, using the FlowSOM plugin in FlowJo. FlowSOM populations were aligned with the previously described populations in Fig. 10 (see Table 26) and were assigned to those populations based on their respective marker expression. Using our novel staining panel for mouse skin tissue, we identified 12 populations based on similarity in surface marker expression (Fig. 11).

In a multicolor dataset, each stained marker represents one dimension within the set. To obtain an overview of the data, so-called dimensional reduction algorithms allow the visualization of multiparametric datasets in a two-dimensional space. Using these techniques, the distances between certain cells in the 2D plot represent their relative similarity regarding their marker expression assessed via flow cytometry. In this way, certain cells belonging to one cell population are clustered close together, and each subset appears as a distinct island within the plot. These clusters can then be annotated using a subset-specific color code (see legend of Fig. 12). Here, we visualized the lineage-positive cell population of mouse skin cells using t-SNE (t-distributed stochastic neighborhood embedding - FlowJo plugin by Van Der Maaten et al. [68]) or UMAP (Uniform Manifold Approximation and Projection - FlowJo plugin by McInnes and Healy et al. [69]). In UMAP, the global structure of the datasets is more preserved in contrast to t-SNE, since the proximity of the clusters to each other also reflects their similarity among each other.

Fig. 12 highlights some advantages and disadvantages of unsupervised clustering over conventional gating. For example, the eosinophil population identified via FlowSOM includes the whole island, whereas not all cells in this group are correctly assigned as eosinophils using manual gating. However, rare

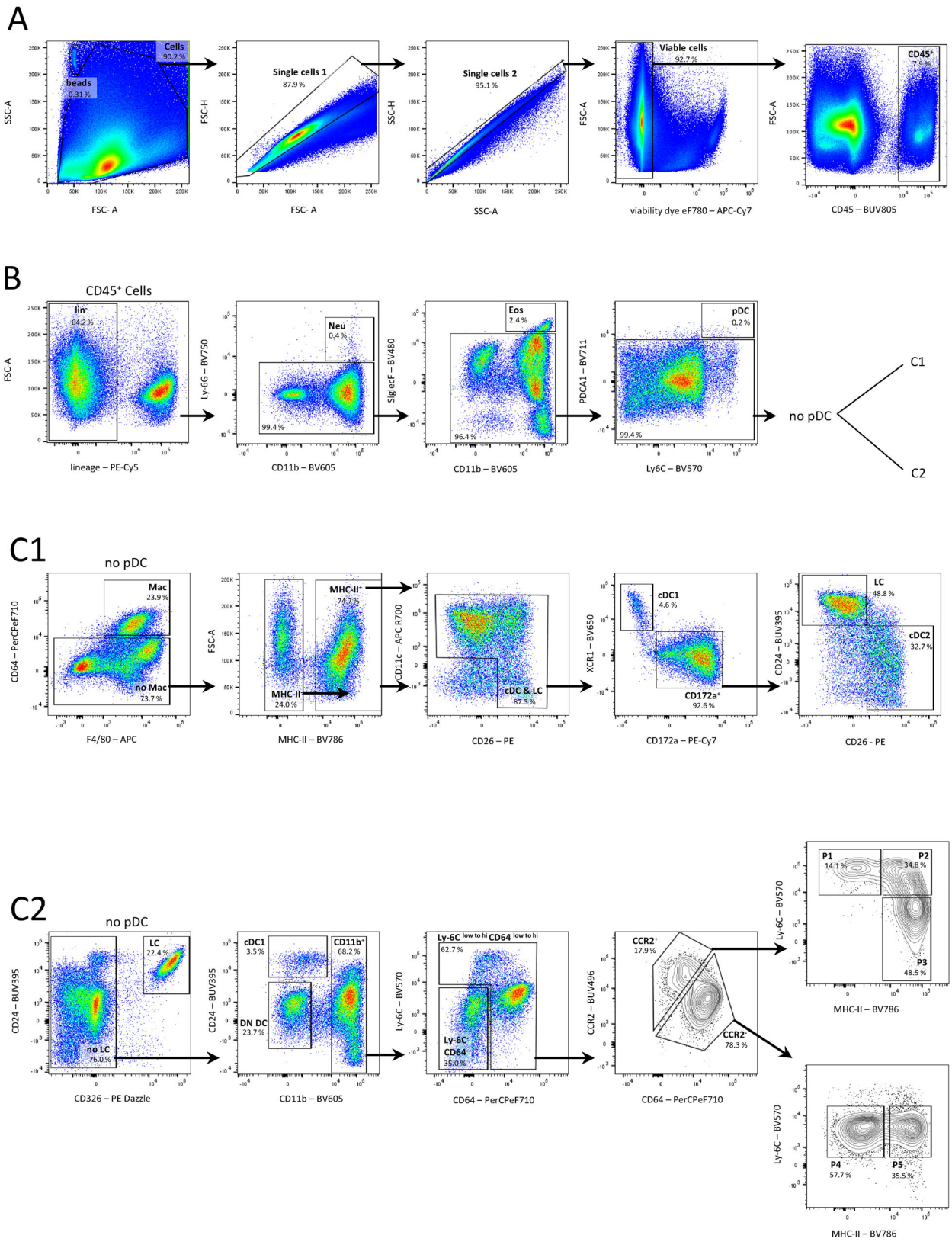

Figure 10. Gating strategy for flow cytometry panel on mouse skin. Ear skin tissue of female wild-type mice (C57BL/6J, 10 weeks old) was enzymatically digested to generate a single-cell suspension. The suspension was stained according to the protocol described here. Representative flow cytometry data of two ears and their analysis are shown. After preprocessing of the dataset (A, then B), two complementary gating strategies (C1 and/or C2) were applied. (A) In the first step, cell debris, doublets, dead cells (eF780$^+$), and stromal cells (CD45$^-$) were excluded. (B) In the

Table 26. Summary of marker expression on analyzed $CD45^+$ cell populations

Population	surface marker
NK-cell	$NK1.1^+$
T-cell	$CD90.2^+$
B-cell	$CD19^+$
Neutrophil	$NK1.1^-$, $CD90.2^-$, $CD19^-$, $CD11b^+$ $Ly6G^+$
Eosinophil	$NK1.1^-$, $CD90.2^-$, $CD19^-$, $CD11b^+$ $SiglecF^+$
Plasmacytoid DC (pDC)	$NK1.1^-$, $CD90.2^-$, $CD19^-$, $PDCA1^+$
Langerhans cell (LC)	$NK1.1^-$, $CD90.2^-$, $CD19^-$, $F4/80^+$, MHC-II^+, $CD11c^+$, $CD26^-$, $CD11b^+$, $CD172a^+$, $XCR1^-$, $CD24^+$, CD326/$EpCAM^+$
Monocyte	$NK1.1^-$, $CD90.2^-$, $CD19^-$, Ly-$6C^+$, Ly-$6G^-$, $F4/80^-$, $CCR2^+$, $CD64^{inter\ to\ +}$, MHC-II^-
Macrophage	$NK1.1^-$, $CD90.2^-$, $CD19^-$, Ly-$6C^+$, Ly-$6G^-$, $F4/80^+$, $CD11b^+$, $CCR2^-$, $CD64^+$, MHC-$II^{low\ to\ high}$
Melanophages	$NK1.1^-$, $CD90.2^-$, $CD19^-$, Ly-$6C^+$, Ly-$6G^-$, $F4/80^+$, $CD11b^+$, $CCR2^-$, $CD64^+$, MHC-$II^{low\ to\ high}$, SSC^{high}
Monocyte derived DC (moDC)	$NK1.1^-$, $CD90.2^-$, $CD19^-$, Ly-$6C^{inter\ to\ low}$, Ly-$6G^-$, $CD64^{inter\ to\ +}$, $F4/80^-$, $CCR2^+$, MHC-$II^{inter\ to\ high}$
Conventional DC type 1 (cDC1)	$NK1.1^-$, $CD90.2^-$, $CD19^-$, Ly-$6C^-$, Ly-$6G^-$, $F4/80^-$, $CD64^-$, MHC-II^+, $CD11c^+$, $CD26^+$, $CD11b^-$, $CD172a^-$, $XCR1^+$
Conventional DC type 2 (cDC2)	$NK1.1^-$, $CD90.2^-$, $CD19^-$, Ly-$6C^-$, Ly-$6G^-$, $F4/80^-$, $CD64^-$, MHC-II^+, $CD11c^+$, $CD26^{low\ to\ high}$, $CD11b^+$, $CD172a^+$, $XCR1^-$
Double negative conventional DC (DN cDC)	$NK1.1^-$, $CD90.2^-$, $CD19^-$, Ly-$6G^-$, $CD326^-$, $CD24^-$, $CD11b^-$

populations are more easily missed when using FlowSOM instead of manual gating, e.g., neutrophils have been assigned to the eosinophil population. In contrast, manual gating delineates those two populations correctly. This can be improved by adjusting the FlowSOM settings, e.g., increasing the number of meta clusters. In another situation when analyzing populations with very similar marker expression properties, FlowSOM seems to be more beneficial for data analysis because all markers are taken into account. In this process, it does not matter whether a suitable gating strategy is available. For example, using the marker CD26 allowed us to distinguish cDC2 from monocyte-derived DC and CD26 was suggested to be included in the minimal set of phenotypic markers to identify cDC, which appear as the $CD26^+$ subset [70]. In summary, accuracy for the annotation of flow cytometry datasets can be achieved using FlowSOM clustering followed by "semisupervised" assignment of cell types to FlowSOM populations based on expression patterns identified using manual gating strategies ideally applied to the same dataset before. In summary, we provide a ready-to-use protocol for the analysis of DC subsets in mouse skin allowing individual adaptation of the staining panel and the application of different approaches for data analysis.

2.1.5 *Pitfalls*

Problem: lack of sensitivity in certain channels

Potential solutions: check cytometer setup for possible changes in the filter system (see Table 25 filter used for detection of fluorochrome).

Problem: Macrophages are not present in the sample

Potential solutions: Use backgating to check if viable lin^- $CD45^+$ cells were accidentally lost during early gating steps. Macrophages appear relatively high in SSC and FSC values (those values depend on how you adjusted the SSC and FSC sensitivity). Make sure to adjust your gates and settings regarding FSC and SSC voltages accordingly. In the mouse skin of a C57BL*/6J* background, so-called melanophages (SSC-A^{high} $CD24^{low}$

next step, the remaining hematopoietic-derived cell ($CD45^+$) lineage-negative cells, meaning T cells (CD90.2), NK cells (NK1.1) and B cells (CD19), were removed. Then, neutrophils ($CD11b^+$ Ly-$6G^+$), eosinophils ($CD11b^+$ $SiglecF^+$) and pDC ($PDCA1^+$ $Ly6C^+$) among the resulting lineage-positive cells were excluded. The remaining population was named 'no pDC' and was further analyzed using the gating strategy C1 or C2. (C1) The gating strategy C1 represents the analysis of DC subsets as shown previously by Guilliams et al. [62]. Using this approach, dermal macrophages ($CD64^+$ $F4/80^+$), cDC1 ($XCR1^+$ $CD172a^-$), LC ($CD24^+$ $CD26^-$) and cDC2 ($CD24^-$ $CD26^+$) were identified. (C2) With the help of the gating strategy, C2 cells derived from monocytes are specified as described by Tamoutounour et al. [5], we included one additional gate to exclude LC, identified based on their CD24 and CD326/EpCAM expression, from the $CD11b^+$ gate. Subsequently, the following populations were identified: LC ($CD24^+$ CD326/$EpCAM^+$), cDC2 ($CD11b^+$ Ly-$6C^-$ $CD64^-$), skin infiltrating monocytes (P1: $CCR2^+$ Ly-$6C^{high}$ MHC-II^{low}), intermediate state subset (P2: $CCR2^+$ Ly-$6C^+$ MHC-II^+), monocyte-derived DC moDC (P3: $CCR2^+$ Ly-$6C^{low}$ to MHC-II^{high}), dermal MHC-II^{low} macrophages (P4: $CCR2^-$ Ly-$6C^-$ MHC-II^{low}) and MHC-II^{high} macrophages (P5: $CCR2^-$ Ly-$6C^-$ MHC-II^{high}). lin-, lineage-negative cells; Neu, neutrophils; Eo, eosinophils; pDC, plasmacytoid dendritic cells; Mac, macrophages; cDC1, conventional dendritic cells type 1; cDC2, conventional dendritic cells type 2; LC, Langerhans cells; DN cDC, double-negative conventional dendritic cells; P1–P5, populations as described previously by Tamoutounour et al.

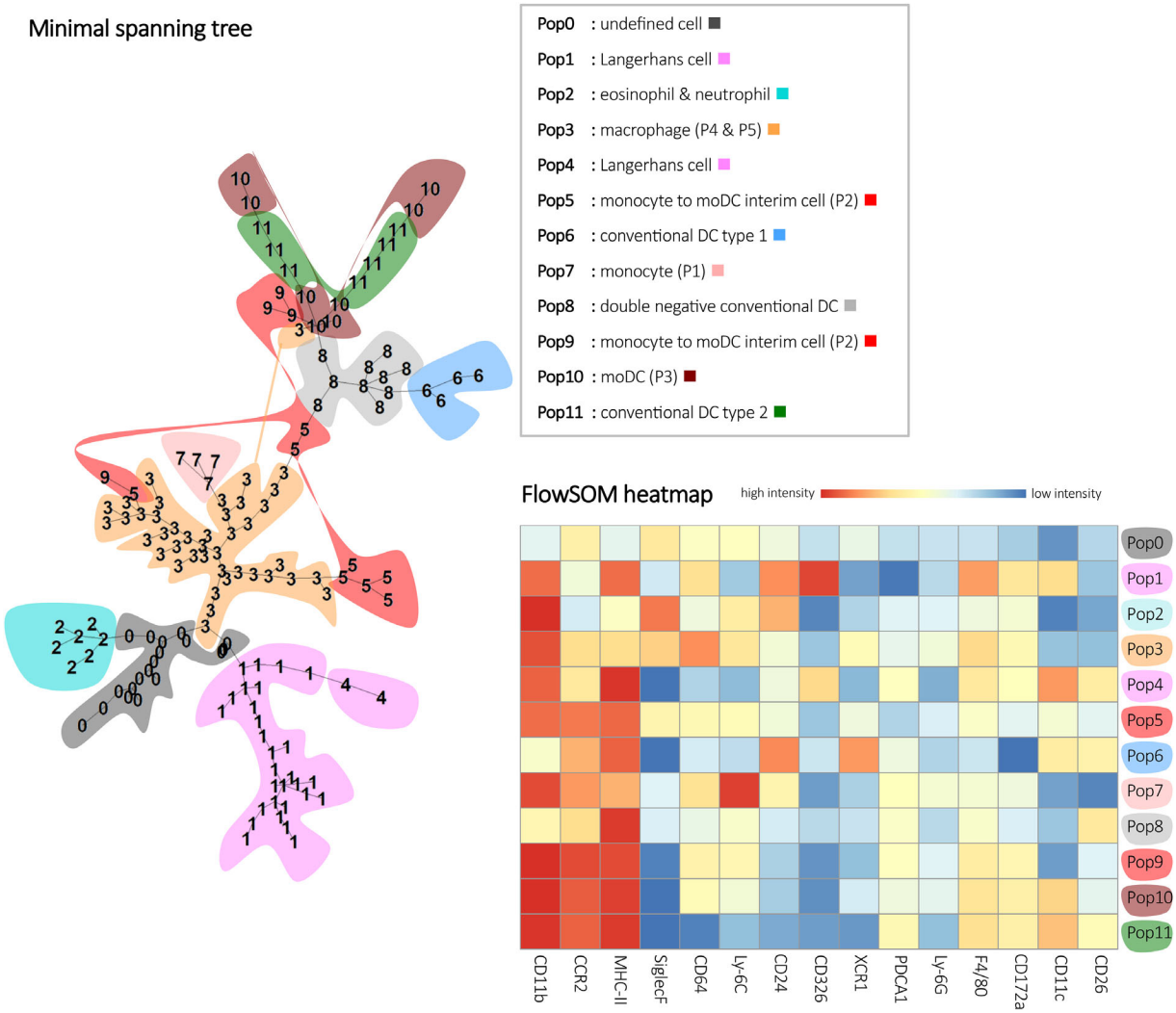

Figure 11. FlowSOM of mouse DC subsets in healthy skin using an 18-parameter flow cytometry panel. After manual pregating on no debris, singlets, eF780$^-$, and CD45$^+$ cells, 60,000 events of lin$^-$ (CD90.2-, NK11-, CD19-) cells were analyzed by FlowSOM using the FlowJo plugin (15 parameter, metacluster 12). All surface markers except those already used in the pregating (eF780, lineage, CD45) were included in the analysis. The minimum spanning tree of the 12 FlowSOM population is shown. Based on the marker expression shown in the FlowSOM heatmap, each FlowSOM population (Pop0-11) was manually assigned to a certain cell type shown in the legend. Those ten cell populations were then used for annotation of the UMAP and t-SNE plot.

CD11b$^+$CD64$^+$ CCR2$^-$MHC-II$^{-\text{ to }+}$) have been identified, which are SSC-A^{high} and are easily left uncharacterised due to gating on SSC-A^{low} cells [64]. These melanophages can be identified based on gating C2, as indicated in Fig. 10, and they appear in gates P4 and P5 due to their macrophage-like phenotype. The respective backgating of P4 and P5 in SSC-A versus FSC-A is shown in Fig. 13. In particular, the MHC-II^{low} subset of melanophages, which are identified as P4, shows a very high granularity (SSC-A^{high}).

Problem: Some cells seem to be false positives for some markers.

Potential solutions: Fc-receptor blocks should be used before the application of staining antibodies to prevent nonspecific binding, which is important if working with cells expressing many Fc-receptors [71]. Additionally, serum of the stained antibody host species could be added to prevent nonspecific binding. Prepare unstained samples, fluorescence minus one control (FMO) or isotype control to assess the respective background of each channel, e.g., autofluorescence could be an issue.

2.1.6 *Top tricks*

Eartags on mice

When working with ear skin tissue, ear-tagged mice can show different results compared to untouched ears. Try to use alternative mouse tagging methods for genotyping/individual identification, e.g., *phalanx distalis* removal.

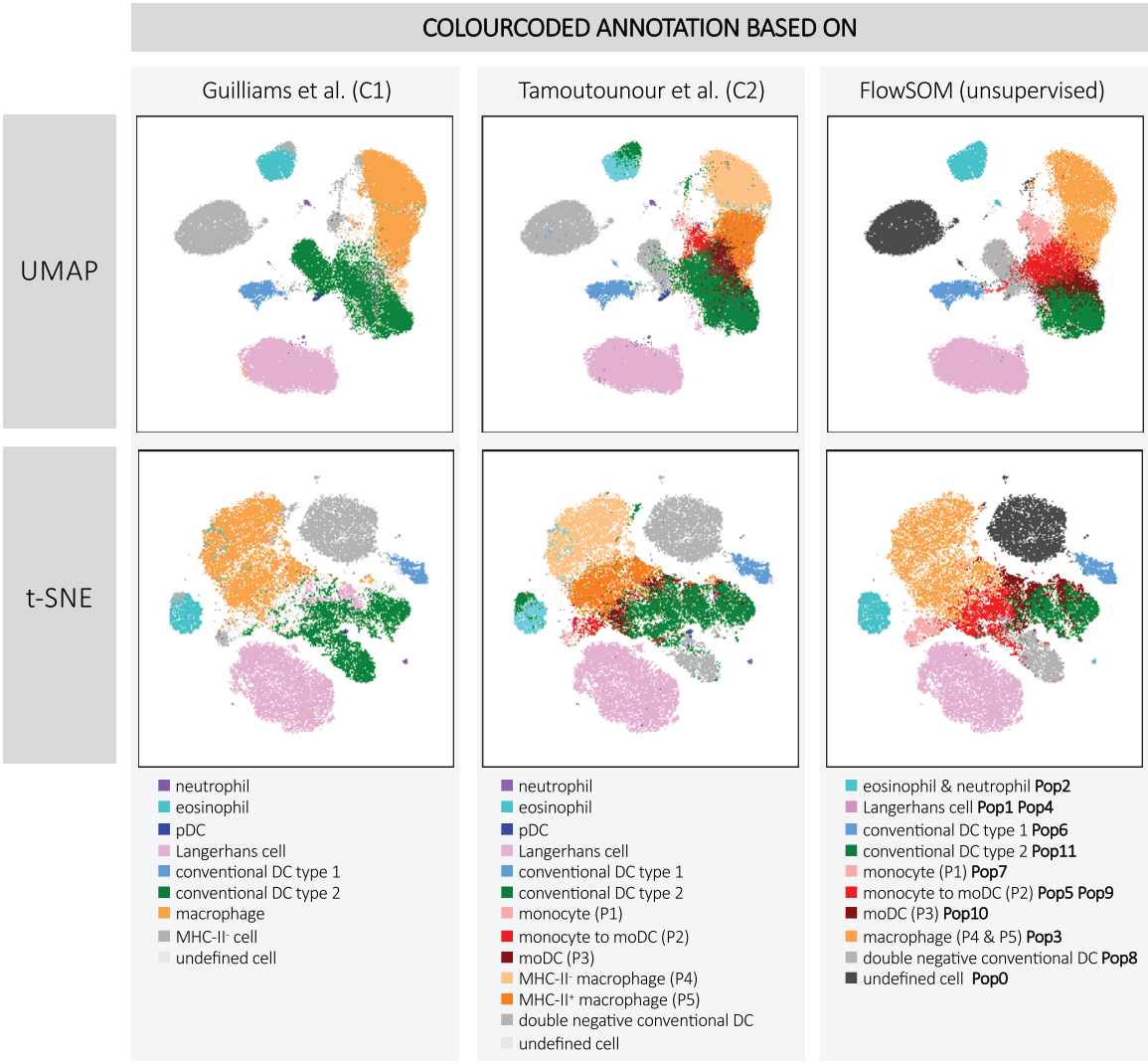

Figure 12. Comparison of data analysis methods for DC subsets in mouse skin tissue. Ear skin tissue of female wild-type mice (C57BL/*6J*, 10 weeks old) was enzymatically digested to generate a single-cell suspension. The suspension was stained according to the protocol as described; thus, the panel allows the identification of DC subsets, among others. Representative flow cytometry data of two ears and their analysis are shown. Per t-SNE (15 parameter, 1000 iterations, 30 perplexity, 4423 eta) or UMAP (15 parameter, Euclidean, nearest neighbor 15, minimal distance 0.5, components 2) plot 60,000 of lin$^+$ (CD90.2$^-$, NK11$^-$, CD19$^-$) cells (pregating on no debris, singlets, efl780$^-$, CD45$^+$ cells) are shown. Either data analysis occurred by manual gating using the respective strategies (C1 and/or C2), or unsupervised clustering based on FlowSOM (15 parameter, metacluster 12) was performed. Identified cell populations are annotated within the plot by using a subset-specific color code (see legend).

Obtaining precise absolute cell numbers per ear

Use Precision Count Beads^{TM} (Cat# 424902 Biolegend) to count the absolute numbers of cells within each sample. See optional step 13 of the staining protocol. Ensure that FSC and SSC are adjusted to allow visualization of beads. An example of how to precisely gate on beads is shown in Fig. 14. To discriminate beads from cells, their characteristic properties (SSC-A^{high} FSC-A^{low}) in size and granularity (first gate: FSC-A versus SSC-A) are used. In addition to the fact that counting beads are excited by a variety of lasers (405 nm, 488 nm, 562 nm, 633 nm), PE Dazzle and APC were used to identify the excited beads (second gate: PE Dazzle versus APC). In this way, the identification of the beads is improved, and in turn, the number of beads per sample is more precise.

Add another layer of information: epidermal or dermal cells/lymph node influx

Dermal and epidermal cells can be separately analyzed; please see Section 1.1.3.3.2 Preparation of single-cell suspensions of epidermis and dermis separately. Additionally, DC subsets in the skin draining lymph node can be identified analogously to the resident skin populations. Furthermore, we recommend using CCR7 as an additional marker to distinguish between migratory and resident DC subsets. Migratory DC are CCR7$^+$, whereas resident DC are CCR7$^-$. CCR7 can be easily integrated into the staining panel using anti-CCR7 in BUV737 (clone 4B12, BD, Cat.741892, final concentration 1:250). CCR7 staining was incubated at 37°C for 30 min immediately after Fc receptor blocking (analogous to

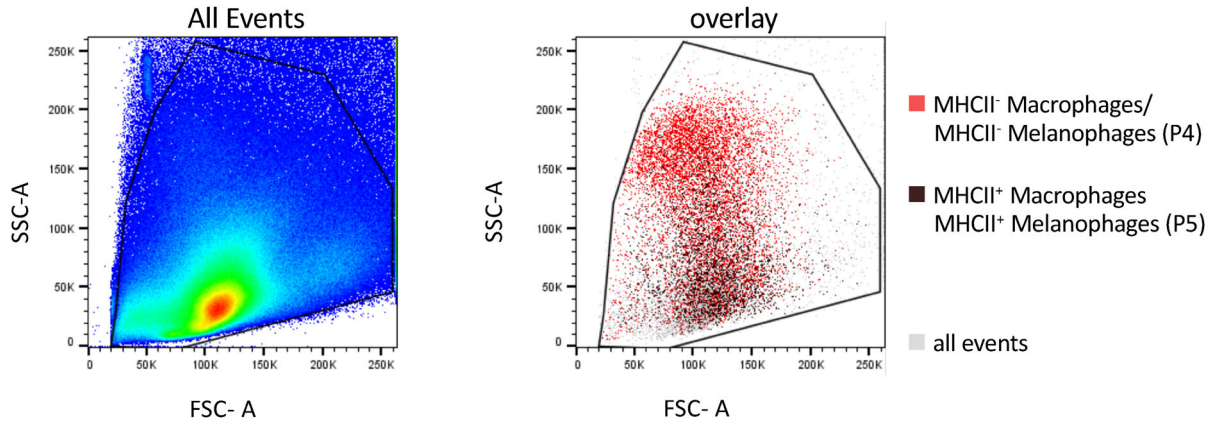

Figure 13. Melanophages and macrophages form an SSC^{high} population. A single-cell suspension of the ears from wild-type C57BL6/J mice was stained with the staining panel as indicated in Table 23. In the first gate (FSC-A vs. SSC-A) of our gating strategy, cells are included or excluded based on their respective size and granularity. On the left, all events as a pseudocolor plot are shown; on the right, an overlay of all events (gray) and the populations P4 (CD24^{low} CD11b^{+} CD64^{+} CCR2^{-} MHC-II^{-}; red) and P5 (CD24^{low} CD11b^{+} CD64^{+} CCR2^{-}MHC-II^{+}; dark red) is shown within the same plot.

staining for the chemokine receptor CCR2: step 8 of the staining protocol).

Resuspension of cells using a vibrating platform shaker

Resuspension of cell pellets within a 96-well plate was performed using a vibrating platform shaker. In this way, sheering stress caused by pipetting is avoided.

Drop in channels for individual adaptation of the staining panel

The staining panel can be adapted in the manner of the investigators' needs. Two very sensitive channels (BB515 and BV421) can be used as drops in channels to be able to stain for your specific marker of interest.

Adaptation of the staining panel for fluorescence-activated cell sorting

In the current version of the staining panel, a fixable viability dye is used, but when sorting cells, a constantly staining live/dead dye would be beneficial. Thus, instead of using eF780, we suggest using 7AAD instead; the lin^{-} channel must then be changed from PE-Cy5 to APC-Cy7.

2.1.7 *Summary of the phenotype*

A summary of surface marker expression on CD45^{+} cells is shown in Table 26.

2.2 Flow cytometry analysis of DC subsets in mouse intestinal tissue

2.2.1 *Introduction*

Dendritic cells (DC) act as central regulators of immune responses that are able to induce protective immunity against pathogens while maintaining tolerance to innocuous self-antigens [72]. In particular, in the intestine, this dual function of DC is challenged on a daily basis by the complex intestinal microbiome and food-borne antigens. To allow for proper analysis of the intestinal

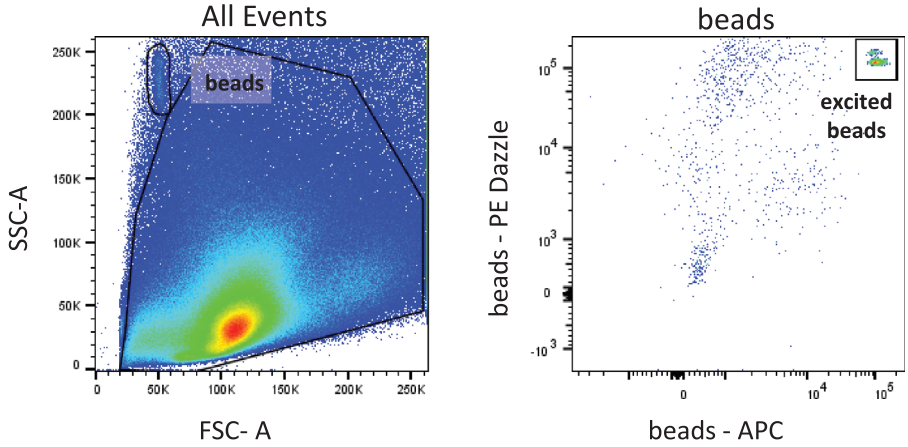

Figure 14. Identification of counting beads within the suspension. Counting beads can be separated from cells using FSC vs. SSC and their emission in two appropriate channels. Counting beads were mixed with a skin tissue single-cell suspension. In the first gate (FSC-A vs. SSC-A), the population beads are identified based on their respective size and granularity (SSC-A^{low} FSC-A^{high} population): on the left, all events as a pseudocolor plot are shown. On the right, this bead population was further purified based on the unique excitation properties of the beads; here, PE Dazzle and APC were used as emission detection channels.

DC subsets, understanding the anatomy of the DC compartment within the intestine and its associated lymphoid tissues, including mesenteric lymph nodes (MLN) and Peyer's patches, is essential. While we have summarized the general architecture of the intestine in Section 1.2, "**Preparation of single-cell suspensions from mouse intestinal tract**", we will now focus on the identification of DC derived from the intraepithelial lymphocytes (IEL) and lamina propria cells (LPC) of the small intestine and colon and its associated lymphoid tissues, including Peyer's patches and mesenteric lymph nodes (MLN).

In general, the expression of markers specific for certain immune lineages, including B cells (CD19, B220), T cells (CD3ε, CD90), NK cells (Nkp46, NK1.1, CD49b), neutrophils (Ly6G), and erythrocytes (Ter-119), is absent on conventional DC (cDC) [72, 73]. Therefore, cDC are often referred to as lineage negative. Additionally, all DC express MHC-II and CD11c. Under steady-state conditions, high levels of MHC-II and intermediate levels of CD11c and *vice versa* allow for the separation of migratory and resident cDC within MLN. cDC themselves can be separated into cDC1 and cDC2 based on the expression of XCR1 and CD172a or CD11b [62, 72, 74]. While migratory cDC1 in MLN and Peyer's patches as well as cDC1 derived from the intestine are $CD103^+CD11b^-$, resident cDC1 in MLN are $CD103^-CD11b^-$. Intestinal cDC2 can be separated into $CD103^+CD11b^+$ and $CD103^-CD11b^+$ cDC2, which is also reflected by CD103 and CD11b expression on migratory cDC2 in MLN [72, 75]. Even though their antigen presenting capabilities and their phenotypic origin are under debate, plasmacytoid DC (pDC) are ascribed to the DC family. pDC can be identified by their expression of PDCA-1, B220, Ly6C and Siglec-H across tissues [72]. In addition, marker-based separation of monocytes from cDC2 can be difficult, requiring their parallel identification during flow cytometry analysis for proper separation.

In the following, we provide an easy and ready-to-use protocol for the analysis of cDC, pDC and monocyte populations isolated from different tissues of the intestinal tract via a conserved core panel by flow cytometry.

2.2.2 *Materials*

2.2.2.1 Reagents. A complete list of reagents is provided in Table 27.

2.2.2.2 Equipment. The necessary equipment is listed in Tables 28 and 29.

2.2.3 *Step-by-step sample preparation*

2.2.3.1 Preparation of stocks and solutions.

DAPI

Dissolve 4′,6-diamidino-2′-phenylindole dihydrochlorid (DAPI) in ultrapure water to create a 1 mg/mL stock solution. Store the solution protected from light at 4°C. Dilute the stock solution 1:10,000 in FACS buffer (PBS+2% FCS) to create a working solution for DAPI staining of cells directly before acquisition by the flow cytometer.

Table 27. Reagents, antibodies, chemicals and solutions

Reagent	Manufacturer	Ordering Number
Antibodies		
αCD3ε Biotin (145-2C11)	BioLegend	100304
αCD19 Biotin (1D3)	BioLegend	553784
αLy6G Biotin (1A8)	BioLegend	127604
αSiglec-H BUV737 (440c)	BD	748293
αNK1.1 BUV395 (PK136)	BD	564144
αCX_3CR_1 BV711 (SA011F11)	BioLegend	149031
αPDCA-1 BV650 (927)	BioLegend	127019
αCD45 BV605 (30-F11)	BD	563053
αLy6C BV570 (HK1.4)	BioLegend	128030
αMHC-II V500 (I-A/I-E) (M5/114.15.2)	BD	562366
αXCR1 BV421 (ZET)	BioLegend	148216
αCD172a PerCp-e710 (P84)	eBioscience	46-1721-82
αB220 PE-Cy5 (RA3-6B2)	BioLegend	103210
αCD11c PE-CF594 (HL3)	BD	562454
αCD103 APC-Cy7 (2E7)	BioLegend	121432
αCD11b A700 (M1/70)	BioLegend	101222
Streptavidin BUV496	BD	612961
Purified αFcγRIIB/III (2.4G2)	BD	101302
Purified αFcγRIV (9E9)	BioLegend	149502
Chemicals & Solutions		
4′,6-diamidino-2-phenylindole (DAPI)	Formatting	62247
Dulbecco's Phosphate Buffered Saline without calcium and magnesium	Sigma	D8537
Fetal Bovine Serum (FCS)	Sigma	F7524
Normal Rat Serum	Stem Cell	13551

FCS

Quickly thaw FCS at 37°C in a water bath. Once completely thawed, incubate for 15 min at 42°C in the water bath to destroy complement activity. Directly filter the warm FCS through a sterile 0.22 μm membrane (Corning #431118) into a sterile storage bottle (Corning #430518) and aliquot into 50 mL portions. Use aseptic techniques during the whole procedure. Aliquoted FCS must be stored at −20°C. Avoid freeze-thaw cycles.

FACS buffer

Add 2% FCS (v/v) to phosphate buffered saline solution (PBS).

2.2.3.2 Antibody staining of single-cell suspensions from intestinal tissue for flow cytometry. In Section 1.2 "**Preparation of single-cell suspensions from mouse intestinal tract**", we described how to prepare single-cell suspensions from mouse intestinal tissue, including cells from Peyer's patches and mesenteric lymph

Table 28. Necessary equipment

Equipment	Company	Purpose
Centrifuge "Allegra X-15R"	Beckman-Coulter	Centrifugation of 50 mL tubes, 15 mL tubes and V-bottom plates
Neubauer chamber 0.100 mm; 0.0025 mm^2	Superior Marienfeld	Cell counting
Corning storage bottle (#430518) and 0.22 μM sterile filter (#431118)	Corning	Sterile filtration and storage of solutions
Sterile bench "Mars Safety Class 2"	Scanlaf	Performance of all aseptic procedures
LSR Fortessa (#647800)	BD	Flow cytometry analysis of single cell suspensions
96-well V-bottom plate (651 180)	Greiner bio-one	Sample preparation for flow cytometry
50 mL tubes (#352070)	Falcon	Centrifugation of cell suspensions; Digestion of intestinal tissues
15 mL tubes (#188271)	Greiner bio-one	Centrifugation of cell suspensions
Serological pipettes (#606180)	Greiner bio-one	Pipetting
FACS tube with 35 μm restrainer cap (#352235)	Corning	Filtration of samples derived from small intestine and colon directly before acquisition at a flow cytometer
FACS tube (#352008)	Corning	Regular FACS tubes for acquisition of single cell suspensions derived from Peyer's patches and MLN at a flow cytometer

nodes (MLN) as well as intraepithelial lymphocytes (IEL) and lamina propria cells (LPC) from the small intestine and colon. Following their preparation, all cells isolated from one mouse were transferred to a 96-well V-bottom plate to perform antibody staining, enabling flow cytometry analysis. Expected cell counts are depicted in Table 9 of Section 1.2 "**Preparation of single-cell suspensions from mouse intestinal tract**".

1. Before centrifugation of the samples, prepare the first staining mix (Table 30);
2. Use 50 μl of FACS buffer per sample and add the antibodies listed in Table 30 in the indicated dilution; Please note that antibody dilutions are dependent on the flow cytometer and its setup; Suggested antibody dilutions were optimized for a BD LSR Fortessa equipped with 355 nm, 405 nm, 488 nm, 561 nm and 640 nm laser lines; If your cell count strongly differs from the expected cellular yields (>factor 1.5), scale the volume of antibody cocktails up and down accordingly to maintain a constant detector antibody to target ratio; Do not stain in less than 35 μl;

Table 29. Detailed configuration of the BD LSR Fortessa

Laser line	Filter		Fluorochrome	Alternatives
	Longpass	Bandpass		
355 nm	–	379/28	BUV395	–
	410LP	470/100	BUV496	DAPI, ZombieUV
	690LP	740/35	BUV737	–
405 nm	–	450/50	BV421	V450, e450, Pacific Blue, CTV
	505LP	525/50	V500	BV510, Pacific Orange
	545LP	585/42	BV570	–
	600LP	610/20	BV605	–
	630LP	670/50	BV650	–
	690LP	710/50	BV711	–
488 nm	–	488/10	FSC/SSC	–
	505LP	530/30	FITC	A488, GFP, CFSE
	685LP	710/50	PerCP-e710	PerCP-Cy5.5, PerCP
561 nm	–	586/15	PE	CMRA
	600LP	610/20	PE-Dazzle 594	PE-CF594
	635LP	670/30	PE-Cy5	PE-Dye649
	750LP	780/60	PE-Cy7	PE-Fire750
640 nm	–	670/14	A647	APC
	690LP	730/45	A700	–
	750LP	780/60	APC-Cy7	APC-Fire750, APC-H7, APC-e780

Table 30. First antibody staining mix for flow cytometry

Fluorophore/Labeling	Antigen	Clone	#Catalog	Company	Dilution
Biotin	CD3ε	145-2C11	100304	BioLegend	1:200
Biotin	CD19	1D3	553784	BioLegend	1:400
Biotin	Ly6G	1A8	127604	BioLegend	1:400
None	FcγRIIB/III	2.4G2	553142	BD	1:400
None	FcγRIV	9E9	149502	BioLegend	1:400

Table 31. Secondary antibody staining mix for flow cytometry

Fluorophore	Antigen	Clone	#Catalog	Company	Dilution
BUV737	Siglec-H	440c	748293	BD	1:400
BUV395	NK1.1	PK136	564144	BD	1:400
BV711	CX_3CR_1	SA011F11	149031	BioLegend	1:400
BV650	PDCA-1	927	127019	BioLegend	1:400
BV605	CD45	30-F11	563053	BD	1:400
BV570	Ly6C	HK1.4	128030	BioLegend	1:800
V500	MHC-II (I-A/I-E)	M5/114.15.2	562366	BD	1:200
BV421	XCR1	ZET	148216	BioLegend	1:400
PerCp-e710	CD172a	P84	46-1721-82	eBioscience	1:400
PE-Cy5	B220	RA3-6B2	103210	BioLegend	1:800
PE-CF594	CD11c	HL3	562454	BD	1:400
APC-Cy7	CD103	2E7	121432	BioLegend	1:100
A700	CD11b	M1/70	101222	BioLegend	1:800
BUV496	Streptavidin (αBiotin)	None	612961	BD	1:50

3. Commercially available, purified αFcγRIIB/III and αFcγRIV are employed to block Fc gamma receptors (FcγRs) IIB, III and IV, thereby avoiding nonspecific recognition of staining antibodies by cell-bound Fc gamma receptors; additionally, FACS buffer can be supplemented with 2% (v/v) rat serum;
4. Centrifuge the sample-containing 96-well V-bottom plates at 700 × g and 4°C for 5 min;
5. Discard the supernatant in one fast and flowing motion, keep the plate upside down and dip it three times on a different location on a fresh paper towel;
6. Resuspend each sample in 50 μl of primary antibody staining mix and incubate for 30 min at 4°C;
7. Fill up with 100 μl FACS buffer per well;
8. Centrifuge at 700 × g and 4°C for 5 min;
9. During the following washing steps, prepare the second antibody staining mix (Table 31);
10. Prepare 50 μl of staining mix per sample utilizing the antibodies in Table 31 in the indicated dilution; Please note that antibody dilutions are dependent on the flow cytometer and its setup; Suggested antibody dilutions were optimized for a BD LSR Fortessa equipped with 355 nm, 405 nm, 488 nm, 561 nm and 640 nm laser lines; If your cell count strongly differs from the expected cellular yields (>factor 1.5), scale the volume of antibody cocktails up and down accordingly to maintain a constant detector antibody to target ratio; Do not stain in less than 35 μl;
11. Discard the supernatant, keep the plate upside down and dip on a paper towel;
12. Resuspend each sample in 160 μl FACS buffer;
13. Centrifuge at 700 × g and 4°C for 5 min;
14. Discard the supernatant, keep the plate upside down and dip on a paper towel;
15. Resuspend each sample in 160 μl FACS buffer;
16. Centrifuge at 700 × g and 4°C for 5 min;
17. Resuspend each sample in 50 μl of the secondary antibody staining mix;
18. Incubate for 30 min at 4°C in the dark;
19. Fill up with 100 μl FACS buffer per well;
20. Centrifuge at 700 × g and 4°C for 5 min;
21. Resuspend each sample in 160 μl FACS buffer;
22. Centrifuge at 700 × g and 4°C for 5 min;
23. Discard the supernatant, keep the plate upside down and dip on a paper towel;
24. Resuspend each sample in 160 μl FACS buffer;
25. Centrifuge at 700 × g and 4°C for 5 min;
26. Resuspend the samples in 100 μl FACS buffer;
27. Samples are ready for acquisition with a flow cytometer;
28. Add 180 μl of FACS buffer containing DAPI at a dilution of 1:10,000 directly before acquisition;
29. While MLN and Peyer's patch samples can be directly acquired, filter IEL and LPC samples via 35 μm cell strainers into FACS tubes;

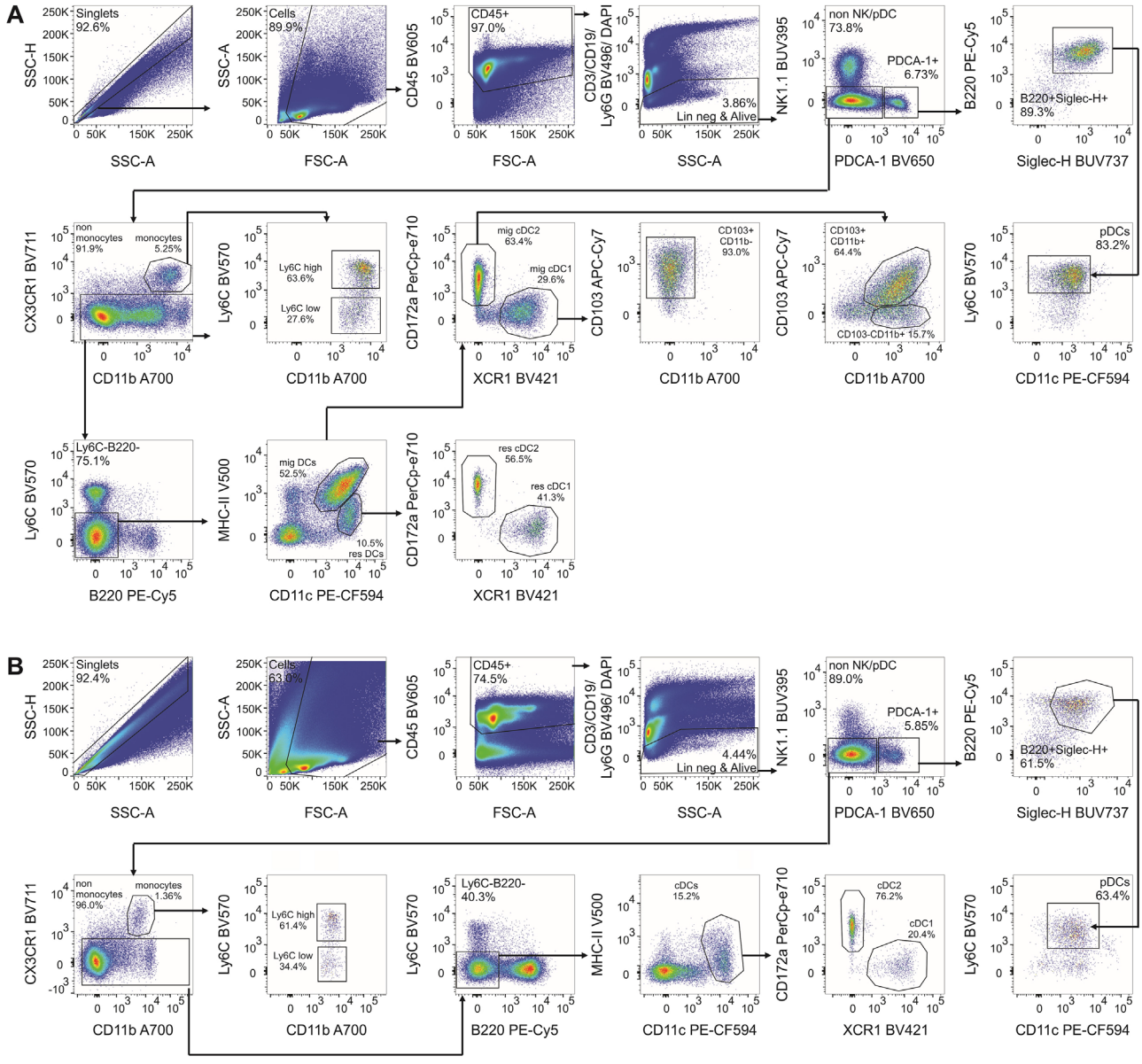

Figure 15. Exemplary gating strategy for the dendritic cell network of mesenteric lymph nodes (A) and Peyer's patches (B). After elimination of doublets and debris, dead cells (DAPI$^+$), T cells (CD3ε), NK cells (NK1.1), B cells (CD19), and neutrophils (Ly6G) were excluded from the CD45$^+$ cell population. pDC were further identified as positive for the markers B220, PDCA-1, Siglec-H and Ly6C. Monocytes were identified by the simultaneous expression of CX_3CR_1 and CD11b. Monocytes can then be separated into Ly6C^{high} and Ly6C^{low} monocytes. DC were further classified as negative for CX_3CR_1, Ly6C and B220. DC located in mesenteric lymph nodes (MLN) separate into migratory (MHC-II^{high}; CD11c^{int}) and resident (MHC-II^{int}; CD11c^{high}) conventional DC (cDC). Both migratory and resident cDC are separated into conventional cDC type 1 (cDC1; XCR1$^+$; CD172a$^-$; CD103$^+$, CD11b$^-$) and type 2 (cDC2; XCR1$^-$; CD172a$^+$) that are further separated into CD103$^+$CD11b$^+$ and CD103$^-$CD11b$^+$ migratory cDC2. Shown is one exemplary gating strategy derived from analysis of a C57BL/6J mouse. Data acquisition was performed at a BD LSR Fortessa, and data were evaluated utilizing FlowJo software.

30. After performing the cytometer setup, data were acquired using an appropriate flow cytometer.

2.2.4 *Data analysis*

Data acquisition was performed using a BD LSR Fortessa SORP equipped with 355 nm, 405 nm, 488 nm, 561 nm, and 640 nm lasers. Subsequently, the data were analyzed utilizing FlowJo software (BD) version 10.8.1. In the following, we provide exemplary gating strategies for all tissues analyzed with an identical panel. An overview of markers expressed on DC and monocyte populations is provided in Table 33 (below). Fig. 15 displays an exemplary gating strategy for the identification of DC and monocyte subsets within mesenteric lymph nodes and Peyer's patches.

Our analysis approach allowed for the straightforward identification of pDC as well as cDC and monocyte subsets within

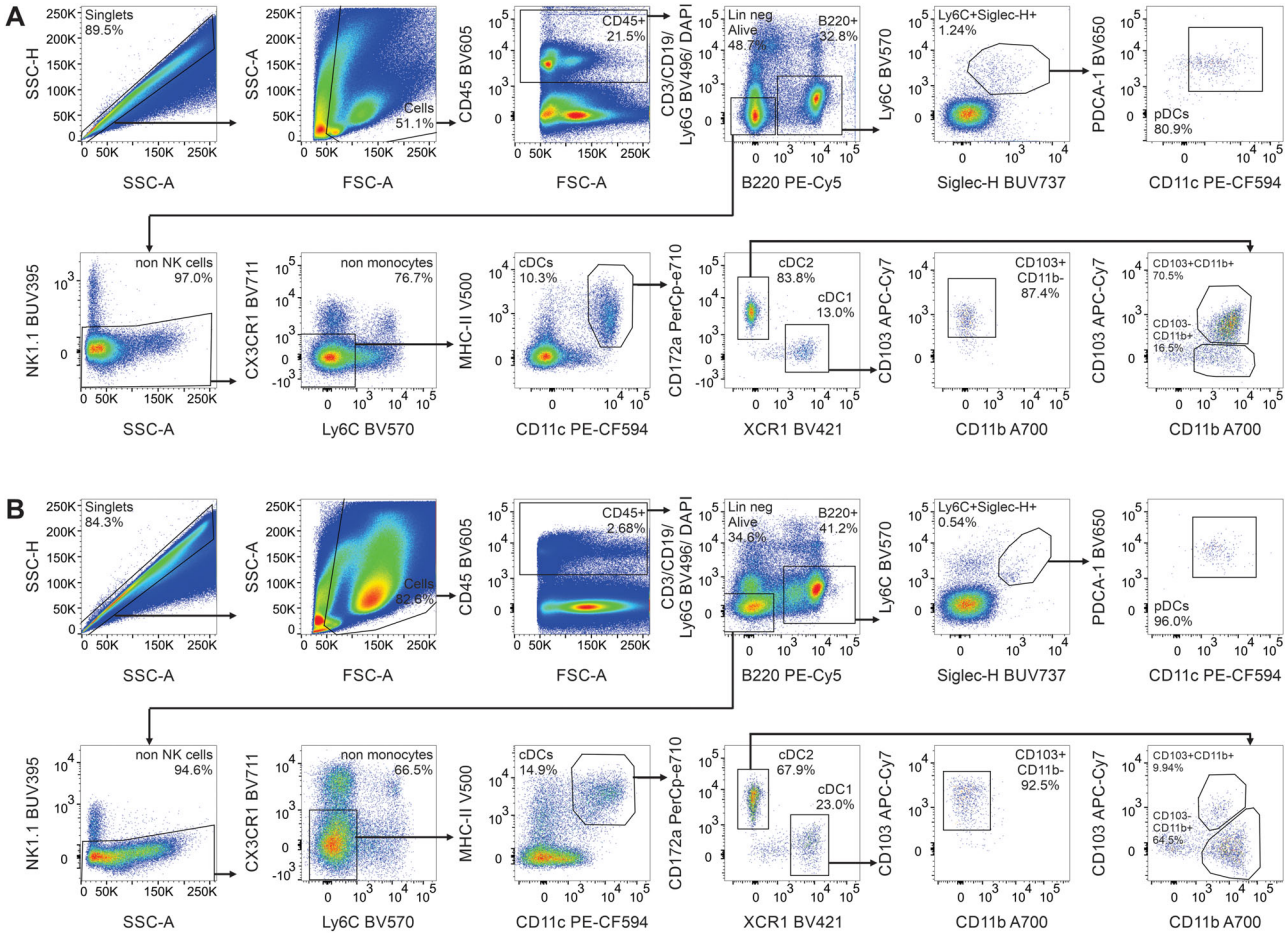

Figure 16. Exemplary gating strategy for the dendritic cell network within lamina propria cells (LPC) derived from the small intestine (A) and colon (B). After elimination of doublets and debris, dead cells (DAPI$^+$), T cells (CD3ε), B cells (CD19, B220), and neutrophils (Ly6G) were excluded from the CD45$^+$ cell population. pDC were further identified as positive for the markers B220, PDCA-1, Ly6C and Siglec-H while expressing intermediate levels of CD11c. Following exclusion of CX_3CR_1, Ly6C and NK1.1 expressing cells, DC were identified via the expression of MHC-II and CD11c, which were subsequently separated into cDC1 and cDC2 cells based on the expression of XCR1 and CD172a, respectively. While cDC1 display a CD103$^+$CD11b$^-$ phenotype, cDC2 can be further separated into CD103$^+$CD11b$^+$ and CD103$^-$CD11b$^+$ cDC2. Shown is one exemplary gating strategy derived from analysis of a C57BL/6J mouse. Data acquisition was performed at a BD LSR Fortessa, and data were evaluated utilizing FlowJo software.

mesenteric lymph nodes (Fig. 15A) and Peyer's patches (Fig. 15B). Mesenteric lymph nodes contained clearly segregated migratory (MHC-II^{high}CD11c^{int}) and resident (MHC-II^{int}CD11c^{high}) cDC populations that each separated migratory and resident cDC1 and cDC2, respectively. While this discrimination is not clearly observable for DC derived from Peyer's patches located in the small intestine, Bonnardel et al. showed that Peyer's patches contain a heterogeneous cDC compartment including three populations of cDC2 (CD11b$^+$ dome cDC, CD11b$^-$ dome cDC and CD11b$^+$ dome-associated villi cDC) that also have been described to differ in their MHC-II expression levels [76]. Peyer's patches comprise clustered domes formed by B cell follicles separated from each other by interfollicular regions (IFRs) enriched in T cells. The follicle-associated epithelium (FAE) contains specialized epithelial cells, called M cells, that bind and rapidly transport microorganisms from the lumen to the subepithelial dome (SED). For a sophisticated analysis of the Peyer's patch DC compartment, our panel already includes the most important markers enabling the identification of these cDC2 populations (MHC-II, CD11c, CD11b, CD172a and PDCA-1).

Within the lamina propria cell fraction, cDC were frequently present, while only small numbers of pDC were identified, which was independent of the intestinal section investigated (Fig. 16). Within cDC, CD172a$^+$ cDC2 have the highest frequency. While CD103$^+$CD11b$^+$ cDC2 have a higher abundance than CD103$^-$CD11b$^+$ cDC2 in the small intestine, the CD103$^-$CD11b$^+$ subset is dominant within the colon. In strong contrast to the DC network analyzed within the lamina propria cell fraction, the intraepithelial lymphocyte fraction barely contains any cDC, while pDC are highly abundant within the small intestine (Fig. 17).

In general, the provided panel is designed to enable researchers with smaller flow cytometers to reliably identify and characterize DC populations of the intestinal tract. Since monocytes and macrophages often display phenotypic similarities with DC, their clear separation from the cDC pool is challenging. While monocytes have been excluded by means of CX_3CR_1 and Ly6C,

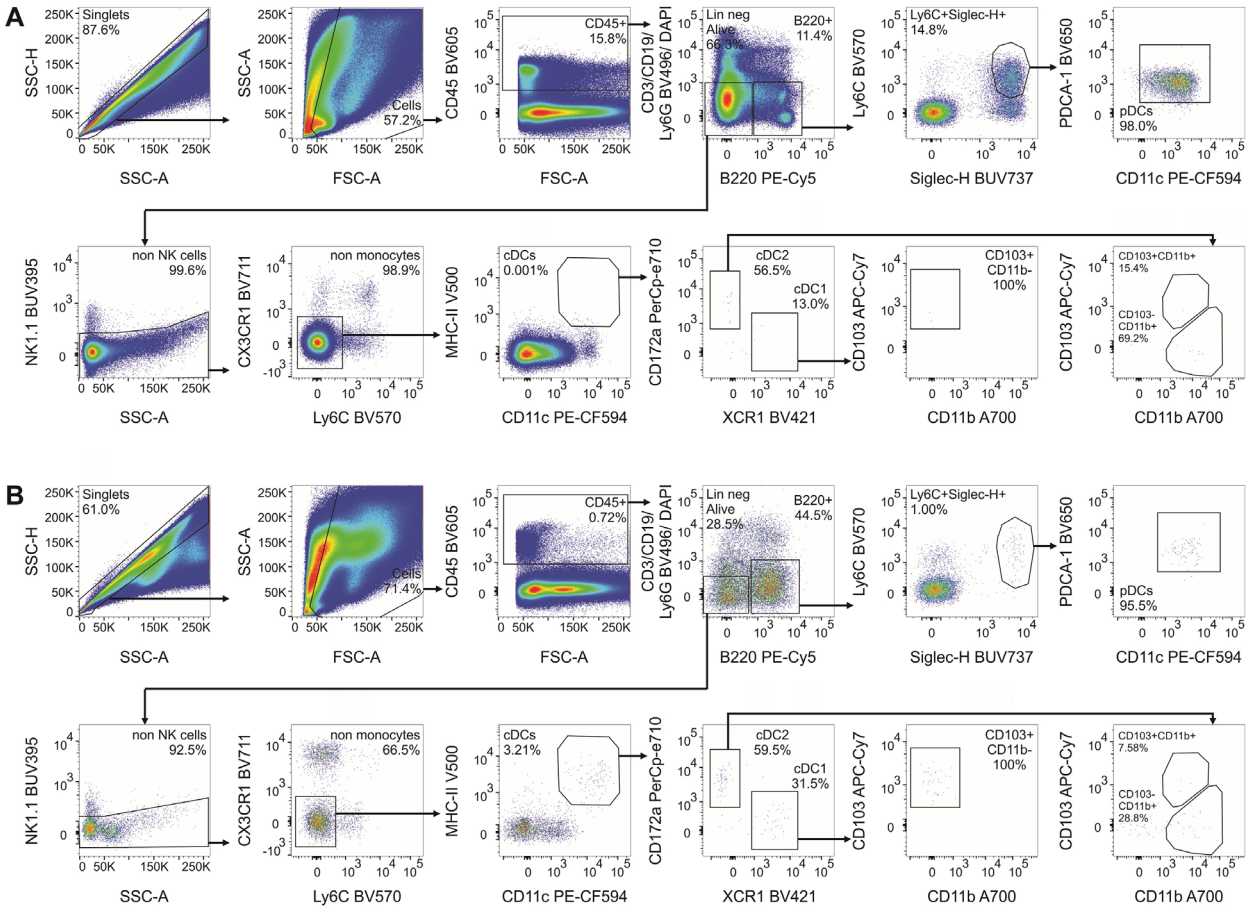

Figure 17. Exemplary gating strategy for the dendritic cell network within intraepithelial lymphocyte preparations (IEL) derived from the small intestine (A) and the colon (B). After elimination of doublets and debris, dead cells (DAPI$^+$), T cells (CD3ε), B cells (CD19, B220), and neutrophils (Ly6G) were excluded from the CD45$^+$ cell population. pDC were further identified as positive for the markers B220, PDCA-1, Ly6C and Siglec-H while expressing intermediate levels of CD11c. Following exclusion of CX_3CR_1, Ly6C and NK1.1 expressing cells, DC were identified via the expression of MHC-II and CD11c, which were subsequently separated into cDC1 and cDC2 cells based on the expression of XCR1 and CD172a, respectively. Shown is one exemplary gating strategy derived from analysis of a C57BL/6J mouse. Data acquisition was performed at a BD LSR Fortessa, and data were evaluated utilizing FlowJo software.

macrophages that are frequently identified by the high simultaneous expression of CD64 (FcγRI) and F4/80, which show a low-level expression on cDC, are not visible with the provided panel [62, 77]. Thus, to provide evidence that the proposed panel reliably identifies cDC, we performed counterstains with αCD64 and αF4/80 antibodies to identify macrophages and to identify cDC via the marker CD26 [62].

As shown in Fig. 18, CD64$^+$ and F4/80$^+$ macrophages that can be identified within the CD45$^+$ fraction are properly excluded from the analyzed MHC-II$^+$ CD11c$^+$ cDC pool. Additionally, all cDC identified across tissues, including XCR1$^+$ CD103$^+$ CD11b$^-$ cDC1 as well as CD172a$^+$ CD103$^+$ CD11b$^+$ and CD172a$^+$ CD103$^-$ CD11b$^+$ cDC2, showed high and uniform expression of CD26 across tissues. Thus, our panel provides a reliable scaffold for the straightforward identification of cDC across the intestinal tissue landscape in the steady state, which can be easily expanded/adapted for the simultaneous analysis of macrophages or to meet the demands for cDC analysis under inflammatory conditions. For further information about panel expansions and potential current limitations, please refer to the sections **2.2.5 Pitfalls** and **2.2.6 Top tricks**.

2.2.5 *Pitfalls*

Problem: The signal resolution of a marker is not high enough to identify positive and negative cells

Potential solutions:

Check, if laser lines and employed filter sets are appropriate for excitation and detection of the employed dyes. Therefore, please refer to Table 32, where we summarized the excitation and emission maxima of the employed dyes.

Check, if the defined PMT voltages are adequate. Check, if the correct antibody clone was employed. Perform an antibody titration with your own flow cytometer set up. If this protocol is used to analyse tissue samples that resulted from pooling of multiple mice, the staining volume has to be scaled up accordingly to maintain a constant staining antibody to target molecule ratio.

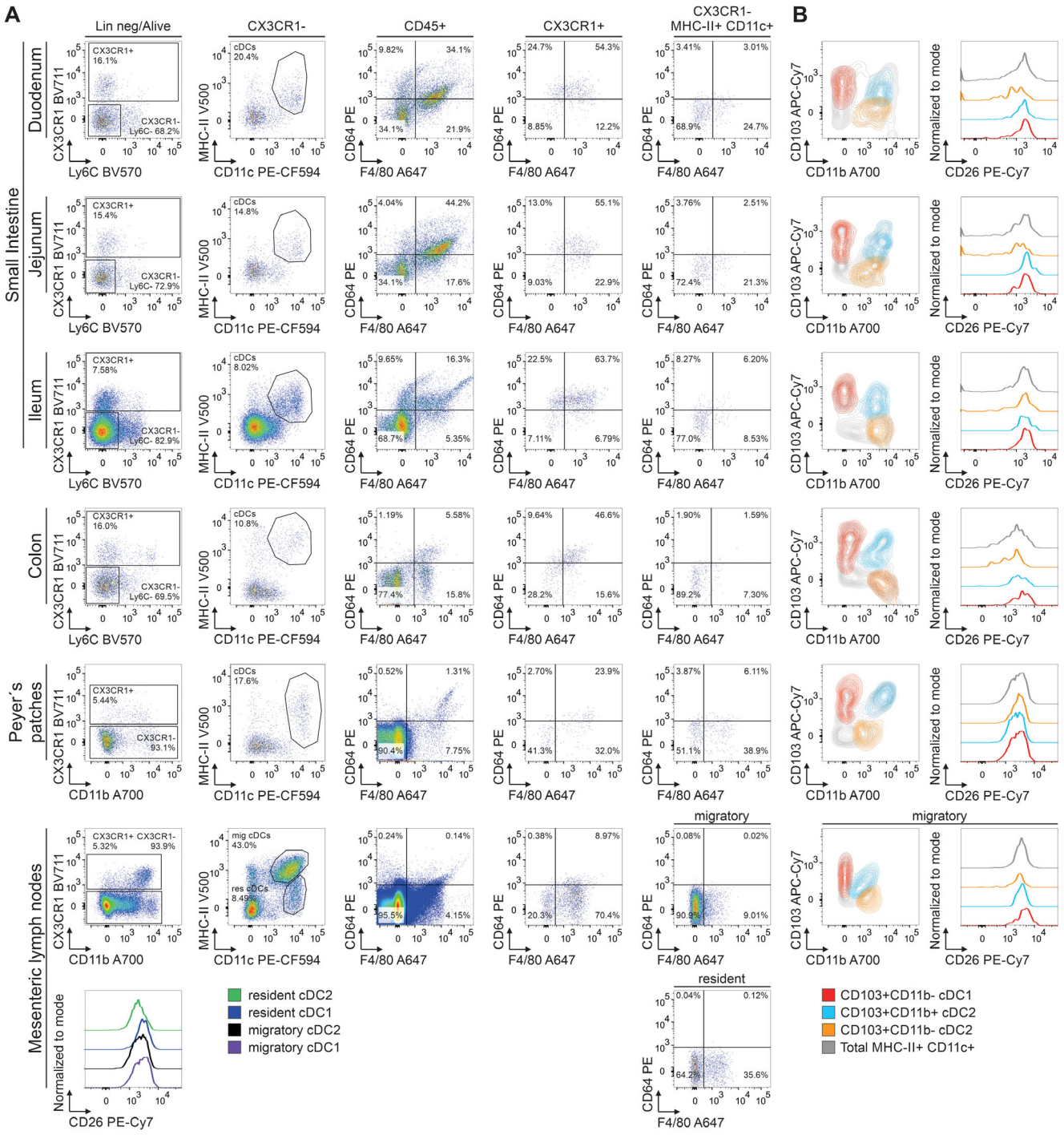

Figure 18. The identified cDC pool is devoid of $CD64^{+}F4/80^{+}$ macrophages, while all identified cDC show high expression of the marker CD26 across intestinal sections, mesenteric lymph nodes and Peyer's patches. Following the preparation of single-cell suspensions from the colon and different parts of the small intestine, comprising duodenum, jejunum and ileum, and single-cell suspensions from mesenteric lymph nodes and Peyer's patches, cells were stained with the proposed antibody panel, including αCD64 PE (X54-5/7.1), αF4/80 A647 (BM8), and αCD26 PE-Cy7 (H194-112). (A) After gating on $CX_3CR_1^{+}$ and $CX_3CR_1^{-}$ Ly6C^{-} cells containing the MHC-II^{+} CD11c^{+} cDC fraction, the expression of CD64 and F4/80 is shown as dot plots within the $CD45^{+\,lineage+}$ fraction, the $CX_3CR_1^{+}$ fraction and within the $CX_3CR_1^{-}$ Ly6C^{-} MHC-II^{+} CD11c^{+} cell pool. (B) Expression of CD26 on total MHC-II^{+} CD11c^{+} cDC containing XCR1^{+} CD103^{+} CD11b^{-} cDC1 as well as CD172a^{+} CD103^{+} CD11b^{+} and CD172a^{+} CD103^{-} CD11b^{+} cDC2 across the intestinal tissue landscape. One representative example derived from the analysis of a C57BL/6J mouse is shown. Data acquisition was performed at a BD LSR Fortessa, and data were evaluated utilizing FlowJo software.

Table 32. Optimal excitation and emission values for employed dyes

Fluorophore	Optimal excitation in nm	Emission maximum in nm
BUV737	348	737
DAPI	358 (bound to dsDNA)	461
BUV496	348	496
BUV395	348	395
BV711	405	711
BV650	405	645
BV605	405	603
BV570	405	570
V500	415	500
BV421	405	421
PerCp-e710	482	710
PE-Cy5	564	670
PE-CF594	564	612
APC-Cy7	650	780
A700	702	723

Problem: There are no positive signals for the staining of MHC-II

Potential solutions:

The MHC-II alloantigens recognized by the employed αMHC-II antibody clone are not expressed in all mouse strains. The MHC-II antibody clone M5/11.15.2 employed in this staining reacts to the I-A^b, I-A^d, I-A^q, I-E^d, and I-E^b alloantigens expressed by mice exhibiting a H-$2^{p,r,q,b,d,u}$ haplotype. Check, if your analysed mouse strain does express the listed alloantigens.

Problem: The repertoire of immune cells included in IEL and LPC samples derived from the small intestine varies strongly between samples

Potential solutions:

Even if Peyer's patches are not the focus of analysis, they have to be removed from the intestinal tissue since their cellular composition substantially differs from intestinal tissue.

Problem: The pDC to cDC ratio in IEL and LPC samples strongly differs from the expected results

Potential solutions:

Prepare fresh IEL buffer for sample preparation (for more information please refer to "**preparation of single-cell suspensions from mouse intestinal tract**").

Ensure that the longitudinal intestine cut before the first digestion is carried out properly, and that all solutions, shakers and incubators are pre-heated to 37°C.

The ratio of pDC to cDC can be used as quality control for the IEL digestion for individual samples.

Problem: The staining of CX_3CR_1 is accompanied by unspecific staining

Potential solutions:

The employed αCX_3CR_1 antibody is a mouse IgG2a,κ antibody. In particular, FcγRIV displays a high binding affinity for mouse antibodies of the IgG2a isotype [78]. Since FcγRIV is frequently expressed on myeloid cells including monocytes and cDC, we perform an obligatory block of FcγRIV (clone 9E9) in addition to the regular protein block (FCS) also blocking FcγRI and the blockade of FcγRIIB and FcγRIII via the 2.4G2 blocking antibody, thereby preventing unspecific binding of the αCX_3CR_1 antibody to FcγRIV expressing cell populations [77].

Problem: Clear demarcation of the cDC network from monocytes and macrophages under inflammatory conditions

Potential solutions:

In general, cDC and in particular cDC2 are often difficult to distinguish from monocytes and macrophages. Clear demarcation of these cell types is even more challenging under inflammatory conditions. To encounter this issue, the provided staining panel can be modified by addition of several markers further specifying the different myeloid populations.

Besides MHC-II and CD11c, CD26 can be included in the staining cocktail as a universal cDC marker across analysed tissues [62, 79]. In combination with markers for cells of the monocyte and macrophage lineage, this potentially allows for a more robust identification of cDC. Besides the already included markers Ly6C and CX_3CR_1 facilitating identification of monocytes, CD88 can be included as an additional monocyte and macrophage marker [80]. With respect to macrophages, MerTK and in particular CD64 in combination with F4/80 might be used to clearly separate macrophages from the cDC pool [62, 81, 82]. If a CD64 based exclusion strategy is used, care should be taken to only exclude CD64 high cells, since cDC also express FcγRI [77]. Under inflammatory conditions, the development of monocyte-derived DC can be observed *in vivo*. Only recently, Bosteels et al. described a population of cDC2 emerging during inflammation that can also be found within mesenteric lymph nodes, which is characterized by the simultaneous expression of CD26, MHC-II, CD11c, CD64 and MAR-1 (antibody clone recognizing FcεRIα) [21]. Since CD64 and MAR-1 are usually expressed on macrophages and monocyte-derived cells, inclusion of CD26 secures that inflammatory cDC2 are not excluded from the cDC2 pool under inflammatory conditions [21].

Finally, inflammation could lead to an upregulation of MHC-II, thereby prohibiting a clear separation of migratory and resident cDC2 within mesenteric lymph nodes based on the expression of MHC-II, while migratory cDC1 are still distinguishable from resident cDC1 via CD103.

2.2.6 *Top tricks*

Modification of the provided staining panel

The currently provided 14-color staining panel scaffold is designed to enable the identification of cDC1, cDC2, pDC, $Ly6C^{high}$ monocytes and $Ly6C^{low}$ monocytes in the intestinal compartment, while flexibility for the experimenters´ individual needs is maintained. Thus, the staining panel does not employ antibodies in the most commonly available colours including

Table 33. Summary of marker expression on analyzed cell populations

Population	Marker negative	Marker positive
Ly6C^{high} monocytes	DAPI, CD3, CD19, Ly6G, B220, PDCA-1, NK1.1	CX_3CR_1, CD11b, Ly6C
Ly6C^{low} monocytes	DAPI, CD3, CD19, Ly6G, B220, PDCA-1, NK1.1	CX_3CR_1, CD11b
cDC1	DAPI, CD3, CD19, Ly6G, B220, PDCA-1, NK1.1	CD11c, MHC-II, XCR1
cDC2	DAPI, CD3, CD19, Ly6G, B220, PDCA-1, NK1.1	CD11c, MHC-II, CD172a
Plasmacytoid DC (pDC)	DAPI, CD3, CD19, Ly6G, NK1.1	B220, Siglec-H, PDCA-1

A647/APC, PE, PE-Cy7 and FITC/A488. Therefore, this panel scaffold can be easily expanded or adapted to allow for a) usage of this panel at flow cytometers with less channels, b) the analysis of receptor expression, c) for the staining of intracellular molecules employing the small dyes A647 and A488 and d) for the analysis and/or more stringent demarcation of other myeloid populations e.g. macrophages or inflammatory cDC2 from monocyte-derived cells under inflammatory conditions by addition of MerTK (Clone DS5MMER,), CD64 (Clone X54-5/7.1), CD26 (Clone H194-112), CD88 (Clone 20/70), FcεRI (Clone MAR-1) and αF4/80 (Clone BM8).

The current use of the live-dead discriminator DAPI is not compatible with fixation and intracellular stainings. To allow for parallel fixation and live-dead cell discrimination employ a fixable viability dye. In particular, the Zombie UV^{TM} Fixable Viability Kit from BioLegend (#Cat 423107) might be attractive, since the dye is usually detected in the same channel as DAPI.

Dependent on analysed populations, the BUV496 dump channel can be shrunk or expanded. For instance, αB220 Biotin (exclusion of pDC) or αSiglec-F Biotin (exclusion of Eosinophils) could be included, if these cells are not of interest. If the employed antibody panel for exclusion of lineage positive cells is modified, a new titration of the Streptavidin BUV496 conjugate has to be performed.

The suggested panel is suitable to analyse DC across various tissues including lympho-hematopoietic (spleen, lymph nodes and thymus) and peripheral tissues (lung, liver) without the need of major modifications.

2.2.7 *Summary of the phenotype*

The overall phenotype of immune cells covered by the markers included in the panel is detailed in Table 33.

2.3 Flow cytometry analysis of DC subsets in mouse lung

2.3.1 *Introduction*

The lung is a barrier tissue that is constantly exposed to the environment and incoming challenges, such as pathogens, allergens and pollutants. Therefore, induction, maintenance and termination of innate and humoral immune responses have to be tightly regulated to ensure efficient pathogen clearance but impede overshooting immune responses [83]. A multitude of myeloid cells, such as dendritic cells (DC), macrophages, monocytes, and granulocytes, form a functionally specialized network to serve as the first line of defense and to mediate tissue homeostasis in the steady state [84]. As professional antigen-presenting cells, DC play a key role in orchestrating immune responses by linking the innate and the adaptive branch of the immune system [85]. After phagocytosis and processing of antigens, DC migrate to lymphoid tissues, present antigens, and subsequently activate T cells in a cell–cell contact-dependent manner [86]. For mouse DC, expression of CD11c, MHC-II, and CD26 is conserved across subpopulations and across organs [62, 85]. Conventional DC (cDC) are found in lymphoid and non-lymphoid tissues and can be subdivided into cDC1 and cDC2 based on their function and localization in the tissue microenvironment [85]. Comparative studies of mice and human cDC showed an occurrence of mouse cDC1 and cDC2 equivalents in human lymphoid and non-lymphoid tissues [85]. Within the mouse lung, cDC1 are closely attached to the epithelial layer around the airways and subpleural region [87]. Extension of their dendrites through the epithelial layer into the air-exposed space allows antigen uptake [88], which subsequently leads to cross-presentation of captured antigens to CD8$^+$ T cells and initiation of Th1 polarization by IL-12 secretion [89, 90]. These functional properties of cDC1 initiate protective immune responses against respiratory viruses, tumor surveillance and intracellular bacteria [90]. In contrast, cDC2 sit next to epithelial layer of the alveolar ducts [87] and preferentially prime CD4$^+$ T cells [91, 92]. Differential expression of transcription factors IRF4, KLF-4, and Notch2 in cDC2 drive Th2 or Th17 polarization triggering allergic reactions or anti-bacterial and –fungal immune responses [92–96]. It was recently described in mice and humans that cDC2 can be further delineated in two subsets based on the transcription factor T-box expressed in T-cells (Tbet). Tbet$^+$ cDC2 are crucial for tissue repair, while Tbet$^-$ cDC2 have a pro-inflammatory transcriptional profile [97]. However, inflammatory or infectious episodes challenge the classical separation of cDC1 and cDC2, recent publications have focussed on the characterization of monocyte-derived DC and inflammatory cDC [21, 62].

To study pulmonary myeloid cells by flow cytometry, it is crucial to efficiently isolate and properly discriminate between the complex heterogeneous cell populations, irrespective of their partially overlapping surface marker expression pattern. cDC1 can be identified by the expression of CD8, CD103, CD24, and XCR1 [62,

Table 34. Reagents, antibodies, chemicals and solutions

Reagent	Manufacturer	Ordering Number
10× Dulbecco's Phosphate Buffered Saline (PBS) without calcium and magnesium	Carl Roth	9130.2
HBSS w/o: Phenol red, w: Ca and Mg, w: 0.35 g/L $NaHCO_3$	PAN Biotech	P04-32505
Heat-inactivated Fetal Calf Serum (FCS)	Sigma-Aldrich	F7524-500ML
BSA (Albumin bovine Fraction V)	SERVA	11930.04
EDTA Solution	Carl Roth	X986.3
NH_4Cl	Carl Roth	K298.1
$NaHCO_3$	Carl Roth	6885.2
DRAQ7	Biolegend	424001
Precision Count Beads	Biolegend	424902

84], while cDC2 express CD4, CD11b, and CD172α [62]. CD301b is exclusively expressed in Tbet$^-$ cDC2 [97, 98]. In the following protocol, we focus on cDC subsets and additionally characterize granulocytes (neutrophils, eosinophils), macrophage subsets (interstitial, alveolar), and monocyte subsets (Ly6c^{high} monocytes, Ly6c^{low} monocytes) in the homeostatic mouse lung using a 15 parameter flow cytometry panel.

2.3.2 *Materials*

2.3.2.1 Reagents. A complete list of reagents is provided in Tables 34 and 35.

2.3.2.2 Equipment. Necessary equipment is listed in Tables 36 and 37.

2.3.3 *Step-by-step sample preparation*

2.3.3.1 Preparation of buffer and antibody mix.

FACS Buffer
1× PBS with 0.5% BSA and 2 mM EDTA

DRAQ7 working solution
1:1000 in FACS buffer

RBC lysis buffer
8.32 g NH_4Cl, 0,84 g $NaHCO_3$, 0.043 g EDTA in 1 liter of H_20

2.3.3.2 Preparation of single cell suspension from mouse lung tissue.

In Section 1.3 "**Preparation of single-cell suspensions from mouse lung**", it is described how to isolate and prepare cell suspensions from mouse lung tissue for flow cytometry.

2.3.3.3 Antibody staining of single-cell suspensions from steady-state lung tissue for flow cytometry.

1. Centrifuge the single cell suspension for 5 min at 4°C and 363 x g. Discard the supernatant;
2. Resuspend cells in 200 μl antibody mix with 15 different surface markers. Transfer the cells to a FACS tube and incubate them for 45 min at 4°C in the dark;
3. Fill up with 3 mL FACS buffer, centrifuge, and discard the supernatant;
4. Resuspend cells in 1 mL RBC lysis buffer to remove erythrocytes. Incubate for 5 min at RT covered by foil. Do not exceed 5 min;
5. Fill up with 3 mL FACS buffer, centrifuge, and discard the supernatant;
6. Resuspend cells in 200 μl DRAQ7 working solution. Incubate 5 min at RT covered by foil. DRAQ7 stains dead cells and can be detected together with the Lineage in channel APC-Cy7;
7. Fill up with 3 mL FACS buffer, centrifuge, and discard the supernatant;
8. Resuspend cells in 500 μl FACS buffer and filter through 40 μm mesh before acquiring cell at flow cytometer;
9. If necessary, manually count your cells or add 30 μl Precision count beads to your sample to determine absolute cell numbers before acquiring your sample;
10. If necessary, add an individual amount of FACS buffer to your sample to adjust the cell concentration and events/s. Usually, we add additional 500 μl of FACS buffer after filtering and record the sample at a medium flow rate with approximately 6500 events/s;
11. Acquire at least 1.5 × 10^6 events.

2.3.4 *Data analysis*

To characterize cDC subsets in the mouse steady-state lung, we performed multicolor flow cytometry with subsequent data analysis using FlowJo (Fig. 19). After exclusion of debris from all events and two doublet exclusion gates, immune cells were identified by the expression of the pan-hematopoietic marker CD45. Next, we excluded lymphoid cells (B220$^+$ CD19$^+$ B cells, TCR-β$^+$ T cells, NK1.1$^+$ NKP46$^+$ NK cells, Ter-119$^+$ erythrocytes) and DRAQ7$^+$ apoptotic/dead cells by gating on Lin$^-$ cells in channel APC-Cy7. Ly-6G expression allowed unambiguous identification of neutrophils. Furthermore, macrophages were identified by a combined MerTk and CD64 expression followed by a subsequent division into alveolar macrophages (AM; CD64$^+$, MerTk$^+$, CD11b$^-$, SiglecF$^+$) and interstitial macrophages (IM; CD64$^+$, MerTk$^+$, CD11b$^+$, SiglecF$^-$). Expression of CD11c and MHC-II accompanied by CD26 expression and CD64 absence led to a clear identification of cDC. Comparison of XCR1 and CD172α expression allowed subdivision of cDC into cDC1 (CD64$^-$, MHC-II$^+$, CD11c$^+$, CD26$^+$, XCR1$^+$) and cDC2 (CD64$^-$, CD11c$^+$, MHC-II$^+$, CD26$^+$, CD172α$^+$). CD301b and CD11b provided additional help to characterize CD301b$^+$ cDC2 and CD301b$^-$ cDC2 subsets

Table 35. Antibodies

ANTIBODIES	FLUOROPHORE + DILUTION	SOURCE	IDENTIFIER
α-mouse B220, Clone: RA3-6B2	APC-Cy7 1:400	BioLegend	Cat# 103224, RRID:AB_313007
α-mouse CD11b, Clone: M1/70	BUV737 1:400	BD Biosciences	Cat#: 612800; RRID:AB_2870127
α-mouse CD11c, Clone: N418	PerCp-Cy5.5 1:100	BioLegend	Cat#: 117328; RRID:AB_2129641
α-mouse CD172α, Clone: P84	PE-CF594 1:200	BioLegend	Cat#: 144015; RRID:AB_2565279
α-mouse CD19, Clone: 6D5	APC-Cy7 1:200	BioLegend	Cat#: 115530; RRID:AB_830707
α-mouse CD26, Clone: H194-112	BV750 1:200	BD Biosciences	Cat# 624380 RRID:customs
α-mouse CD301b, Clone: URA-1	APC 1:200	BioLegend	Cat#: 146813; RRID:AB_2566024
α-mouse CD43, Clone: S7	BUV563 1:200	BD Biosciences	Cat# 741238, RRID:AB_2870790
α-mouse CD45, Clone: 30-F11	BUV805 1:200	BD Biosciences	Cat#: 748370; RRID:AB_2872789
α-mouse CD64, Clone: X54-5/7.1	PE-Cy7 1:100	BioLegend	Cat#: 139314; RRID:AB_2563904
α-mouse Ly-6c, Clone: HK1.4	BV711 1:200	BioLegend	Cat#: 128037; RRID:AB_2562630
α-mouse Ly-6g, Clone: 1A8	PE 1:200	BioLegend	Cat# 127608, RRID:AB_1186099
α-mouse MerTk, Clone: 2B10C42	BV421 1:200	BioLegend	Cat# 151510, RRID:AB_2832533
α-mouse MHC-II, Clone: M5/114.15.2	BV510 1:200	BioLegend	Cat#: 107636; RRID:AB_2734168
α-mouse NK1.1, Clone: PK136	APC-Cy7 1:200	BioLegend	Cat#: 108724; RRID:AB_830871
α-mouse NKP46, Clone: 29A1.4	APC-Cy7 1:200	BioLegend	Cat# 137631, RRID:AB_2617040
α-mouse SiglecF, Clone: E50-2440	BUV395 1:200	BD Biosciences	Cat#: 740280; RRID:AB_2740019
α-mouse TCR-β, Clone: H57-597	APC-Cy7 1:400	BioLegend	Cat# 109219, RRID:AB_893626
α-mouse TER-119, Clone: TER-119	APC-Cy7 1:200	BioLegend	Cat#: 116223; RRID:AB_2137788
α-mouse TruStain fcXTM (CD16/32), Clone: 93	- 1:200	BioLegend	Cat# 101319, RRID:AB_1574973
α-mouse XCR1, Clone: ZET	BV650 1:200	BioLegend	Cat# 148220, RRID:AB_2566410

in the mouse lung. After the exclusion of cDC, CD11b$^+$ positive cells were gated and further subdivided into SiglecF$^+$ eosinophils and monocytes (CD64^{mid}, CD11b$^+$, CD11c$^-$, MHC-II$^-$). Monocytes differentially express Ly6c and CD43 allowing grouping into Ly6c^{high} monocytes (Ly6c$^+$, CD43$^-$) and Ly6c^{low} monocytes (Ly6c$^-$, CD43$^+$). Taken together, the here shown gating approach is a solid tool to reliably characterize the myeloid cell compartment with focus on cDC subsets in the mouse steady-state lung.

To further visualize the pulmonary myeloid compartment in an unbiased manner, we performed an uniform-manifold approximation and projection (UMAP) analysis as previously described [99]. Single CD45$^+$ Lin$^-$ DRAQ7$^-$ cells were exported from FlowJo and used for the clustering. The clustering was based on the parameters of our 15-marker flow cytometry panel including FSC-A and SSC-A, but excluding CD45 – BUV805 and Lin – APC-Cy7. With the help of the gating strategy provided in Fig. 19, we were able to identify and annotate all relevant myeloid populations of the mouse lung (Fig. 20). AMs, neutrophils and eosinophils form clearly separated cluster, probably due to their exclusive expression of Ly-6g or SiglecF. Based on their overlapping surface marker expression pattern, IMs, cDC, and monocyte subsets cluster more closely together. We speculate

Table 36. Necessary equipment

Equipment	Company	Purpose
1.5 or 2 mL reaction tube	Eppendorf	For the preparation of the antibody staining mix
FACS tubes	Sarstedt	For FACS staining
Centrifuge "Allegra X-15R"	Beckman-Coulter	Centrifugation of 50 mL tubes, 15 mL tubes, and FACS tubes
FACS Symphony A5	BD	FACS analysis
FlowJo	Version 10.7.1	https://www.flowjo.com/solutions/flowjo/downloads
RStudio	Version 1.2.5033	https://www.rstudio.com/products/rstudio/download/

that unidentified cells between Ly6c^{hi} monocyte and cDC clusters might be immature precursor cells, such as pre-DC and pre-cDC, that are derived from MDPs (macrophage and DC precursors) [100] Furthermore, we hypothesize that the separated cluster of unidentified cells located to the right side of Ly6c^{hi} monocyte cluster might be lymphoid cells negative for our lineage markers, such as T cell subsets or innate lymphoid cells. Altogether, the resolution of our 15-marker flow cytometry panel allowed identification of all relevant myeloid subsets in the mouse steady-state lung in a manual gating analysis (Fig. 19) and in a non-linear dimensionality-reduction approach (Fig. 20).

2.3.5 *Pitfalls*

- Macrophages, especially alveolar macrophages, are high in forward and side scatter. Adjust the voltage carefully before recording the sample and be careful to not exclude them in the FSC-A vs. SSC-A gate of all events and in the subsequent doublet exclusion gates.
- pDC express B220, which is in our panel part of the lineage. Remove B220 from the lineage and add Siglec-H for pDC identification.

Table 37. Configuration of the flow cytometer FACS Symphony A5 in terms of lasers, power, position, filters and the fluorochrome of the respective channel

Laser	Power	Position	Filter	Longpass filter	Fluorochrome
355 nm	60 mW	A	810/40	770	BUV805
UV		B	735/30	690	BUV737
		C	670/25	630	BUV661
		D	605/20	595	BUV615
		E	580/20	550	BUV563
		F	515/30	450	BUV496
		G	379/28	–	BUV395
405 nm	200 mW	A	780/60	750	BV786
Violet		B	750/30	735	BV750
		C	710/20	685	BV711
		D	677/20	635	BV650
		E	605/40	595	BV605
		F	586/15	550	BV570
		G	525/50	505	BV510/BV480
		H	450/50	–	BV421
488 nm	200 mW	A	780/60	750	BB790
Blue		B	710/50	685	PerCp-Cy5.5
		C	670/30	635	BB660
		D	610/20	600	BB630
		E	530/30	505	FITC
		F	488/10		SSC
561 nm	200 mW	A	780/60	750	PE-Cy7
Yellow-Green		B	710/50	685	
		C	670/30	635	PE-Cy5
		D	610/20	600	PE-CF594
		E	586/15	570	PE
637 nm	140 mW	A	780/60	750	APC-Cy7
Red		B	730/45	690	Alexa Fluor 700
		C	670/14	665	APC/ Alexa Fluor 647

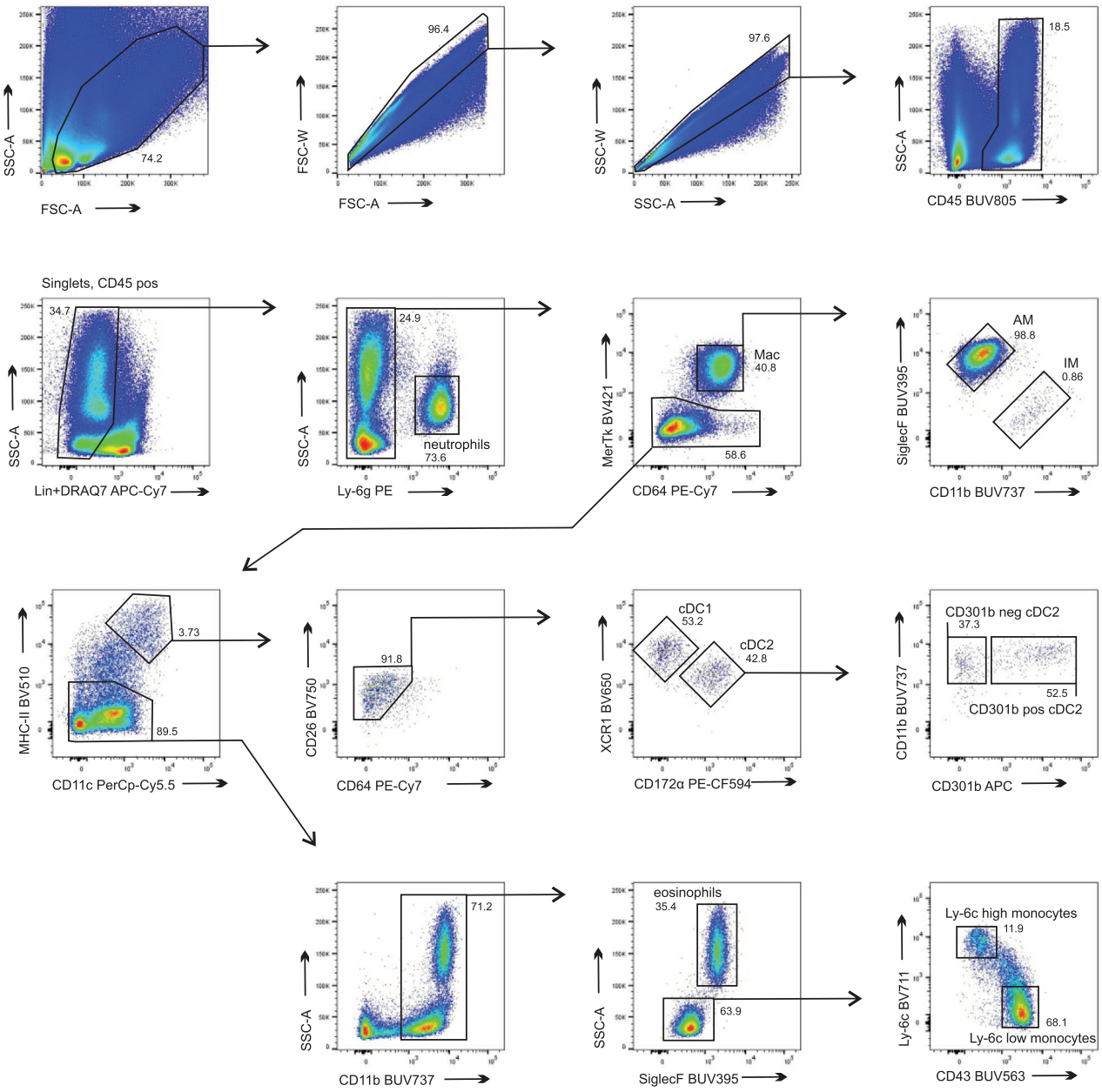

Figure 19. Representative gating strategy of the mouse pulmonary myeloid cell compartment with focus on cDC in the steady-state. Single cell suspension was prepared by enzymatic digestion of 8 weeks old C57BL/6 mouse lungs and afterward stained with a set of 15 surface markers. 3×10^6 events were recorded for subsequent identification of pulmonary myeloid populations. After the exclusion of debris and doublets, immune cells were identified by expression of CD45. Lineage-positive lymphoid cells ($B220^+$, $CD19^+$, $Nk\text{-}1.1^+$, $NKP46^+$, $Ter\text{-}119^+$, $TCR\text{-}\beta^+$) and dead cells ($DRAQ7^+$, in APC-Cy7) were excluded. Based on their surface marker expression pattern, all myeloid populations present in the mouse lung were identified.

- This panel was designed to detect myeloid cells and cDC subsets in the mouse steady-state lung and might need to be adjusted to detect DC during inflammatory conditions.
- PreDC, Pre-cDC1, and Pre-cDC2 can be detected by further addition of CD135, all progenitor subsets are positive for CD135. They can be separated from pDC by Siglec-H and CD135.
- CD301b is sensitive to cleavage by Dispase, do not use Dispase in your digestion mix if you are interested in CD301b detection.
- We do not recommend using CD3e as an additional T cell marker in the lineage as it can be expressed by macrophages in inflammatory conditions.

2.3.6 *Top tricks*

- As shown in Fig. 19, cDC1 and cDC2 can be nicely separated using XCR1 and CD172α.

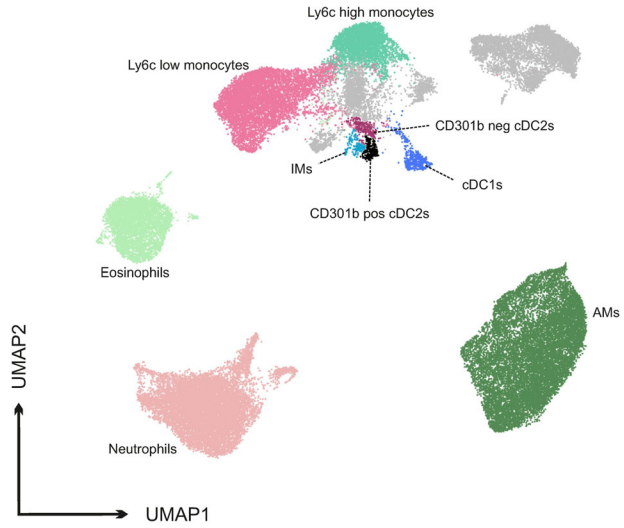

Figure 20. UMAP of the mouse pulmonary myeloid cell compartment with focus on cDC in the steady-state lung using a 15 marker flow cytometry panel. Single, CD45$^+$, Lin$^-$ DRAQ7$^-$ cells were exported after manual gating in FlowJo. Computational analysis was performed using the R script of *Becht et al.* as previously described by the authors [99]. SSC-A and FSC-A were included as parameters next to all surface markers except for CD45 and Lin. Threshold of cells included in the UMAP was set to 50k events. Cluster annotation was performed in FlowJo using the gating strategy described in Fig. 19. Unidentified cells are depicted in grey.

- In the case of monocyte subsets, CD43 can be replaced by CCR2 to obtain the classical monocyte waterfall.
- We recommend performing the RBC lysis after the antibody stain in order to preserve the epitopes.
- Alveolar macrophages are highly autofluorescent. An empty FITC channel can be used to further separate AMs from IMs.
- To obtain a clean population of living myeloid cells, include clean-up gates in your gating strategy, especially FCS-A vs. SSC-A to remove debris and SSC-A vs. Lin to remove dead cells.
- The cell quality after digestion of the mouse lung is suitable for single-cell RNA sequencing. We suggest to enrich myeloid cells using CD45 microbeads.
- This flow cytometry panel was designed to characterize DC subsets in the homeostatic mouse lung. In order to reliably characterize monocyte-derived DC and inflammatory cDC2 during inflammatory or infectious events, we recommend including Mar-1 and CD88. Monocyte-derived DC are CD11b$^+$ CD172α^+ F4/80$^+$ Mar-1$^+$ CD26$^-$, while inflammatory cDC2 can be identified by CD26$^+$ CD88$^+$ CX3CR1$^+$.
- If the reader is interested in pDC, B220 should be removed from the lineage and separately stained in a different channel, or alternatively PDCA-1/CD317 can be used.

2.3.7 *Summary of the phenotype*

The phenotype of granulocytes and myeloid cells identified by our panel is summarized in Table 38.

2.4 Flow cytometry analysis of DC subsets in mouse oral mucosa

2.4.1 *Introduction*

Dendritic cells (DC) represent a heterogeneous family of professional antigen-presenting cells (APC) that are key regulators balancing immunity versus tolerance [107]. Consequently, they are strategically positioned at epithelial borders to the environment like the oral mucosa, where they constantly probe the environment for invading pathogens and harmless foreign antigens. Upon capture of these antigens, DC migrate to draining lymph nodes (LN) to induce appropriate protective or tolerogenic T cell response [6, 108]. This balance is vital since its breakdown leads to dysbiosis resulting in periodontal diseases [31]. To be able to investigate and understand how DC execute these opposing tasks a detailed analysis of the phenotypically and functionally distinct DC subsets of the oral mucosa is necessary. An optimized digestion protocol for the mouse oral mucosa is provided in Section 1.4.

To date, we can distinguish three major subsets among APC present in oral tissues: Langerhans cells (LC), which are located in the epithelium, interstitial DC of the lamina propria, and macrophage-like cells that lack CD11c expression [30]. In the oral epithelium, LC represent 80–90% of APC and can be identified by the expression of CD11c, MHC-II, Langerin, and EpCam. They can be further separated into three subsets: CD103$^+$ LC which are CD11b^{low} and CD64^{neg}, CD11b$^+$ LC that are negative for both CD103 and CD64, and monocyte-derived (mo)LC (CD11b$^+$CD64$^+$CD103^{neg}). In contrast to LC, DC in the lamina propria lack expression of EpCam and can thereby be distinguished by flow cytometry. These interstitial DC can be divided into two main subsets according to their Sirpα and XCR1 expression. The major population of interstitial DC expresses Sirpα and CD11b (cDC2). Within the cDC1 population that express XCR1 a small subset of cells expressing CD103 can be identified.

In recent years, a lot of progress has been made to disentangle the phenotypic heterogeneity within the oral DC compartment, however, the exact functions of the different LC and DC subsets are only beginning to emerge. Using Langerin-DTR mice to inducibly deplete LC from the oral epithelium, we could demonstrate a protective immunoregulatory role of LC in a model of inflammation-induced alveolar bone resorption [32]. In contrast to epidermal LC, which originate from yolk sac-derived progenitors and fetal liver monocytes, oral mucosal LC arise from bone marrow-derived pre-DC and monocytes that enter the lamina propria via the circulation and differentiate into CD11c$^+$MHC-II$^+$ cells [109]. Signaling via BMP7 and its receptor ALK3 leads to the expression of CCR2 and CCR6, which facilitate the chemokine-dependent translocation of the precursors to the epithelium [110]. Here, TGF-β1 promotes the final LC differentiation [111]. To better understand the exact role of the different LC and DC subsets in the oral tissues it is important to study them by flow cytometry. In the following, we describe a detailed analysis of how to distinguish the different LC and DC populations.

Table 38. Summary of surface markers, localization of cells, and transcription factors of granulocytes and myeloid cells in the steady-state lung tissue

Population	Surface marker	Localization in tissue	Transcription factor
Alveolar macrophage	CD64$^+$, CD11b$^-$, CD11c$^+$, MHC-II$^+$, SiglecF$^+$	alveolar space	Bhlhe40, Bhlhe41 [101] PU.1, Egr1, Egr, MafB and c-Maf [102]
Interstitial macrophage	CD64$^+$, CD11b$^+$, CD11c$^+$, MHC-II$^+$, MerTk$^+$	interstitial space	Egr, MafB and c-Maf [102]
Ly6c^{high} monocytes	CD64^{mid}, CD11b$^+$, CD11c$^-$, MHC-II$^-$, Ly6c$^+$	interstitial space / intravascular space	Egr, MafB and c-Maf [102]
Ly6c^{low} monocytes	CD64^{mid}, CD11b$^+$, CD11c^{mid}, MHC-II$^-$, Ly6c$^-$, CD43$^+$	interstitial space /intravascular space	Egr, MafB and c-Maf [102]
CD301b$^+$ cDC2	CD64$^-$, CD11b$^+$, CD11c$^+$, MHCI-I$^+$, CD26$^+$, CD172α^+, CD301b$^+$	interstitial space, next to alveolar ducts	ZBTB46 [103] IRF4 [104] RORγt$^+$, Tbet$^-$ [97]
CD301b$^-$ cDC2	CD64$^-$, CD11b$^+$, CD11c$^+$, MHC-II$^+$, CD26$^+$, CD172α^+, CD301b$^-$	interstitial space, next to alveolar ducts	ZBTB46 [103] IRF4 [104] Tbet [97]
cDC1	CD64$^-$, CD11b$^-$, MHC-II$^+$, CD11c$^+$, CD26$^+$, XCR1$^+$	interstitial space, next to airways and subpleural region	ZBTB46 [103] IRF8, ID2 [105] BATF3 [90]
Neutrophils	CD64$^-$, CD11b$^+$, CD11c$^-$, MHC-II$^-$, Ly6g$^+$	interstitial space / intravascular space	PU.1, C/EBPα, Gfi1, MPO, ELANE, CEBPE, LEF-1 later stages: PU.1, C/EBPβ, C/EBPδ and C/EBPγ [106]
Eosinophils	CD64$^-$, CD11b$^+$, CD11c$^-$, MHC-II$^-$, SiglecF$^+$	interstitial space / intravascular space	PU.1^{int}, GATA-1/2^{hi}, C/EBPα^{hi} [106]

2.4.2 *Materials*

2.4.2.1 Reagents. A complete list of reagents is provided in Table 39.

2.4.2.2 Equipment. Necessary equipment is listed in Tables 40 and 41.

2.4.3 *Step-by-step sample preparation*

2.4.3.1 Preparation of buffer and antibody mix.

FCS: Quickly thaw FCS at 37°C in a water bath. Once completely thawed, incubate for 60 min at 56°C in the water bath to destroy complement activity. Aliquot the FCS into 50 mL portions and store at −20°C. Avoid freeze-thaw cycles. Use aseptic techniques during the whole procedure.

FACS buffer: Add 2% FCS (v/v) to 500 mL of PBS.

Intracellular staining buffer: Intracellular staining will be performed using the BD Cytofix/Cytoperm^{TM} Fixation/Permeabilization Kit according to the manufacturer's instructions (BD Biosciences). For this, prepare the 1× working solution of Permeabilization/Wash (Perm/Wash) buffer by mixing 1 part of the 10× concentrate with 9 parts of MilliQ. Alternatively, cells can be fixed with 2% Roti®-Histofix and permeabilized using Saponin buffer (FACS buffer containing 0.5% Saponin). Use the Saponin buffer also to dilute the intracellular antibody and for the washing steps after intracellular staining.

Antibody mix: Basic antibody staining mix (in Brilliant Stain Buffer Plus): Prepare 50 µl of antibody staining mix per sample containing the final dilution of the antibodies listed in Table 41. Intracellular antibody staining mix (in 1× Perm/Wash buffer): Prepare 50 µl of antibody staining mix per sample containing the final dilution of the antibody listed in Table 42.

2.4.3.2 Isolation and preparation of single cell suspensions from oral mucosal tissues. In Section 1.4 "**Preparation of single cell suspensions from mouse oral mucosa**", we provide a detailed protocol on how to isolate the gingiva, buccal mucosa, and tongue from the mouse oral cavity, followed by instructions on how to obtain single-cell suspensions from these tissues for further analysis by flow cytometry.

2.4.3.3 Antibody staining of single-cell suspensions from oral mucosal tissues for flow cytometry.

1. Transfer the isolated cells to a 96-well V-bottom plate and store it at 4°C or on ice until the staining mix is prepared;
2. Prepare 50 µl of antibody staining mix per sample in a 1.5 mL Eppendorf tube;
3. Centrifuge the cells for 5 min at 400 × *g* and 4°C;

Table 39. Reagents, antibodies, chemicals, and solutions

Reagent	Manufacturer	Ordering Number
Antibodies		
αB220 BUV496 (RA3-6B2)	BD	612950
αCD172a (SIRP α) BUV563 (P84)	BD	741349
αCD24 BUV661 (M1/69)	BD	750679
αF4/80 BUV737 (T45-2342)	BD	749283
αCD45pan BUV805 (30-F11)	BD	748370
αLy6C BV570 (HK1.4)	BioLegend	128030
αCD11b BV605 (M1/70)	BD	563015
αXCR1 BV650 (ZET)	BioLegend	148220
αLy6G BV750 (1A8)	BD	747072
αI-A/I-E (MHC-II) BV786 (M5/114.15.2)	BD	742894
αCD103 PerCP-Cy5.5 (2E7)	BioLegend	121416
αCD64 PE (X54-5/7.1)	BioLegend	139304
αCD11c APC-R700 (N418)	BD	565872
αCX3CR1 BB790-P (Z8-50)	BD	Costum
αCD326 (EpCam) PE-Cy7 (G8.8)	eBioscience	25-5791
αCD207 (Langerin) Alexa-647 (929F3.01)	Dendritics	DDX0362
Chemicals & Solutions		
Dulbecco's Phosphate Buffered Saline (PBS) without calcium and magnesium	Sigma	D8537
Fetal Bovine Serum (FCS)	Sigma	F7524
Brilliant Stain Buffer Plus	BD	566385
Cytofix/Cytoperm™ Fixation/Permeablization Kit	BD	554714
4% Roti®-Histofix	Roth	P087.5
Fixable Viability Stain (FVS780)	eBioscience	65-0865

Table 41. Data acquisition setup of the Symphony flow cytometer

Laser line	Filter Longpass	Filter Bandpass	Fluorochrome
Ultra Violet 355 nm	450 LP	515/30 BP	BUV496
	550 LP	580/20 BP	BUV563
	660 LP	670/25 BP	BUV661
	690 LP	735/30 BP	BUV737
	770 LP	810/40 BP	BUV805
Violet 405 nm	550 LP	586/15 BP	BV570
	595 LP	605/40 BP	BV605
	635 LP	677/20 BP	BV650
	735 LP	750/30 BP	BV750
	750 LP	780/60 BP	BV786
Blue 488 nm	770 LP	820/60 BP	BB790-P
	685 LP	710/50 BP	PerCP-Cy5.5
YellowGreen 561 nm	570 LP	586/15 BP	PE
	750 LP	780/60 BP	PE-Cy7
	635 LP	670/30 BP	PE-Cy5
Red 637 nm	690 LP	730/45 BP	APC-R700
	750 LP	780/60 BP	eF780
	655 LP	670/30 BP	AF647

4. Discard the supernatant and dip the plate on a paper towel up-side-down to remove any residual liquid;
5. Calculate the amount of Fc-block and prepare it in 25 μl FACS buffer per well (to avoid unspecific recognition of staining antibodies by cell-bound Fc-gamma receptors);
6. Resuspend the cells in 25 μl of Fc-Block and incubate for 10 min at 4°C;
7. Centrifuge the plate for 5 min at 400 × *g* and 4°C;
8. Discard the supernatant and dip the plate on a paper towel up-side-down to remove any residual liquid;
9. Resuspend each sample in 50 μl of the first antibody staining mix and incubate for 30 min at 4°C;
10. Add 100 μl of FACS buffer per sample;
11. Centrifuge the plate for 5 min at 400 × *g* and 4°C;
12. Discard the supernatant and dip the plate on a paper towel up-side-down to remove any residual liquid;
13. Wash the cells by adding 150 μl FACS buffer and pipetting up and down;
14. Centrifuge the plate for 5 min at 400 × *g* and 4°C;
15. Discard the supernatant and dip the plate on a paper towel up-side-down to remove any residual liquid;
16. Repeat step 13–15;
17. Resuspend the cells in 100 μl Fixation/Permeabilization solution (BD Cytofix/Cytoperm™ Kit);
18. Incubate the cells for 30 min at 4°C in the dark;

Table 40. Necessary equipment

Equipment	Company	Purpose
Centrifuge Z 446 K	HERMLE Labortechnik GmbH	Centrifugation of 50 mL tubes and V-bottom plates
PipetBoy	Fisher Scientific	Pipetting
96-well V-bottom plate	Greiner bio-one	Sample preparation for flow cytometry
50 mL tubes	Falcon	Centrifugation of single-cell suspensions
1.5 mL Eppendorf tubes	SARSTEDT AG & Co. KG	For the preparation of the antibody staining mix
FACS tubes	BD	For sample acquisition at the flow cytometer
FACSymphony™ A5	BD	Flow cytometry analysis of single-cell suspensions

Table 42. Dilution of antibodies used for flow cytometry

Excitation Laser Line	Fluorophore	Antigen	Clone	#Catalog	Company	Dilution
Ultra Violet (355 nm)	BUV496	B220	RA3-6B2	612950	BD	1:500
	BUV563	CD172a (SIRP α)	P84	741349	BD	1:400
	BUV661	CD24	M1/69	750679	BD	1:500
	BUV737	F4/80	T45-2342	749283	BD	1:500
	BUV805	CD45pan	30-F11	748370	BD	1:400
Violet (405 nm)	BV570	Ly6C	HK1.4	128030	BioLegend	1:400
	BV605	CD11b	HK1.4	563015	BD	1:500
	BV650	XCR1	ZET	148220	BioLegend	1:500
	BV750	Ly6G	1A8	747072	BD	1:400
	BV786	αI-A/I-E (MHC-II)	M5/114.15.2	742894	BD	1:400
Blue (488 nm)	BB790-P	CX3CR1	Z8-50	Costum	BD	1:200
	PerCP- Cy5.5	CD103	2E7	121416	BioLegend	1:100
YellowGreen (561 nm)	PE	CD64	X54-5/7.1	139304	BioLegend	1:500
	PE-Cy7	CD326 (EpCam)	G8.8	25-5791	eBioscience	1:800
Red (637 nm)	APC-R700	CD11c	N418	565872	BD	1:500
	FVS780	Live/Dead		65-0865	eBioscience	1:1000

Table 43. Dilution of intracellular antibody used for flow cytometry

Exitation Laser Line	Fluorophore	Antigen	Clone	#Catalog	Company	Dilution
Red (637 nm)	Alexa647	CD207 (Langerin)	929F3.01	DDX0362	Dendritics	1:200

19. In the meantime, prepare 50 μl of intracellular antibody staining mix (Table 42) per sample in a 1.5 mL Eppendorf tube;
20. Centrifuge the plate for 5 min at 400 × *g* and 4°C;
21. Discard the supernatant and dip the plate on a paper towel up-side-down to remove any residual liquid;
22. Wash the cells by adding 150 μl FACS buffer and pipetting up and down;
23. Centrifuge the plate for 5 min at 400 × *g* and 4°C;
24. Discard the supernatant and dip the plate on a paper towel up-side-down to remove any residual liquid;
25. Repeat step 22 to 24;
26. Resuspend each sample in 50 μl of intracellular antibody staining mix (Table 43) and incubate for 60 min at 4°C;
27. Wash the cells by adding 150 μl Perm/Wash buffer and pipetting up and down;
28. Centrifuge the plate for 5 min at 400 × *g* and 4°C;
29. Discard the supernatant and dip the plate on a paper towel up-side-down to remove any residual liquid;
30. Repeat step 27 to 29;
31. Resuspend the cells in 100 μl FACS buffer;
32. The cells can be acquired directly or kept dark in the fridge until acquiring at the flow cytometer.

2.4.4 *Data analysis*

Data acquisition was performed at a FACSymphony (BD) equipped with 355 nm, 405 nm, 488 nm, 561 nm, and 637 nm laser lines. Data were analyzed using the FlowJo 10.5.3 software. The gating strategy provided in Fig. 21 shows an example for the identification of LC and DC in the gingiva and can be applied to other oral tissues like the buccal mucosa and tongue.

First, cells were gated according to their size (FSC-A/SSC-A) to exclude debris. After doublet removal (FSC-A/FSC-H) living $CD45^+$ hematopoietic cells were selected by gating on viability $dye^{neg}CD45^+$ cells. Neutrophils which are present in higher numbers in the gingiva compared to the buccal mucosa and tongue were identified by the expression of Ly6G. From the $Ly6G^{neg}$ population APC were analyzed by gating CD11c versus MHC-II. While the majority of $MHC\text{-}II^+CD11c^{neg}$ cells represent B cells, macrophages can be identified by the expression of CD11b and F4/80. In order to distinguish the different gingival DC populations, $CD11c^+MHC\text{-}II^+$ cells were further divided into interstitial DC and LC. While LC express the epithelial cell adhesion molecule EpCam interstitial DC can be identified as $EpCam^{neg}$ cells. In contrast to skin LC oral mucosal LC can be further distinguished into

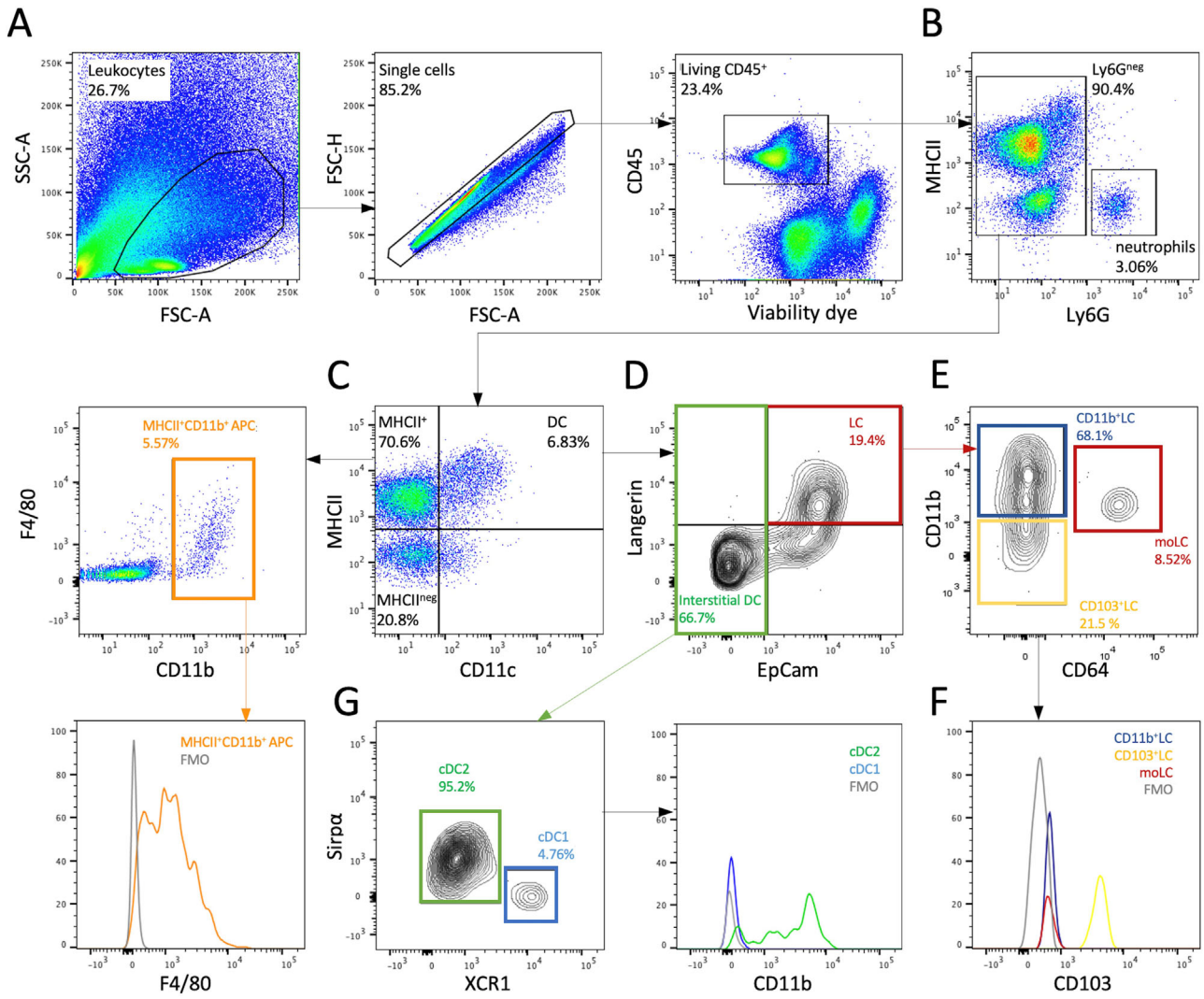

Figure 21. Flow cytometry analysis of DC and LC subsets in oral mucosal tissue. (A) Cells are pre-gated according to their size (FSC-A/SSC-A) to exclude debris. Single cells are determined by the area and height of FSC. After the elimination of dead cells by gating on the fixable viability dye negative population, living CD45$^+$ hematopoietic cells were selected. (B) Neutrophils were excluded by their Ly6G expression and MHC-II$^+$ cells were further gated on (C) MHC-II$^+$CD11c^{neg} APC or MHC-II$^+$CD11c$^+$ DC. While the majority of MHC-II$^+$ APC represent B cells (according to their size and granularity) a minor population of MHC-II$^+$CD11b$^+$ macrophages can be identified by the expression of CD11b and F4/80. CD11c$^+$MHC-II$^+$ cells consist of (D) EpCam$^+$Langerin$^+$ LC and EpCam$^-$ interstitial DC. (E) LC can be further separated into 3 subsets using CD11b and CD64: CD11b$^+$ LC which are CD11b$^+$CD64^{neg}, CD103$^+$ LC which are CD11b^{low}CD64^{neg} and moLC that express CD11b together with CD64. (F) Depiction of the CD103 expression on the different LC subsets. While CD11b$^+$LC (F: blue line) and moLC (F: red line) are negative for CD103, CD103$^+$ LC are positive (F: yellow line). (G) Interstitial DC were divided into cDC1 and cDC2 according to their Sirpα and XCR1 expression. While cDC1 (Sirpα^{neg}XCR1$^+$) are negative for CD11b (G: blue line), the majority of cDC2 (Sirpα$^+$XCR1^{neg}) express CD11b (G: green line). Data acquisition was performed at a BD FACSymphony A5 cell analyzer and data was analyzed using FlowJo V10.5.3 software. APC: antigen-presenting cells, cDC1: conventional dendritic cells type 1, cDC2: conventional dendritic cells type 2, LC: Langerhans cells, FMO: fluorescence minus one.

three different subpopulations based on their CD11b and CD64 expression. MoLC are the minor LC population in all oral tissues characterized by the coexpression of CD11b and CD64. Among the CD64^{neg} cells CD11b$^+$ LC and CD103$^+$ LC (CD11b^{neg}) can be identified. Within the lamina propria cDC can be further separated into cDC1 and cDC2 based on the expression of XCR1 and Sirpα, respectively. While cDC1 represent only a small population of DC high frequencies of cDC2 can be detected in all different oral mucosal tissues.

2.4.5 *Pitfalls*

- Please note that antibody concentrations need to be adjusted to the flow cytometer and its lasers and the suggested antibody dilutions in Table 42 are optimized for the FACSymphony^{TM} A5 cell analyzer from BD.
- Varying DC subset distribution in the different oral mucosal tissues can be observed as every tissue has its unique leukocyte compartment.

Table 44. Summary of marker expression on the analyzed mononuclear phagocyte populations

Population	Marker negative	Marker positive
CD11b$^+$LC	Ly6G, CD103, CD64	CD11c, MHC-II, CD24, Langerin, EpCam, CD11b
CD103$^+$LC	Ly6G, CD64	CD11c, MHC-II, CD24, Langerin, EpCam, CD11b^{int}, CD103
moLC	Ly6G, CD103	CD11c, MHC-II, CD24, Langerin, EpCam, CD11b, CD64
cDC2	Ly6G, EpCam, CD24, Langerin	CD11c, MHC-II, Sirpα, CD11b
cDC1	Ly6G, EpCam, Sirpα, Langerin	CD11c, MHC-II, CD24, XCR1, CD103$^{+/-}$
Macrophage-like cells	Ly6G, CD11c, EpCam, Langerin, Sirpα, XCR1	MHC-II, CD11b, F4/80, CD64

- Unspecific recognition of staining antibodies by cell-bound Fc-gamma receptors can be avoided by commercially available purified rat anti-mouse anti-CD16/32 to block the Fc-gamma RIIB/III receptors.
- In contrast to the skin, in oral tissues CD24 does not correlate with Langerin and can therefore not be used as a replacement to avoid intracellular staining.

2.4.6 *Top tricks*

- To analyze subpopulations of rare cell types like LC we recommend pooling oral tissues from 3 to 5 mice per sample to ensure a proper FACS analysis.
- To avoid cell loss during acquisition, increase the volume of FACS buffer used to resuspend the cells before acquiring.
- It is recommended to use a specialized Brilliant Stain Buffer for the first antibody staining mix to eliminate non-specific reactivity between the polymer-based fluorochromes as this can result in under-compensation of the data.

2.4.7 *Summary of the phenotype*

The overall phenotype of DC and LC covered by the markers included in the panel is detailed in Table 44.

2.5 Flow cytometry analysis of DC subsets in mouse kidney

2.5.1 *Introduction*

Dendritic cells (DC) are potent inducers of immune responses that are particularly proficient at presenting antigens to T cells. They continuously survey tissues for signs of infection or tissue damage and help control barrier integrity and tissue homeostasis [112]. In kidneys, DC exhibit a prominent phenotypic overlap with other mononuclear phagocytes (MPs), particularly macrophages [33, 34]. As a result, few studies have addressed the unique functions of kidney DC subsets in immunity. Studies in rodents indicate that renal MPs can promote but also dampen inflammation and the resulting kidney damage [33–35]. Therefore, a better understanding of DC dynamics and function in steady state and inflammation could help improve immune therapies for patients suffering from kidney disease.

The adult mouse kidney contains at least four subsets of MPs with prominent *Clec9a*-expression history, which is indicative of a DC origin [113, 114]. These cells express varying levels of CD11c and include the main cDC1 and cDC2 subtypes as well as two CD64-expressing subtypes that can be identified as CD11b^{hi}F4/80^{low} and F4/80^{hi}CD11b^{low} cells. Kidney cDC1 express the canonical cDC1 markers, including XCR-1, CLEC9A, CD24 as well as high levels of IRF8, whereas cDC2 are marked by CD11b, CD172a and express high levels of IRF4 [62, 113, 114]. CD64$^+$CD11b^{hi}F4/80^{low} DC strongly resemble CD64 negative cDC2, however, they are transcriptionally distinct and exhibit some differences in their ability to respond to pathogenic stimuli. F4/80^{hi} MPs phenotypically and transcriptionally resemble embryonic-derived macrophages, although they appear ontogenetically distinct and can be distinguish from embryonic macrophages by the expression of MHC-II and a lack of TIM4 and MerTK [114]. Whether F4/80^{hi} cells in the kidney should be classified as macrophages or DC has been matter of a long-standing debate [114, 115–119] and therefore it is important to note that these cells have been referred to as DC and macrophages.

With the advancement of single cell transcriptomics and multiparameter flow cytometry, the phenotypic heterogeneity within the kidney DC compartment has become obvious. However, the exact functions of the different DC subsets in the kidney remain poorly studied. We have recently revisited the role of MPs in cisplatin-induced kidney injury using cell type-specific depletion models. We found that the intrinsic potency reported for CD11c$^+$ cells to limit cisplatin toxicity is specifically attributed to CD64$^+$ DC, while cDC1 and cDC2 are dispensable [120]. In nephrotoxic nephritis on the other hand, it has been shown that cDC1 protect the tissue, while cDC2 seem to play a pro-inflammatory role [121, 122]. These data highlight the need to better understand the exact role of the different DC and macrophage subsets in the

Table 45. Antibodies

Antibodies	Fluorophore	Company	Clone	Dilution
CD3ε	PeCy5	BioLegend	145-2C11	1:300
CD11b	BUV737	BD	M1/70	1:800
CD11c	BV786	BioLegend	N418	1:200
CD16/CD32	Purified	BD	2.4G2	1:300
CD19	BV650	BioLegend	6D5	1:200
CD24	BUV395	BD	M1/69	1:400
CD45.2	PeCy7	BioLegend	104	1:300
CD45R/B220	PE	BioLegend	RA3-6B2	1:200
CD64 (FcγRI)	PE	BioLegend	X54-5/7.1	1:200
CD103	BUV395	BD	M290	1:300
XCR1	BV650	BioLegend	ZET	1:200
F4/80	AF647	BioLegend	BM8	1:300
I-A/I-E (MHC-II)	AF700	BioLegend	M5/114.15.2	1:300
Ly-6C	BV605	BioLegend	HK1.5	1:200
Ly-6G	PerCPCy5.5	BioLegend	1A8	1:200
DAPI		Sigma		1:50

kidney, which necessitates to study them by flow cytometry. In the following, we describe a detailed analysis of how to distinguish the different DC populations in the steady state kidney.

2.5.2 *Materials*

2.5.2.1 Reagents. A complete list of reagents is provided in Tables 45–48.

2.5.3 *Step-by-step sample preparation*

2.5.3.1 Preparation of buffer and antibody mix.

FACS buffer (PBS, 1% FCS, 0,2% Sodium Azide)

Thaw heat-inactivated FCS. Avoid freeze–thaw cycles for FCS. When kept sterile FCS can be stored contamination free at 4°C for some time. Under sterile conditions (cell culture hood) add 5 mL FCS and 2.5 mL of 0.5 M EDTA solution to 500 mL of Phosphate buffered saline (PBS). Finally, add 1 mL of a 10% Sodium Azide solution. Sodium Azide is anti-microbial and therefore helps keep the FACS buffer contamination free. It also interferes with membrane mobility, which increases surface staining intensity of some epitopes, as it inhibits endocytosis-mediated downregulation of receptors. **TIP**: Sodium Azide leads to cell death and must not be used when cells are to be sorted for functional analyses.

Table 46. Reagents

Reagent	Manufacturer	Order number
Dulbecco's Phosphate Buffered Saline without calcium and magnesium	Sigma	D8537-500ML
Fetal Bovine Serum (FCS)	Sigma	F7524
0,5M EDTA	Thermo Fisher	15575020
Sodium Azid	MERCK	26628-22-8

2.5.3.2 Isolation and preparation of single-cell suspensions from mouse kidneys. In Section 1.4 "**Preparation of single-cell suspensions from mouse kidney**" we provide a detailed protocol on how to isolate the kidney followed by instructions on how to obtain single-cell suspensions from these tissues for further analysis by flow cytometry.

2.5.3.3 Antibody staining of single-cell suspensions from the kidney for flow cytometry.

1. Transfer the required amount of cells into a 96-well V-bottom plate. Centrifuge at 400 × g (ca. 1350 rpm at Rmax) for 3 min at 4°C.
2. Discard supernatant by quickly inverting the plate over a waste container and then tap the plate onto a paper towel to collect the last drops of liquid (for this step it is critical to hold the plate upside down until dipping onto paper to avoid cell loss).
3. Resuspend cells in 25 μl FACS buffer. (Cells can be stored at 4°C or on ice until the Fc-Block and staining mix are prepared).
4. Prepare a 2× master mix of Fc-block reagent by multiplying the number of samples (plus one extra well) by 25 μl. Then add the required amount of Fc-block (to avoid unspecific binding of staining antibodies to Fc-gamma receptors).
5. Add 25 μl 2× Fc-block mix and incubate for 10 min at 4°C (or on ice). **TIP**: This incubation step can be extended (for instance if preparation of the staining master mix takes longer).
6. Prepare 50 μl of 2× antibody staining mix per sample in a 1.5 mL Eppendorf tube;
7. Add 50 μl 2× antibody staining mix to each sample and incubate for 30 min at 4°C.
8. Add 100 μl of FACS buffer per sample.
9. Centrifuge at 400 × *g* for 3 min at 4°C.
10. Discard supernatant by quickly inverting the plate over a waste container and then dipping the plate onto a paper towel to collect the last drops of liquid.
11. Resuspend cells in 200 μl of FACS buffer.
12. Repeat steps 9–11.
13. Resuspend cells in 100 μl and store in the dark until acquisition.
14. Before acquisition filter cells through a 100 μm strainer to avoid clogging of the FACS machine. **TIP**: Check the standard operating procedures of your local FACS facilities to help you prepare your samples properly and according to standards of the local facility.

Table 47. Necessary equipment/Software

Equipment	Manufacturer	Step
Centrifuge 'MULTIFUGE X3R'	Thermo Fisher	Centrifugation of 50 mL tubes, 15 mL tubes, and V-bottom plates
1.2 mL individual reaction tubes 'E1710-0000'	Starlab	To store kidney immune cell suspension
96well v-bottom plate '277143'	Thermo Fisher	To stain cell suspension with antibody for FACS
Strainer 'PA80N'	Josef Hepfinger KG München	To filter cell isolated from kidney
LSR Fortessa	BD	Data Acquisition
FlowJo v.10	FlowJo, LLC	Data analysis (alternative software can be used)

Preparation of single color control samples

For each fluorophore, a single color control sample must be prepared to compensate fluorescent spill over. This is a sample that is stained with only one antibody from the antibody mix. Single color controls can be generated using compensation beads, which bind antibodies nonspecifically. This is preferable if cells are limited or the antibody that needs to be compensated produces a weak fluorescent signal or stains only a small fraction of cells. We recommend using mouse spleen cells, when possible, to generate single color controls, as this also takes into account other properties of cells such as size, granularity, and autofluorescence. In this case, about 2–4 million splenocytes are stained with individual antibodies as described above and at the same concentration. Fc-block is not necessary for single-color controls. Importantly, the staining intensity of the single color control must be as bright or brighter as in the sample for the experiment to be set up and compensated properly.

Table 48. Equipment Specifications Fortessa

Laser	Long pass filter	Band Pass Filter	Fluorophore
UV 355 nm		**379/28**	BUV395
		450/50	DAPI
	690	**740/35**	BUV737
Violet 405 nm		**450/50**	
	505	**525/50**	
	595	**610/20**	BV605
	630	**670/30**	BV650
	685	**710/50**	
	750	**780/60**	BV786
Blue 488 nm	**505**	**530/30**	
	595	**710/50**	PerCPCy5.5
YG 561 nm		**586/15**	Pe
	600	**610/20**	
	635	**670/30**	PeCy5
	750	**780/60**	PeCy7
Red 640 nm		**670/14**	AF647
	690	**730/45**	AF700
	750	**780/60**	

2.5.4 *Data analysis*

Cell acquisition is performed by using BD LSR Fortessa equipped with 355 nm, 405 nm, 488 nm, 561 nm, and 640 nm lasers. Analysis was performed using FlowJo software (v.10). In the following, we show the gating strategy of kidney immune cell populations, all antibodies we used in this panel are shown in Table 45.

Figure 22 shows the gating strategy for DC identification in adult mouse kidney. First, CD45.2 live cells are gated, followed by a leukocyte scatter gate that identifies leukocytes based on their size (FSC) and granularity (SSC). Single cells are then identified as indicated and are first distinguished into MHC-II$^-$ and MHC-II$^+$ cells. Within the MHC-II$^+$ gate Ly-6C-negative cells are then gated. Ly-6C$^+$ cells resemble monocytes, but a connection to transitional DC cannot be excluded. In a further step, CD19$^+$ B cells are identified and DC are gated as CD19-negative cells and first subdivided into CD11c$^+$CD64$^-$ and CD64$^+$ cells. The CD11c$^+$CD64$^-$ cDC can be separated into CD24$^+$ cDC1 and CD11b$^+$ cDC2. The CD64$^+$ cells can further be divided into F4/80^{hi} and CD11b^{hi} DC. These cell types do not fit the classical cDC1/cDC2 scheme and F4/80^{hi} cells resemble macrophages and have been called as such, while CD11b^{hi} cells have also been called CD64$^+$ cDC2 [62]. Within the MHC-II$^-$ kidney fraction CD11b$^+$ cells contain neutrophils and monocytes based on Ly-6G and Ly-6C expression, respectively. CD11b$^-$ cells contain mostly CD3$^+$ T cells. Please note that CD24$^+$ cDC1 from mouse kidney also express the cDC1 marker XCR1 whereas only a fraction of cells express the cDC1 activation marker CD103 (Fig. 22B). It is also important to note that DC dynamics change in conditions of inflammation (Fig. 22C).

2.5.5 *Pitfalls*

- Please note that antibody concentrations may need to be adjusted to your experimental conditions and the flow cytometer used. The described panel has been optimized BD LSR Fortessa equipped with 355, 405, 488, 561, and 640 nm lasers.
- The kidney contains many autofluorescent non-leukocytes that can appear as a diagonal tails in the live/dead marker against CD45 plot. To avoid this population which makes it difficult to discern leukocytes, make sure to optimize the collection step

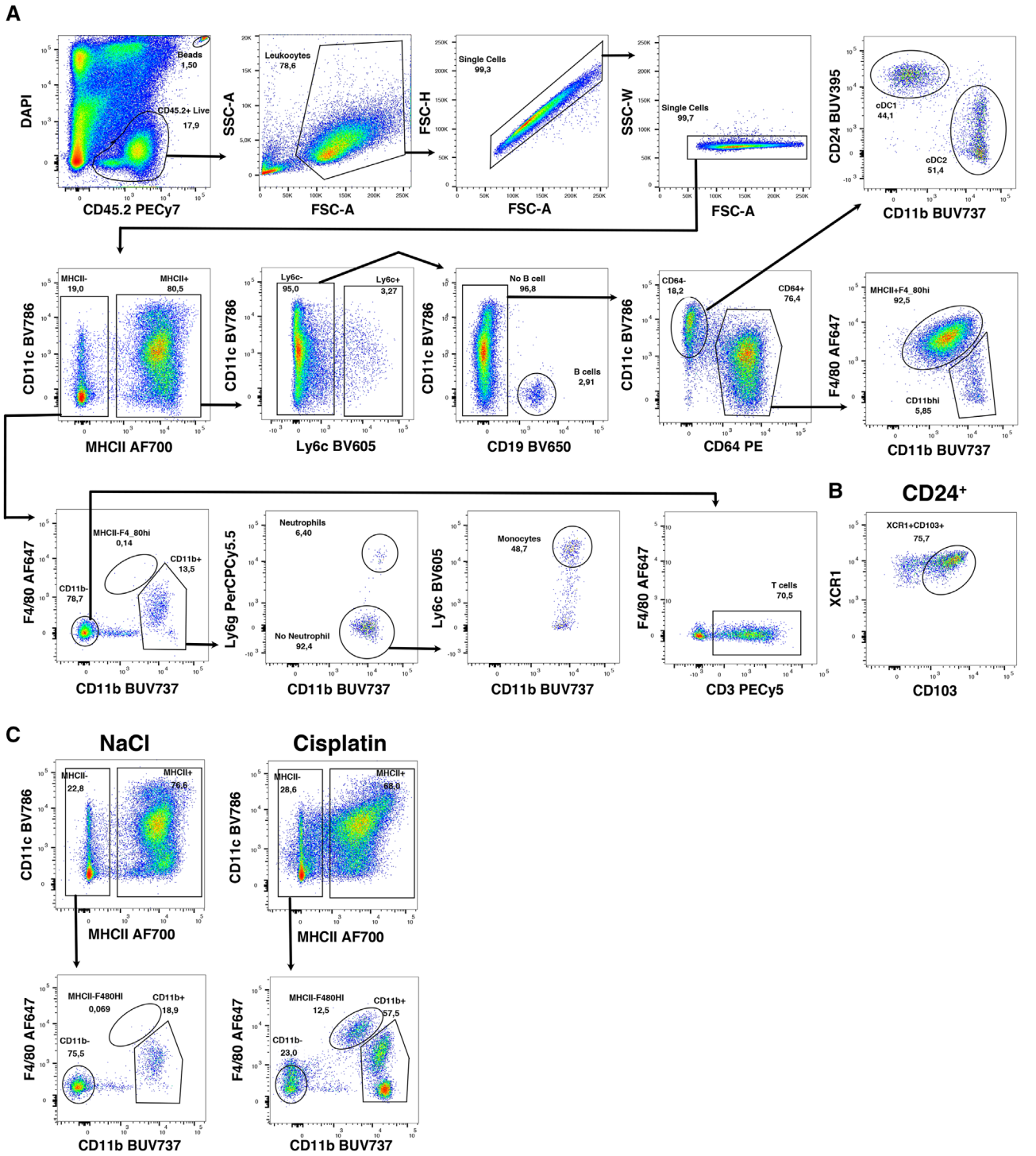

Figure 22. Gating strategy to identify the main DC subsets and other kidney resident immune cells. **A.** CD45.2 live cells are gated, followed by a leukocyte scatter gate that is based on the size and granularity of leukocytes. Single cells are then identified as indicated. Within single leukocytes, cells are first distinguished as MHC-II$^-$ and MHC-II$^+$ cells. Within the MHC-II$^+$ gate Ly-6C-negative cells are then gated. In a further step CD19$^+$ B cells and CD19$^-$ cells are identified, the latter can be further subdivided into CD11c$^+$CD64$^-$ and CD64$^+$ cells. The CD11c$^+$CD64- cDC can be separated into CD24$^+$ cDC1 and CD11b$^+$ cDC2. The CD64$^+$ cells can further be divided into F4/80^{hi} and CD11b^{hi} DC. Within the MHC-II$^-$ cells, the CD11b$^+$ cells contain neutrophils and monocytes based on Ly-6G and Ly-6C expression, respectively. CD11b$^-$ cells contain mostly CD3$^+$ T cells. **B.** A representative staining of XCR1 and CD103 on CD24$^+$ DC from mouse kidney is shown. Please note that all CD24$^+$ cDC1 as identified above express the cDC1 marker XCR1 whereas only a fraction of cells expresses the cDC1 activation marker CD103. **C.** DC dynamics change in inflammation. Shown are representative FACS plots of single leukocytes isolated from mouse kidney three days after treatment of mice with NaCl or Cisplatin to induce acute kidney inflammation. Please note the downregulation of MHC-II and appearance of an MHC-II$^-$F4/80^{hi} population that results from downregulation of MHC-II from CD64$^+$F4/80^{hi} DC [114, 117].

Table 49. Summary of the phenotypes of the main DC subsets in the adult mouse kidney

Population	Phenotype summary as used in the panel (all subsets $CD3^-$, $CD19^-$, $Ly6C^-$)	Additional markers delineating these subsets (5–7, 16–19)
cDC1	MHC-II^+, $CD11c^+$, $XCR1^+$, $CD24^+$, $CD103^+$	$ZBTB46^+$, $IRF8^{high}$, $IRF4^{low}$, $CX3CR1^-$, $CLEC9A^+$
cDC2	MHC-II^+, $CD11c^+$, $CD24^-$, $CD103^-$, $CD11b^+$, $CD172a^+$, $F4/80^{int/low,}$	$ZBTB46^+$, $IRF4^+$, $IRF8^{low}$, $CX3CR1^{low}$
$CD11b^{high}$	MHC-II^+, $CD11c^+$, $CD24^-$, $CD103^-$, $CD64^+$, $CD11b^{high}$, $CD172a^+$, $F4/80^{int/low}$,	$ZBTB46^+$, $IRF4^+$, $IRF8^{low}$, $CX3CR1^{high}$
$F4/80^{high}$	MHC-II^+, $CD11c^+$, $CD24^-$, $CD103^-$, $CD172a^+$, $CD64^+$, $CD11b^{low}$, $F4/80^{high}$	$ZBTB46^{low}$, $IRF4^{low}$, $IRF8^{low}$, $CX3CR1^{high}$, $CD14^+$

from the Percoll gradient or try to increase the amount of viability dye.
- The above panel does not include markers to reliably identify plasmacytoid DC (pDC) because steady state kidney contains few. As pDC contribute to kidney immunity markers to survey pDC may prove important during analysis in inflammatory conditions.
- DC dynamics change in inflammation (Fig. 22C), which needs to be considered during experimental planning.
- Please note that kidney DC subsets exhibit age-dependent developmental heterogeneity, also leading to age-dependent differences in marker expression [114].
- CD26 expression may additionally help to distinguish $F4/80^{high}$ cells from the other DC subtypes in the mouse kidney [62].

2.5.6 *Top tricks*

- Kidneys contain many non-leukocytes. Despite the use of Percoll gradient for the generation of a single cell suspension, many autofluorescent non-leukocytes will be isolated during the procedure. To distinguish leukocytes we strongly advise to include the pan leukocyte marker CD45 in the analysis (see Fig. 22).
- Varying DC subset distribution has been observed between medulla and cortex. It is possible generate single cell suspension from the separate areas and analyze cortex and medulla DC separately (see our protocol on single cell isolation from mouse kidneys).
- The above protocol uses DAPI to distinguish dead cells. However, the use of alternative and fixable viability dyes is possible.
- Staining time can be reduced or may need to be extended.
- Staining of some surface receptors require incubations steps at room temperature or 37°C for optimal staining.
- Characterizing DC may require cell quantification. This can be achieved using counting beads by adding counting beads at a defined concentration to the FACS sample before acquisition.

2.5.7 *Summary of Phenotype*

Table 49 gives an overview on the main myeloid populations that can be identified the mouse kidney.

2.6 Flow cytometry analysis of DC subsets in mouse mammary glands

2.6.1 *Introduction*

Mammary gland (MG) is a very dynamic, secretory organ, undergoing remodeling at various phases during adult life [38]. At puberty, for example, the MG ductal tree massively expands into a highly branched network of ducts. Pregnancy and lactation are another phase of enormous tissue remodeling, with lobuloalveolar structures that develop to produce and secrete milk proteins. Finally, weaning induces the MG to revert to its pre-pregnancy state via a process called involution characterized by massive cell death. MG is seeded with immune cells, which change in relative abundance throughout the various phases of tissue remodeling [123]. Several immune cell populations contribute to tissue remodeling [38]. Macrophages are best studied in this context [124].

Dendritic cells (DC) have also been found in MG [41–43]. Very little, however, is known about their subset composition, function, and phenotype at the various phases of MG remodeling. Interestingly, Betts et al. classified MG as a temporal mucosal tissue, especially during lactation and involution [41]. The presence of milk proteins and microbes during lactation, and the potential exposure to self-antigens during involution, likely requires a state of immune tolerance in MG. Indeed, tolerogenic DC and reduced Ag-dependent T cell proliferation were found in MG. So far, a detailed analysis of DC subsets in MG lacks, as does the understanding about their precise location. Moreover, CD11c and MHC-II, markers typically used to identify classical DC (cDC) are also expressed by MG macrophages. It is, therefore, important to carefully separate macrophage from cDC, especially cDC2, which requires the inclusion of macrophage markers such as F4/80 or CD64 [42].

Here we describe a gating strategy for DC subsets in stromal and ductal fractions of MG, using markers that are generally used to identify DC in other lymphoid and non-lymphoid tissues. These markers include XCR1 and CD24 for cDC1, CD11b, and CD172a for cDC2, and Siglec-H for plasmacytoid DC (pDC). Expression of other markers such as CD103 and CD8-α was analyzed as well. In the stromal fraction, we find enrichment of cDC, pDC, stromal macrophages, and eosinophils. The ductal fraction is enriched in ductal macrophages and epithelial cells, but also contains some DC.

Table 50. Reagents, antibodies, chemicals, and solutions*

Reagent	Manufacturer	Ordering Number
Antibodies		
αCD3ε Biotin (145-2C11)	BioLegend	100304
αCD19 Biotin (1D3)	BioLegend	553784
αNK1.1 Biotin (PK136)	BioLegend	108704
αTer119 Biotin (TER-119)	BioLegend	116204
αCD8α PE-cy7 (53-6.7)	BioLegend	100722
αCD11b PE-Dazzle594 (M1/70)	BioLegend	101256
αCD11b BV510 (M1/70)	BioLegend	101263
αF4/80 APC (BM8)	BioLegend	123116
αCD45.2 BV650 (104)	BioLegend	109836
αCD24 FITC (M1/69)	eBioscience	11-0242
αMHC-II BV785 (I-A/I-E) (M5/114.15.2)	BioLegend	107645
αMHC-II PerCP-cy5.5 (I-A/I-E) (M5/114.15.2)	BioLegend	107626
αXCR1 BV421 (ZET)	BioLegend	148210
αXCR1 FITC (ZET)	BioLegend	148216
αCD172a PerCP-cy5.5 (P84)	BioLegend	144010
αSiglec-H SB600 (440c)	eBioscience	63-0333
αCD11c PE-cy7 (N418)	BioLegend	117318
αCD11c BV785 (N418)	BioLegend	117336
αCD103 PE (2E7)	eBioscience	12-1031
αSiglec-F BV421 (E50-2440)	BD	562681
Streptavidin PE-cy5.5	Thermo Scientific	SA1018
Purified αFcγRIIB/III (2.4G2)	BioLegend	101302
Chemicals & Solutions		
Zombie NIR Fixable Viability Kit	BioLegend	423106
Dulbecco's Phosphate Buffered Saline (PBS), no calcium, no magnesium	Thermo Scientific	14190169
Fetal Bovine Serum (FBS)	Gibco	10270106
UltraPure 0.5M EDTA, pH8.0	Thermo Scientific	15575020
Brilliant stain buffer	BD	566349

* Reagents can be purchased from other vendors. For antibodies, alternative clones and fluorophores can be used but should be tested in advance.

Table 51. Necessary equipment*

Equipment	Company	Purpose
Centrifuge "Heraeus megafuge 16 series"	Thermo Scientific	Centrifugation of 50 mL tubes
PipetteBoy	Integra	Pipetting
Serological pipettes 5 mL (#606180)	Greiner bio-one	Pipetting
Sample tube, 5 mL (#55.1579)	Sarstedt	5 mL polystyrene tubes used for staining and acquiring single cell suspensions
Round-Bottom Tubes with Cell Strainer Cap, 5 mL (#352235)	Corning	Filtration of cell suspensions
LSR Fortessa (4 lasers)	BD	Flow cytometry acquisition
Flowjo Software version 10.5.3	BD	Analysis of acquired flow cytometry data

* Equipment can be purchased from other vendors

Table 52. Data acquisition setup: LSR Fortessa 4 laser flow cytometer

Laser line	Filter		Fluorochrome	
	Long pass	Band pass	Standard	Alternative
405 nm	NA	450/50	BV421	
	505 LP	525/50	BV510	
	595 LP	610/20	BV605	SB600
	630 LP	670/30	BV650	
	690 LP	710/50	BV711	
	750 LP	780/60	BV786	
488 nm	NA	488/10	SSC	
	505 LP	530/30	FITC	
	655 LP	695/40	PerCP-cy5.5	
561 nm	570 LP	586/15	PE	
	600 LP	610/20	PE-CF594	PE-Dazzle594
	635 LP	670/30	PE-cy5	
	685 LP	710/50	PE-cy5.5	
	750 LP	780/60	PE-cy7	
640 nm	NA	670/14	APC	
	690 LP	730/45	AF700	
	750 LP	780/60	APC-cy7	Zombie NIR

2.6.2 *Materials*

2.6.2.1 Reagents. A complete list of reagents is provided in Table 50.

2.6.2.2 Equipment. Necessary equipment is listed in Tables 51 and 52.

2.6.3 *Step-by-step sample preparation*

2.6.3.1 Preparation of stocks and solutions.

Zombie NIR

Dissolve lyophilized Zombie NIR dye in 100 μl of anhydrous DMSO (delivered with the kit) at room temperature. Resuspend until all powder is dissolved. Prepare 5 μl aliquots and store at −20°C. Right before use, thaw one aliquot and dilute Zombie NIR 1:1000 in PBS at room temperature. Prepare 100 μl per sample.

Staining buffer

Supplement PBS with 1% FBS (v/v) and 5 mM EDTA and use at 4°C.

Table 53. Antibody mix 1

Fluorophore	Antigen	Clone	#Catalog	Company	Dilution
Biotin	CD3ε	145-2C11	100304	BioLegend	1:400
Biotin	CD19	1D3	553784	BioLegend	1:400
Biotin	NK1.1	PK136	108704	BioLegend	1:400
Biotin	Ter119	TER-119	116204	BioLegend	1:400
BV421	Siglec-F	E50-2440	562681	BD	1:200
BV510	CD11b	M1/70	101263	BioLegend	1:200
BV650	CD45.2	104	109836	BioLegend	1:200
BV785	MHC-II	M5/114.15.2	107645	BioLegend	1:2000
FITC	XCR1	ZET	148216	BioLegend	1:200
PerCP-cy5.5	CD172a	P84	144010	BioLegend	1:200
PE	CD209	927	127019	BioLegend	1:200
PE-cy7	CD11c	N418	117318	BioLegend	1:200
APC	F4/80	BM8	123116	BioLegend	1:200

Table 54. Antibody mix 2

Fluorophore	Antigen	Clone	#Catalog	Company	Dilution
Biotin	CD3ε	145-2C11	100304	BioLegend	1:400
Biotin	CD19	1D3	553784	BioLegend	1:400
Biotin	NK1.1	PK136	108704	BioLegend	1:400
Biotin	Ter119	TER-119	116204	BioLegend	1:400
BV421	XCR1	ZET	148210	BioLegend	1:200
SB600	Siglec-H	440c	63-0333	eBioscience	1:200
BV650	CD45.2	104	109836	BioLegend	1:200
BV785	CD11c	N418	117336	BioLegend	1:200
FITC	CD24	M1/69	11-0242	eBioscience	1:200
PerCP-cy5.5	MHC-II	M5/114.15.2	107626	BioLegend	1:800
PE	CD103	2E7	12-1031	eBioscience	1:200
PE-CF594	CD11b	M1/70	101256	BioLegend	1:1000
PE-cy7	CD8α	53-6.7	100722	BioLegend	1:200
APC	F4/80	BM8	123116	BioLegend	1:200

Table 55. Streptavidin solution

Fluorophore	Antigen	Clone	#Catalog	Company	Dilution
PE-cy5.5	Streptavidin	–	SA1018	Thermo Scientific	1:1000

Blocking solution

Prepare 50 μl blocking solution per sample by diluting purified αFcγRIIB/III 1:50 in staining buffer.

Antibody mixes

Dilute the antibodies and streptavidin as indicated in Tables 53–55 in brilliant stain buffer, use 50 μl per sample. Fluorochrome combinations are chosen in function of the flow cytometer used, in this case, a 4 laser LSR Fortessa (405 nm, 488 nm, 561 nm, and 640 nm, Table 52).

2.6.3.2 Preparation of single cell suspension from mammary gland.

In Section 1.6 "**Preparation of single cell suspensions from mouse mammary gland**", it is described how to isolate stromal and ductal fractions of mammary gland tissue for flow cytometry. For both fractions, all cells isolated from one mouse are stained with fluorophore-labeled antibodies for analysis of DC subsets.

2.6.3.3 Antibody staining of single-cell suspensions from mammary gland for flow cytometry.

1. Transfer single cell suspensions into sample tubes, each sample is split over 2 tubes;
2. Spin cells down for 5 min at 400 × *g*;
3. Resuspend pellet in 2 mL PBS;
4. Spin cells down again for 5 min at 400 × *g*;
5. Resuspend cells in 100 μl diluted Zombie NIR;
6. Incubate cells for 30 min in the dark at room temperature;
7. Add 2 mL staining buffer;
8. Spin cells down for 5 min at 400 × *g* and 4°C;
9. Resuspend pellet in 50 μl blocking solution;
10. Incubate cells for 10 min at 4°C;

Table 56. Overview of identified immune cell populations and their phenotype

Population	Marker negative	Marker positive
cDC1	Zombie-NIR, CD3, CD19, Ter-119, NK1.1, Siglec-F, F4/80, CD172a, Siglec-H	CD11c, MHC-II, XCR1, CD24
cDC2	Zombie-NIR, CD3, CD19, Ter-119, NK1.1, Siglec-F, F4/80, XCR1, Siglec-H	CD11c, MHC-II, CD172a, CD11b
Plasmacytoid DC (pDC)	Zombie-NIR, CD3, CD19, Ter-119, NK1.1, F4/80,	Siglec-H
Ductal macrophages (DM)	Zombie-NIR, CD3, CD19, Ter-119, NK1.1, Siglec-F	F4/80, CD11c, MHC-II
Stromal macrophages (SM)	Zombie-NIR, CD3, CD19, Ter-119, NK1.1, Siglec-F	F4/80, MHC-II
Eosinophils	Zombie-NIR, CD3, CD19, Ter-119, NK1.1,	Siglec-F

11. Prepare antibody mix 1 and 2 according to Tables 53 and 54, respectively;
12. Add 50 μl antibody mix to the cells;
13. Mix well and incubate further for 30 min at 4°C;
14. Add 2 mL staining buffer;
15. Spin cells down for 5 min at 400 × *g* and 4°C;
16. Prepare streptavidin solution according to Table 55;
17. Resuspend pellet in 100 μl streptavidin solution;
18. Incubate cells for 20 min at 4°C;
19. Add 2 mL staining buffer;
20. Spin cells down for 5 min at 400 × *g* and 4°C;
21. Resuspend pellet in 300 μl staining buffer;
22. Right before acquiring, filter the cell suspension through a cell strainer;
23. Acquisition was done on the same day.

2.6.4 *Data analysis*

Data acquisition was performed at a BD LSR Fortessa equipped with 405, 488, 561, and 640 nm laser lines. Data analysis was done using FlowJo software. We used two panels of antibodies to identify DC subsets, macrophages, eosinophils, and epithelial cells in stroma and ducts of mouse mammary gland (Fig. 23A and B). In addition, we show expression of further surface markers specific for cDC1 and cDC2 (Fig. 23C).

The gating strategy for cDC1, cDC2, stromal and ductal macrophages, and eosinophils is shown in Fig. 23A. Siglec-F^{+} eosinophils (Eos) are clearly enriched in the stromal fraction. To separate cDC from macrophages (mPh), we used F4/80 but in addition CD64 can be used, as virtually all macrophages in mammary gland express both markers. Several surface markers to identify cDC, such as MHC-II, CD11c, and CD11b, are expressed by macrophages as well. During digestion, we separated stromal and ductal fractions of mammary gland. Indeed, stromal macrophages (SM), which are identified as MHC-II^{high} CD11c^{low} CD11b^{high}, are more frequent in the stromal fraction whereas ductal macrophages (DM), characterized as F4/80^{+} MHC-II^{high} CD11c^{high} CD11b^{low}, are enriched in the ductal fraction (Fig. 23A). In the F4/80^{-} MHC-II^{high} CD11c^{high} fraction, the typical cDC1 and cDC2 markers XCR1 and CD172a are used to separate these two cDC subsets. They are both found in stromal and ductal fractions. Furthermore, all cDC1 express CD24 but only part of them is positive for CD103 and CD8-α (Fig. 23C). The majority of cDC2 expresses CD11b. In Fig. 23B, the gating strategy for pDC and epithelial cells (EC) is presented. As expected, CD24^{+} CD45.2^{-} EC are strongly enriched in the ductal fraction. Small populations of Siglec-H^{+} CD11c^{low} pDC are found in stromal and ductal fractions.

The summary of markers to identify DC subsets, macrophages, eosinophils, and epithelial cells is given in Table 56.

2.6.5 *Pitfalls*

Problem: Suboptimal signal for surface markers

- Different antibodies, antibody clones, fluorophores and their combinations can be used, but should always be tested and titrated. Which fluorophores to use depends a lot on the flow cytometer used. Always check the laser lines and filter sets, as they might vary from standard settings. If that is the case, alternative fluorophores might have to be selected to avoid suboptimal results. In this protocol two panels of antibodies are listed (Table 53 and 54). However, depending on the flow cytometer at hand and the antibodies of interest, the two panels can be combined in one panel.
- If significantly more or less cells are used per staining e.g., when cells from several mice are pooled or if cells from one single MG are used, it is recommended to adjust the antibody dilutions to avoid a too low or too high fluorescent signal.
- Enzymes used for tissue digestion and single-cell preparation might affect cell surface proteins. The protocol "**Preparation of single-cell suspensions from mouse mammary gland**" (Section 1.6) uses collagenase IV and DNase I, of which no influence on surface markers was noticed. However, several other protocols used to digest mammary gland tissue apply hyaluronidase, trypsin, or other blends of proteases. It should be tested carefully how these enzymes affect the surface markers.

2.6.6 *Top tricks*

- 96 well plates can be used to stain cells for flow cytometry, in case many samples need to be stained at once or if the

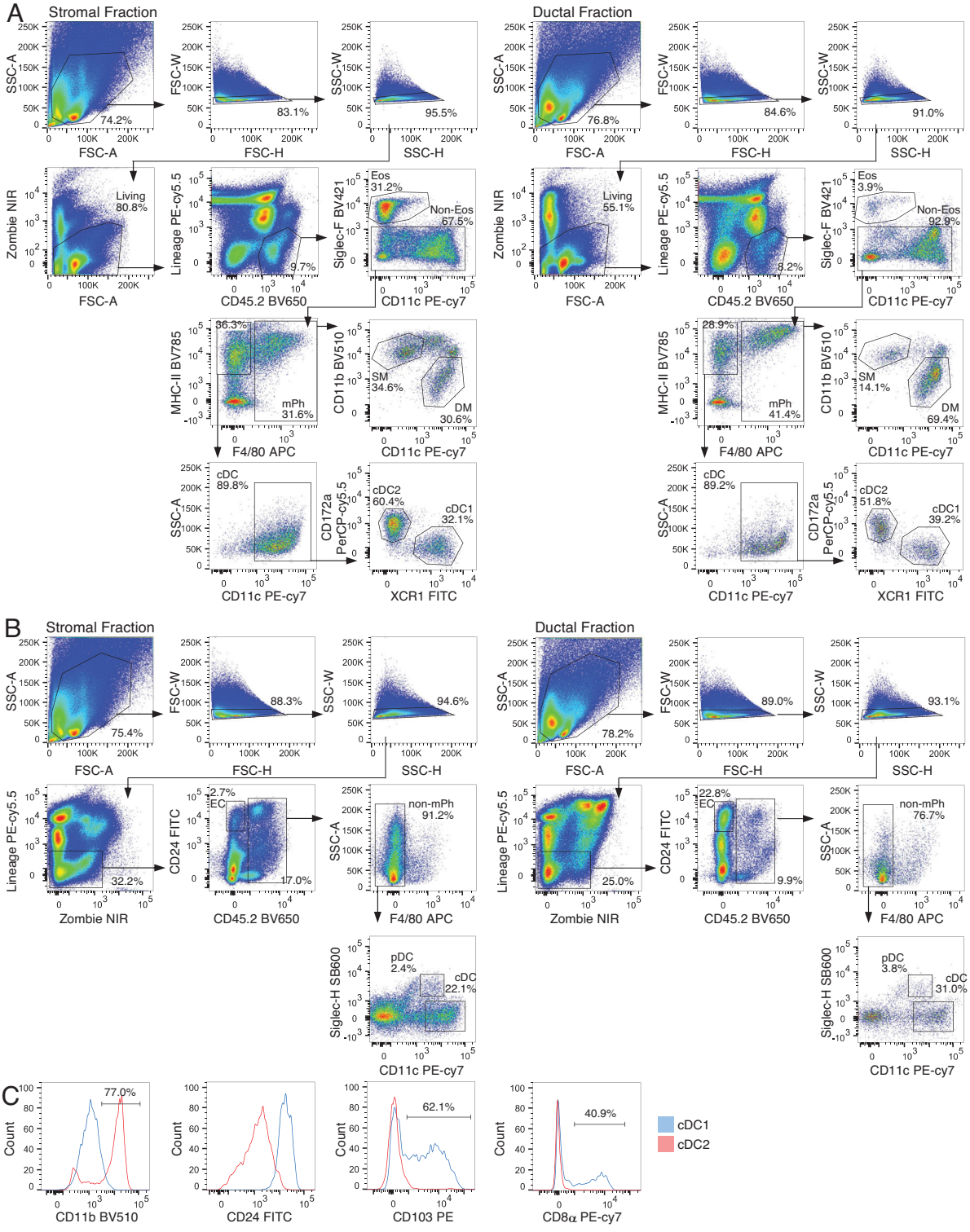

Figure 23. Gating strategy for dendritic cell subsets in mammary gland. (A) Cells from stromal and ductal fractions stained with antibody mix 1. First, dead cells (Zombie-NIR$^+$) and doublets are excluded. Next, CD45.2$^+$, lineage-negative cells are selected. After excluding Siglec-F$^+$ eosinophils (Eos), macrophages (mPh, F4/80$^+$) and DC (F4/80$^-$ MHC-II$^+$) are separated. Macrophages are split into ductal macrophages (DM, CD11c^{high} CD11b^{low}) and stromal macrophages (SM, CD11c^{low} CD11b^{high}). cDC are further selected by CD11c expression and split into cDC1 (XCR1$^+$ CD172a$^-$) and cDC2 (XCR1$^-$ CD172a$^+$). (B) Cells from stromal and ductal fractions stained with antibody mix 2. Single, living (Zombie-NIR$^-$), lineage-negative cells are selected. Next, hematopoietic (CD45.2$^+$) cells are separated from epithelial cells (EC, CD24$^+$ CD45.2$^-$). From the CD45.2$^+$ population, macrophages are excluded by F4/80 and non-macrophage cells are further split into Siglec-H$^+$ CD11c^{intermediate} pDC and Siglec-H$^-$ CD11c^{high} cDC. (C) Expression of further surface marker on cDC1 (blue) and cDC2 (red). Gates show the frequency of cDC2 positive for CD11b and of cDC1 positive for CD103 and CD8-α.

Table 57. Reagents, antibodies, chemicals and solutions

Reagent	Manufacturer	Ordering Number
Dulbecco's Phosphate Buffered Saline (PBS) without calcium and magnesium	Gibco	14190-094
Heat-inactivated Fetal Calf Serum (FCS)	PAN Biotech	P30-3031
BSA (Albumin bovine Fraction V)	SERVA	11930
AccuGENE^{TM} 0.5 M EDTA Solution	Lonza AccuGene	51201
Deoxyribonuclease I (DNAse I)	Sigma Aldrich	DN-25
Fc-Block – purified anti-CD16/CD32 antibody (clone 2.4G2)	TONBO Bioscience	70-0161
eFluor-780 fixable viability dye (eF780)	eBioscience	65-0865-14
Brilliant Staining buffer	BD	563794

centrifuge at hand does not have suitable holders for the sample tubes used in this protocol.
- Splitting the MG ductal and stromal fraction helps to discriminate cDC from macrophages. Although the separation is not absolute, CD11c^{high} MHC-II^{high} cDC are clearly enriched in the stromal fraction whereas CD11c^{high} MHC-II^{high} ductal macrophages are mostly found in the ductal fraction.
- Using a fixable viability dye allows to include intracellular staining protocols for example for transcription factors or cytokines.
- The set of biotinylated antibodies can be expanded to exclude more cell populations in the 'lineage-positive' fraction. This might allow using more antibodies to stain DC.

2.6.7 *Summary of the phenotype*

Table 56 lists the immune cell populations that can be identified using the antibody combinations described in this protocol.

2.7 Flow cytometry analysis of DC subsets in transplantable mouse melanoma

2.7.1 *Introduction*

Dendritic cells (DC), as the most potent antigen-presenting cells of the immune system, have the ability to capture and present antigens and activate T lymphocytes via co-stimulatory receptor-upregulation and cytokine production. By inducing CD4$^+$ and CD8$^+$ T cell responses, DC play a crucial role in adaptive immunity and contribute to immune responses against pathogens, allergens and cancer [125, 126]. This unique function makes them key regulators in the context of cancer. Within the tumor microenvironment (TME), DC capture antigens from tumor cells and migrate to the tumor-draining lymph nodes, where they present them to T cells [127].

Mouse DC are characterized by the expression of CD11c and MHC class II and can be divided into two major branches, the conventional DC (cDC), which can be further subdivided into cDC1 and cDC2, and the plasmacytoid DC (pDC). The latter are responsible for the production of type I interferons in response to pathogens, while showing poor ability to prime naïve T cells [128, 129]. The development of cDC1 is regulated by the transcription factors (TF) BATF3, IRF8, and ID2 [130]. This DC subset can be characterized by the surface expression of the chemokine receptor XCR1 [131]. cDC1 are known as the main producers of IL-12 and they are specialized for cross-presentation of antigens to CD8$^+$ T cells. Several studies have underlined the relevance of cDC1 in anti-tumor immunity [132–134]. In contrast, cDC2 development depends on the TF IRF4, ZEB2, and RELB. cDC2 are defined by their surface expression of CD11b and are mainly responsible for polarizing CD4$^+$ T helper cell responses [129, 130].

We here describe the flow cytometry protocol for the characterization of myeloid cell populations with a specific focus on DC from mouse transplantable D4M tumors. The panel allows a detailed separation of the mouse DC subsets cDC1 and cDC2 with simultaneous identification of NK cells, T cells, B cells as well as monocytes, neutrophils, and macrophages. Due to inclusion of additional markers characterizing DC, the migratory status (CCR7), activation (CD40) and expression of inhibitory molecules (PD-L1, PD-L2) can be determined on the various DC subsets. The definition of myeloid subsets relies on markers described in healthy tissue [5, 62, 135]. As myeloid cells show high plasticity, many of those discriminatory markers change in the TME and as DC share many markers with macrophages, especially under inflammatory conditions or in tumor context, multiple markers are required to allow DC subset discrimination from other myeloid cells. Moreover, by using a DC-specific reporter mouse, namely the Zbtb46-GFP, in which all cDC express a GFP signal, we are able to confirm the proper dissection of DC and macrophages [103].

2.7.2 *Materials*

2.7.2.1 Reagents. A complete list of reagents is provided in Tables 57 and 58.

2.7.2.2 Equipment. Necessary equipment is listed in Tables 59 and 60.

Table 58. Antibodies and reagents

Specificity	Fluorochrome	Clone	Manufacturer	Catalog #	Dilution
NK1.1	BB630	PK136	BD	Custom-made	1:200
CD19	BB660	1D3	BD	Custom-made	1:400
CD40	BB700	3/23	BD	742136	1:100
CD103	BB790	M290	BD	Custom-made	1:200
F4/80	PE-Dazzle594	BM8	Biolegend	123146	1:100
CD3e	PE-Cy5	145-2C11	BD	553065	1:200
CD64	PE-Cy7	X54	Biolegend	139314	1:200
CCR7	APC	4B12	Biolegend	120108	1:50
PD-L2	APC-R700	TY25	BD	Custom-made	1:100
Viabilty dye eF780	APC-Cy7	–	eBioscience	65-0865-14	1:5000
Ly-6C	BV421	HK1.4	Biolegend	128031	1:200
MHC class II	BV480	M5/114	BD	566086	1:400
Ly-6G	BV570	1A8	BD	Custom-made	1:200
CD115	BV605	T38-320	BD	743640	1:100
XCR1	BV650	ZET	Biolegend	148220	1:400
CCR2	BV711	475301	BD	747964	1:400
pDCA-1	BV750	927	BD	747608	1:400
CD24	BV786	M1/69	BD	744470	1:400
CD11c	BUV395	N418	BD	744180	1:100
CD11b	BUV496	M1/70	BD	Custom-made	1:400
MerTK	BUV563	108928	BD	Custom-made	1:50
PD-L1	BUV615	MIH5	BD	Custom-made	1:400
CD4	BUV661	RM4-5	BD	741461	1:400
CD8a	BUV737	53-6.7	BD	612759	1:400
CD45	BUV805	30-F11	BD	748370	1:200

2.7.3 *Step-by-step sample preparation*

2.7.3.1 Preparation of Buffers.

Staining buffer:

Supplement PBS with 1% BSA, 50 μM EDTA and 50 μg/mL DNase I.

Live/Dead dye solution:

Dilute eFluor-780 fixable viability dye 1:5000 in PBS.

Brilliant Staining buffer

Mix 1 part of Staining buffer with 1 part of Brilliant Staining buffer.

2.7.3.2 Preparation of single cell suspension from mouse transplantable tumors. In Section 1.7 "**Preparation of single-cell suspensions from transplantable mouse melanoma**", it is described how to digest transplantable tumors to obtain single cell suspension for flow cytometry.

2.7.3.3 Antibody staining protocol for tumor single cell suspensions.

1. Use between 3-4 × 10^6 cells per staining. Pellet cells by centrifugation at 485 × *g* for 5 min at 4°C in 5 mL polystyrene round bottom tubes;
2. Resuspend cells in 1 mL of Staining buffer and centrifuge cells at 485 × *g* for 5 min at 4°C and discard supernatant;

Table 59. Necessary equipment

Equipment	Company	Purpose
1.5 mL or 2 mL reaction tube	Eppendorf	For preparation of the antibody staining mix
15 mL canonical tube	FALCON	For preparation of live/dead dye solution
5 mL polystyrene round bottom tubes	FALCON	For flow cytometry staining
Serological pipettes (5 mL/10 mL/25 mL)	Greiner Bio-One	Pipetting
50 mL tubes	Falcon	Centrifugation of single-cell suspensions
Incubator	Thermo Scientific	For staining of chemokine receptors at 37°C
Centrifuge	Heraeus Multifuge 3 S-R	Centrifugation of 5 mL polystyrene round bottom tubes
Aurora spectral flow cytometer	Cytek®	Flow cytometry analysis

Table 60. Aurora Configuration

Wavelength (nm)	Laser power (mW)	Channel	Center Wavelength (nm)	Bandwidth (nm)	Fluorochrome (Peak intensity)
UV laser					
355	20	UV1	373	15	
		UV2	388	15	BUV395
		UV3	428	15	
		UV4	443	15	
		UV5	458	15	
		UV6	473	15	
		UV7	514	28	BUV496
		UV8	542	28	
		UV9	582	31	
		UV10	613	31	BUV615
		UV11	664	27	BUV661
		UV12	692	28	
		UV13	720	29	
		UV14	750	30	BUV737
		UV15	780	30	
		UV16	812	34	BUV805
Violet laser					
405	100	V1	428	15	BV421
		V2	443	15	
		V3	458	15	
		V4	473	15	
		V5	508	20	BV480
		V6	525	17	
		V7	542	17	
		V8	581	19	BV570
		V9	598	20	
		V10	615	20	BV605
		V11	664	27	BV650
		V12	692	28	
		V13	720	29	BV711
		V14	750	30	BV750
		V15	780	30	BV786
		V16	812	34	
Wavelength (nM)	Laser power (mW)	Channel	Center Wavelength (nm)	Bandwidth (nM)	Fluorochrome (Peak intensity)
Blue laser					
488	50	B1	508	20	
		B2	525	17	FITC
		B3	542	17	
		B4	581	19	
		B5	598	20	
		B6	615	20	BB630
		B7	661	17	BB660
		B8	679	18	
		B9	697	19	BB700
		B10	717	20	
		B11	738	21	
		B12	760	23	
		B13	783	23	
		B14	812	34	BB790

(Continued)

Table 60. (Continued)

Wavelength (nM)	Laser power (mW)	Channel	Center Wavelength (nm)	Bandwidth (nM)	Fluorochrome (Peak intensity)
Yellow Green laser					
561	50	YG1	577	20	PE
		YG2	598	20	
		YG3	615	20	PE-Dazzle594
		YG4	661	17	
		YG5	679	18	PE-Cy5
		YG6	697	19	
		YG7	720	29	
		YG8	750	30	PE-Cy7
		YG9	780	30	
		YG10	812	34	
Red laser					
640	80	R1	661	17	APC
		R2	679	18	
		R3	697	19	
		R4	717	20	APC-R700
		R5	738	21	
		R6	760	23	
		R7	783	23	eFluor 780
		R8	812	34	

3. Resuspend cells in freshly prepared 100 μl Live/Dead dye solution;
4. Incubate for 3 min at room temperature in the dark;
5. Wash cells by adding 1 mL of Staining buffer, centrifuge tubes at 485 × *g* for 5 min at 4°C and discard supernatant;
6. Resuspend cells in 100 μl of Fc block (diluted 1:100 - purified anti-mouse CD16/CD32, clone 217 2.4G2) in Staining Buffer;
7. Incubate for 30 min at 4°C, protected from light;
8. Wash cells by adding 1 mL of Staining buffer, centrifuge tubes at 485 × *g* for 5 min at 4°C and discard supernatant;
9. Resuspend cells in 100 μl of antibody staining mix containing the correct final dilution of CCR7 and CCR2 antibodies in Brilliant Staining Buffer;
10. Incubate for 30 min at 37°C in the dark;
11. Wash cells by adding 1 mL of Staining buffer, centrifuge tubes at 485 × *g* for 5 min at 4°C and discard supernatant;
12. Resuspend cells in 100 μl of antibody staining mix with the proper final dilutions of all antibodies for surface staining (and the required FMO mixes) diluted in Brilliant Staining Buffer;
13. For surface staining incubate for 30 min at 4°C, protected from light;
14. Wash cells two times by adding 1 mL of Staining buffer, centrifuge tubes at 485 × *g* for 5 min at 4°C and discard supernatant;
15. Resuspend cells in 100–200 μl of Staining buffer and keep in dark at 4°C until analysis on Cytek Aurora.

The staining procedure and antibody solutions are summarized in Table 61 shown below.

2.7.4 *Data analysis*

Data acquisition was performed with a Cytek Aurora spectral flow cytometer equipped with 5 lasers and 64 detectors. We took advantage that full spectrum cytometry allows the measurement of the entire emission spectra for each fluorochrome, across all lasers, in comparison to classical flow cytometry, which measures the peak emission of every fluorochrome [136–138]. Data were analyzed using FlowJo v10.8.0 software. A representative gating tree of the 26-color staining on mouse D4M tumor tissue to identify immune cell populations is shown in Fig. 24. After removing cellular debris, dye aggregates, and cellular doublets, dead cells were excluded from the analysis using the fixable viability dye eF780. CD45 enables the separation of the hematopoietic cell lineage from contaminating tumor cells and stroma cells (Fig. 24A). Next, NK cells (NK1.1$^+$) and T cells (CD3$^+$) were identified. Furthermore, this multiparameter panel allows the subdivision into CD4$^+$ T cells and CD8$^+$ T cells (Fig. 24B). Based on the surface expression of CD19 and MHC-II, B cells were characterized from the CD3$^-$ NK1.1$^-$ cells. After gating lymphocytes as separate populations and excluding them from further subset delineation, monocytes (Ly-6C$^+$ Ly-6G$^-$) and neutrophils (Ly-6C$^+$ Ly-6G$^+$) were identified. Tumor-associated macrophages (TAM) were characterized by their expression of MerTK and F4/80 (Fig. 24C). From the remaining cells (non-TAM), DC were identified by gating CD11c versus MHC-II. Tumor-infiltrating DC can be further subdivided into XCR1 expressing cDC1, consisting of CD103$^-$ cDC1 and CD103$^+$ cDC1, and CD11b expressing cDC2 (Fig. 24D). DC are characterized by a high functional plasticity, as they express co-stimulatory molecules, i.e. CD40 and CD86, but also inhibitory

Table 61. Staining workflow for DC mouse panel

	Marker	Fluorochrome	Dilution	Diluent	Incubation (min/Temp)
1	Viability dye eF780	APC-Cy7	1:5000	PBS	3'/RT
2	**Wash (Staining buffer)**				
3	Fc Block	–	1:100	Staining Buffer	30'/4°C
4	**Wash (Staining buffer)**				
5	CCR7	APC	1:50	Brilliant Stain Buffer	30'/37°C
	CCR2	BV711	1:400		
6	**Wash (Staining buffer)**				
7	NK1.1	BB630	1:200	Brilliant Stain Buffer	30'/4°C
	CD19	BB660	1:400		
	CD40	BB700	1:100		
	CD103	BB790	1:200		
	F4/80	PE-Dazzle594	1:100		
	CD3e	PE-Cy5	1:200		
	CD64	PE-Cy7	1:200		
	PD-L2	APC-R700	1:100		
	Ly-6C	BV421	1:200		
	MHC class II	BV480	1:400		
	Ly-6G	BV570	1:200		
	CD115	BV605	1:100		
	XCR1	BV650	1:400		
	pDCA-1	BV750	1:400		
	CD24	BV786	1:400		
	CD11c	BUV395	1:100		
	CD11b	BUV496	1:400		
	MerTK	BUV563	1:50		
	PD-L1	BUV615	1:400		
	CD4	BUV661	1:400		
	CD8a	BUV737	1:400		
	CD45	BUV805	1:200		
8	**2X Wash (Staining buffer)**				
9	**Resuspend cells in 100–200 μl of Staining buffer and keep in dark at 4°C until acquisition**				

proteins, like PD-L1 and PD-L2. The two PD-1 ligands are known for their ability to suppress T cell activation [139]. We have included antibodies for CD40, PD-L1 and PD-L2, which allows a more detailed phenotypical characterization of the different DC subsets. Proper discrimination of DC from other myeloid cells was verified by expression of Zbtb46-GFP and inclusion of CD24 and CCR7 allows a more detailed characterization of the DC subsets in the tumor. (Fig. 24E). Moreover, we determined the expression of CCR2, CD64, and CD115 on monocytes, neutrophils, and TAM (Fig. 24F).

2.7.5 *Pitfalls*

- Every transplantable tumor model shows different myeloid cell infiltrate. Therefore, the gating strategy needs be adapted for different mouse tumor cell lines.
- Cellular debris of tumors can interfere with the staining. Make sure to vortex thoroughly when adding a new staining.
- By using the DC-specific reporter mouse strain Zbtb46-GFP in which all cDC express the GFP signal [103], the identified cDC subsets can be double-checked for their preDC origin. Moreover, the other myeloid subtypes such as monocytes and TAMs can be further investigated for possible contamination by DC which was not the case in the tumor model used for this panel description.

2.7.6 *Top Tricks*

- **Antibody Titration**: All used antibodies were titrated, either to a selected optimal concentration or to saturation. Optimal antibody concentrations were considered as the lowest amount of antibody that shows the best signal separation with minimal background staining.
- **Single Color Reference Control**: Using cells as single stained reference controls is superior to beads in our experience. Therefore, we used beads only in cases, when we could not achieve a proper separation of positive and negative signals with the

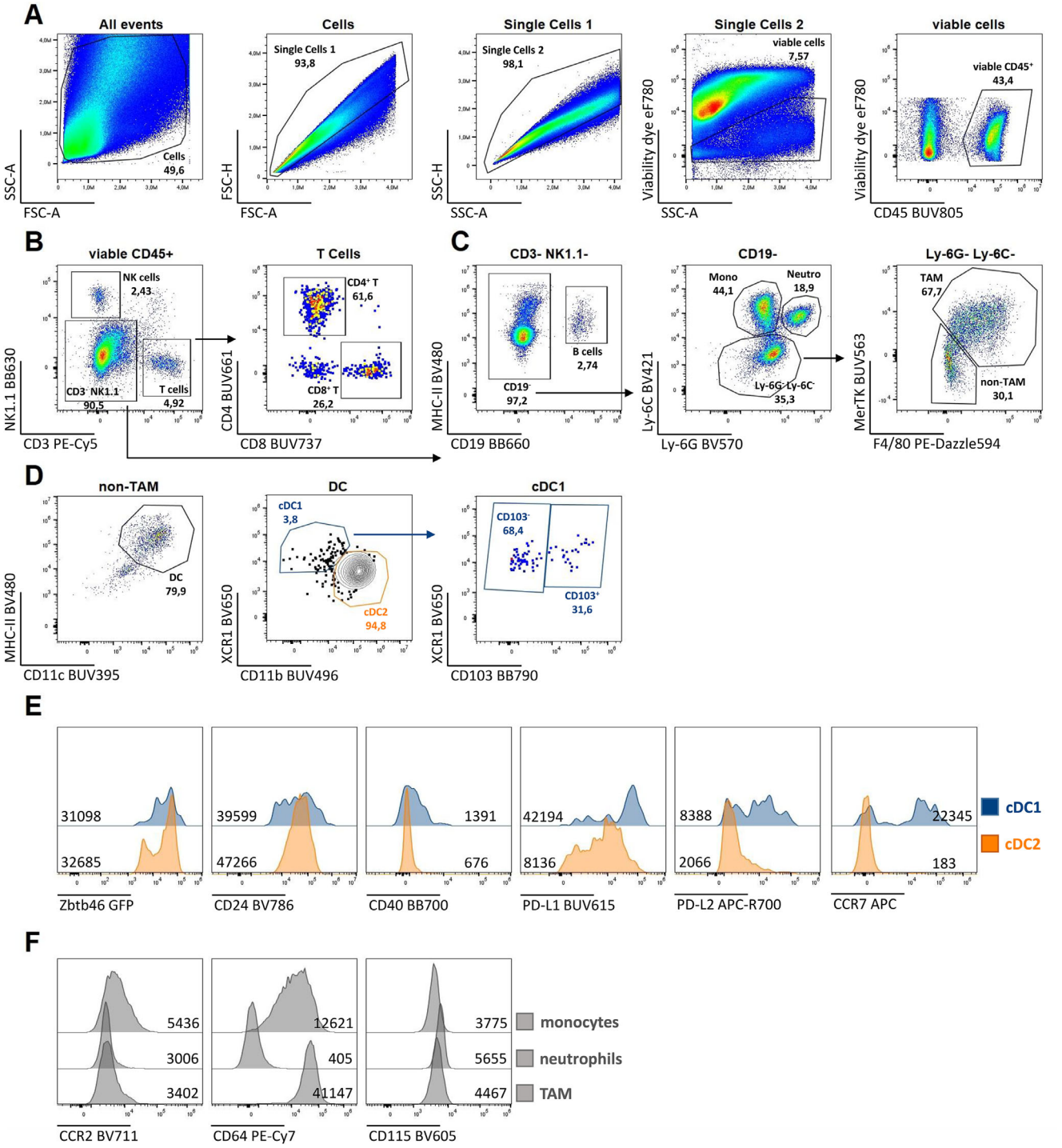

Figure 24. Gating strategy for flow cytometry panel on mouse transplantable tumor. D4M tumor tissue was enzymatically digested to generate single-cell suspensions. A. Gating strategy for viable CD45$^+$ cells after exclusion of cellular debris, doublets, and dead cells. B. CD3$^+$ T cells and NK1.1$^+$ NK cells were gated. Inclusion of CD4 and CD8 allows further characterization of T cell subsets. C. From the CD3$^-$ NK1.1$^-$ cells, B cells (CD19$^+$) can be identified. Next, monocytes (Ly-6C$^+$) and neutrophils (Ly-6C$^+$ Ly-6G$^+$) can be discriminated. Tumor-associated macrophages (TAM) were characterized by their expression of MerTK and F4/80. From the remaining double-negative cells, DC were identified by gating CD11c versus MHC-II. Tumor-infiltrating DC consist of cDC1 (XCR1$^+$ CD11b$^-$), which can be further subdivided into CD103$^-$ and CD103$^+$ cDC1, and cDC2 (XCR1$^-$ CD11b$^+$). E. DC gating was verified by Zbtb46 GFP expression. Furthermore, inclusion of CD24, CD40, PD-L1, PD-L2, and CCR7 allows a more detailed characterization of the different DC subsets. F. Expression of several surface markers on the indicated myeloid cell subsets: monocytes, neutrophils, and TAM. For E. and F. MFI values are shown. CD4$^+$ T: CD4$^+$ T cells, CD8$^+$ T: CD8$^+$ T cells, Mono: monocytes, Neutro: neutrophils, TAM: tumor-associated macrophages.

Table 62. Summary of marker expression on analyzed cell populations

Population	Surface marker
NK cells	NK1.1$^+$, Zbtb46-GFP$^-$
CD8$^+$ T cells	CD3$^+$, CD8$^+$, CD4$^-$, Zbtb46-GFP$^-$
CD4$^+$ T cells	CD3$^+$, CD8$^-$, CD4$^+$, Zbtb46-GFP$^-$
B cells	NK1.1$^-$, CD3$^-$, CD19$^+$, MHC-II$^+$, Zbtb46-GFP$^-$
Monocytes	NK1.1$^-$, CD3$^-$, CD19$^-$, Ly-6C$^+$, Ly-6G$^-$ CD64$^{int/+}$, Zbtb46-GFP$^-$
Neutrophils	NK1.1$^-$, CD3$^-$, CD19$^-$, Ly-6C$^+$, Ly-6G$^+$, CD64$^-$, Zbtb46-GFP$^-$
Tumor-associated macrophages (TAM)	NK1.1$^-$, CD3$^-$, CD19$^-$, Ly-6C$^+$, Ly-6G$^-$, MerTK$^+$, F4/80$^+$, CD64$^+$, Zbtb46-GFP$^-$
CD103$^-$ cDC1	NK1.1$^-$, CD3$^-$, CD19$^-$, Ly-6C$^-$, Ly-6G$^-$, MerTK$^-$, F4/80$^-$, MHC-II$^+$, CD11c$^+$, XCR1$^+$, CD103$^-$, CD11b$^-$, Zbtb46-GFP$^+$
CD103$^+$ cDC1	NK1.1$^-$, CD3$^-$, CD19$^-$, Ly-6C$^-$, Ly-6G$^-$, MerTK$^-$, F4/80$^-$, MHC-II$^+$, CD11c$^+$, XCR1$^+$, CD103$^+$, CD11b$^-$, Zbtb46-GFP$^+$
cDC2	NK1.1$^-$, CD3$^-$, CD19$^-$, Ly-6C$^-$, Ly-6G$^-$, MerTK$^-$, F4/80$^-$, MHC-II$^+$, CD11c$^+$, XCR1$^-$, CD11b$^+$, Zbtb46-GFP$^+$

original antibody or the dummy approach (substitute with fluorochrome from the same company conjugated to an antibody against an abundantly expressed marker). Correct unmixing was monitored with single stained cells. Spectral unmixing is the mathematical method used to differentiate the fluorescence signals from each fluorochrome in an experiment. A major advantage of unmixing in comparison to conventional compensation is that autofluorescence can be handled as a separate parameter, making it possible to extract autofluorescence of a sample. This can be very useful when working with tissues that exhibit a high autofluorescence which might affect the resolution of the other fluorescent signals.

- **Chemokine receptor staining**: During the optimization process of this panel, we realized that a separate incubation of CCR7 APC antibody at 37°C for 30 min results in a better CCR7 staining. Thus, we adjusted our staining workflow and preincubate antibodies for chemokine receptor CCR7 and CCR2 for 30 min at 37°C, before proceeding with the staining of the remaining surface molecules.
- **Brilliant Stain Buffer**: When using two or more BD Brilliant dye-conjugated antibodies, we recommend to use Brilliant Stain Buffer, as fluorescent dye interactions might lead to staining artifacts.
- **Panel optimization**: For future use, several adaptions of the panel are possible, e.g., to use a viability dye excitated by the UV laser (FVS 440UV) to free up APC-Cy7. The FITC-channel can be used for different GFP reporter mouse models. Furthermore, PE as one of the brightest and most commonly available fluorochrome is not employed at the moment. A fixation step after staining for surface molecules would allow to include additional intracellular markers, e.g. cytokines or transcription factors. This optimized panel for flow cytometry allows the high-dimensional immune phenotyping of myeloid cell subsets with a special focus on DC. In addition to resolving the complex cellular heterogeneity of myeloid immune cells, this panel also provides additional information about the major subsets of the lymphoid cell compartment. This multiparameter panel has also been tested on skin-draining lymph nodes and mouse skin, where the inclusion of CD207 PE antibody allows for the identification of Langerhans cells [140]. Fixation does not compromise the proper separation of the various immune cell populations and detection of the GFP signal.

2.7.7 *Summary of the phenotype*

Table 62 lists the immune cell populations that can be identified using the described 26-color flow cytometry panel in this protocol.

Acknowledgements: Section 1.1 and Section 2.1: The Probst laboratory was supported by the German Research Foundation [Deutsche Forschungsgemeinschaft (DFG)] (SFB TR156-B02, CRC1292-TP13).
Section 1.2: The Dudziak laboratory is thankful to its members for fruitful discussions. Parts of this methods paper are also included in the PhD thesis of Lukas Amon and Master's thesis of Lukas Jacobi. The Dudziak laboratory was supported by the German Research Foundation [Deutsche Forschungsgemeinschaft (DFG)] (CRC1181-TPA7 261193037, DU548/5-1, SFB TRR305 – B05, RTG2504-401821119, RTG2599 421758891), the Interdisziplinäres Zentrum für klinische Forschung (IZKF) (IZKF-A80, IZKF-A87) and the Bavarian State Ministry of Science and Art (Bayresq.Net-IRIS). Laurence Zitvogel and Diana Dudziak were co-funded by the Agence Nationale de la Recherche (ANR, Ileobiome - 19-CE15-0029-01) and the DFG (DU548/6-1).

Section 1.3: We thank members of the Clausen laboratory for fruitful discussions and critical reading of the manuscript. Work in the Clausen laboratory is supported by grants from the German Research Foundation (Deutsche Forschungsgemeinschaft, DFG) to B.E.C. (CL 419/2-2 [Project Nr. 315501751], CL 419/4-1, CL 419/7-1 [Project Nr. 503972215], and SFB1292/2 TP20N [Project Nr. 318346496]) and R.A.B. (BA 5939/2-1). B.E.C. and R.A.B. are members of the Research Center for Immunotherapy (Forschungszentrum Immuntherapie, FZI) of the University Medical Center Mainz.
Section 1.4: We thank members of the Clausen and the Hovav laboratories for fruitful discussions and critical reading of the manuscript. Work in the Clausen laboratory is supported by grants from the German Research Foundation (Deutsche Forschungsgemeinschaft, DFG) to B.E.C. (CL 419/2-2 [Project Nr. 315501751], CL 419/4-1, CL 419/7-1 [Project Nr. 503972215], and SFB1292/2 TP20N [Project Nr. 318346496]), and B.E.C. is a member of the Research Center for Immunotherapy (Forschungszentrum Immuntherapie, FZI) of the University Medical Center Mainz.
Sections 1.5 and Section 2.5: We thank members of the Schraml lab for helpful discussions and critical reading of the manuscript. Work in the Schraml lab is supported by the European Research Council - Starting Grant ERC-2016-STG-715182 and the German Research Foundation - Emmy Noether Grant Schr-1444/1-1, project-ID 360372040–SFB 1335-P08 and 322359157-FOR2599-A03.
Section 1.6: This work was supported by the Confocal Microscopy Facility, a core facility of the Interdisciplinary Center for Clinical Research (IKZF) Aachen within the Faculty of Medicine at RWTH Aachen University.
Section 1.7: We would like to thank the whole team of the Laboratory for Langerhans Cell Research at the Department of Dermatology, Venereology & Allergology. This work was financially supported by the Austrian Science Fund (FWF) with the projects P-21487-B13, P-27001-B13, P-33855-B and DOC82. Additional funding was received from the European Union's Horizon 2020 research and innovation program under the Marie Sklodowska-Curie grant agreement no 641549/Immutrain and by a PhD-fellowship of the Austrian Academy of Sciences (OAW DOC/26015) to Florian Hornsteiner.
Section 2.2: The Dudziak laboratory is thankful to its members for fruitful discussions and to the Core Unit for cell sorting and immunomonitoring (FAU Erlangen). Parts of this methods paper are also included in the PhD thesis of Lukas Amon and Master's thesis of Lukas Jacobi. The Dudziak laboratory was supported by the German Research Foundation [Deutsche Forschungsgemeinschaft (DFG)] (CRC1181-TPA7 261193037, DU548/5-1, SFB TRR 305 - B05, RTG2504-401821119, RTG2599 421758891), the Interdisziplinäres Zentrum für klinische Forschung (IZKF) (IZKF-A80, IZKF-A87) and the Bavarian State Ministry of Science and Art (Bayresq.Net-IRIS). Laurence Zitvogel and Diana Dudziak were co-funded by the Agence Nationale de la Recherche (ANR-Ileobiome - 19-CE15-0029-01) and the DFG (DU548/6-1).
Section 2.3: We would like to thank all members of the Schlitzer Lab for fruitful discussions. Parts of this methods paper are included in the PhD thesis of Hannah Theobald. This work was supported by the German Research Foundation [Deutsche Forschungsgemeinschaft (DFG)] (RTG1873, INST217/1034-1, SCHL2116/6-1, SCHL2116/7-1) and under Germany's Excellence Strategy – EXC2151 – 390873048, and an Emmy Noether research grant (SCHL2116/1-1 to AS).
Section 2.4: We thank members of the Clausen and the Hovav laboratories for fruitful discussions and critical reading of the manuscript. Work in the Clausen laboratory is supported by grants from the German Research Foundation (Deutsche Forschungsgemeinschaft, DFG) to B.E.C. (CL 419/2-2 [Project Nr. 315501751], CL 419/4-1, CL 419/7-1 [Project Nr. 503972215], and SFB1292/2 TP20N [Project Nr. 318346496]), and B.E.C. is a member of the Research Center for Immunotherapy (Forschungszentrum Immuntherapie, FZI) of the University Medical Center Mainz.
Section 2.7: We would like to thank the whole team of the Laboratory for Langerhans Cell Research at the Department of Dermatology, Venereology & Allergology. This work was supported by the Austrian Science Fund (FWF) with the project P-33855-B. Additional funding was received from the European Union's Horizon 2020 research and innovation program under the Marie Sklodowska-Curie grant agreement no 641549/Immutrain. Additional funding was received by a PhD-fellowship of the Austrian Academy of Sciences (OAW DOC/26015) to Florian Hornsteiner and a grant of the Austrian Research Promotion Agency to Sieghart Sopper (FFG 858057).
Open access funding enabled and organized by Projekt DEAL.

Conflict of interest: The authors declare no commercial or financial conflict of interest

Data availability statement: The data that support the findings of this study are available from the corresponding authors upon reasonable request

Peer review: The peer review history for this article is available at https://publons.com/publon/10.1002/eji.202249819

Author contributions: Section 1.1: Nadine Kamenjarin, Katrin Hodapp and Hans Christian Probst; lead author Hans Christian Probst.

Section 1.2: Lukas Amon*, Christian H. K. Lehmann*, Anna Seichter, Lukas Jacobi, Lukas Rossnagel, Lukas Heger, Katharina Lahl, Imran Lahmar, Jianzhou Chen, Marion Picard, Maria Paula Roberti, Laurence Zitvogel and Diana Dudziak; * contributed equally, lead author Diana Dudziak.

Section 1.3: Jelena Lakus, Ronald Backer and Björn E. Clausen; lead author Björn E. Clausen.

Section 1.4: Anna Brand, Yasmin Saba, Avi-Hai Hovav and Björn E. Clausen; lead author Björn E. Clausen.

Section 1.5: Xingqi Ji and Barbara U. Schraml; lead author Barbara U. Schraml.

Section 1.6: Carmen Schalla and Kristin Seré; lead author Kristin Seré.

Section 1.7: Helen Strandt, Florian Hornsteiner, Christoph H. Tripp, Athanasios Seretis, Daniela Ortner, Sophie Dieckmann and Patrizia Stoitzner; lead author Patrizia Stoitzner.

Section 2.1: Nadine Kamenjarin, Kristian Schütze, Katrin Hodapp and Hans Christian Probst; lead author Hans Christian Probst.

Section 2.2: Lukas Amon*, Christian H. K. Lehmann*, Anna Seichter, Lukas Jacobi, Lukas Rossnagel, Lukas Heger, Katharina Lahl, Imran Lahmar, Jianzhou Chen, Marion Picard, Maria Paula Roberti, Laurence Zitvogel and Diana Dudziak; * contributed equally, lead author Diana Dudziak.

Section 2.3: Hannah Theobald and Andreas Schlitzer, lead author Andreas Schlitzer.

Section 2.4: Anna Brand, Yasmin Saba, Avi-Hai Hovav and Björn E. Clausen, lead author Björn E. Clausen.

Section 2.5: Xingqi Ji and Barbara U. Schraml, lead author Barbara U. Schraml.

Section 2.6: Carmen Schalla and Kristin Seré; lead author Kristin Seré.

Section 2.7: Florian Hornsteiner, Martina M Sykora, Christoph H Tripp, Athanasios Seretis, Helen Strandt, Sieghart Sopper and Patrizia Stoitzner, lead author Patrizia Stoitzner.

References

1 **Watt, F. M.**, Mammalian skin cell biology: at the interface between laboratory and clinic. *Science*. 2014. **346**: 937–940.

2 **Chambers, E. S. and Vukmanovic-Stejic, M.**, Skin barrier immunity and ageing. *Immunology*. 2020. **160**: 116–125.

3 **Merad, M., Ginhoux, F. and Collin, M.**, Origin, homeostasis and function of Langerhans cells and other langerin-expressing dendritic cells. *Nat. Rev. Immunol.* 2008. **8**: 935–947.

4 **Nielsen, M. M., Witherden, D. A. and Havran, W. L.**, γδ T cells in homeostasis and host defence of epithelial barrier tissues. *Nat. Rev. Immunol.* 2017. **17**: 733–745.

5 **Tamoutounour, S., Guilliams, M., Sanchis, M., Liu, H., Terhorst, D., Malosse, C., Pollet, E. et al.**, Origins and functional specialization of macrophages and of conventional and monocyte-derived dendritic cells in mouse skin. *Immunity*. 2013. **39**: 1–14.

6 **Clausen, B. E. and Stoitzner, P.**, Functional specialization of skin dendritic cell subsets in regulating T cell responses. *Front. Immunol.* 2015. https://doi.org/10.3389/fimmu.2015.00534.

7 **Allan, R. S., Waithman, J., Bedoui, S., Jones, C. M., Villadangos, J. A., Zhan, Y., Lew, A. M. et al.**, Migratory dendritic cells transfer antigen to a lymph node-resident dendritic cell population for efficient CTL priming. *Immunity*. 2006. **25**: 153–162.

8 **Pasparakis, M., Haase, I. and Nestle, F. O.**, Mechanisms regulating skin immunity and inflammation. *Nat. Rev. Immunol.* 2014; **14**:289–301.

9 **Mairhofer, D. G., Ortner, D., Tripp, C. H., Schaffenrath, S., Fleming, V., Heger, L., Komenda, K. et al.**, Impaired gp100-specific CD8+ T-cell responses in the presence of myeloid-derived suppressor cells in a spontaneous mouse melanoma model. *J. Invest. Dermatol.* 2015. **135**: 2785–2793.

10 **Brand, A., Diener, N., Zahner, S. P., Tripp, C., Backer, R. A., Karram, K., Jiang, A. et al.**, E-Cadherin is dispensable to maintain langerhans cells in the epidermis. *J. Invest. Dermatol.* 2020. **140**: 132–142.e3.

11 **Treuting, P. M., Arends, M. J. and Dintzis, S. M.**, Upper Gastrointestinal Tract. In Treuting, P. M., Dintzis, S. M. and Montine, K. S. (Eds.) *Comparative Anatomy and Histology*. Academic Press, San Diego 2018, pp 191–211.

12 **Treuting, P. M., Arends, M. J. and Dintzis, S. M.**, Lower Gastrointestinal Tract. In Treuting, P. M., Dintzis, S. M. and Montine, K. S. (Eds.) *Comparative Anatomy and Histology*. Academic Press, San Diego 2018, pp 213–228.

13 **Houston, S. A., Cerovic, V., Thomson, C., Brewer, J., Mowat, A. M. and Milling, S.**, The lymph nodes draining the small intestine and colon are anatomically separate and immunologically distinct. *Mucosal. Immunol.* 2016. **9**: 468–478.

14 **Mayer, J. U., Brown, S. L., MacDonald, A. S. and Milling, S. W.**, Defined intestinal regions are drained by specific lymph nodes that mount distinct Th1 and Th2 responses against schistosoma mansoni eggs. *Front. Immunol.* 2020. **11**: 592325.

15 **Cook, P. C. and MacDonald, A. S.**, Dendritic cells in lung immunopathology. *Semin. Immunopathol.* 2016. **38**: 449–460.

16 **Gilliet, M., Cao, W. and Liu, Y. J.**, Plasmacytoid dendritic cells: sensing nucleic acids in viral infection and autoimmune diseases. *Nat. Rev. Immunol.* 2008. **8**: 594–606.

17 **de Heer, H. J., Hammad, H., Soullie, T., Hijdra, D., Vos, N., Willart, M. A., Hoogsteden, H. C. et al.**, Essential role of lung plasmacytoid dendritic cells in preventing asthmatic reactions to harmless inhaled antigen. *J. Exp. Med.* 2004. **200**: 89–98.

18 **Guilliams, M., Lambrecht, B. N. and Hammad, H.**, Division of labor between lung dendritic cells and macrophages in the defense against pulmonary infections. *Mucosal. Immunol.* 2013. **6**: 464–473.

19 **Plantinga, M., Hammad, H. and Lambrecht, B. N.**, Origin and functional specializations of DC subsets in the lung. *Eur. J. Immunol.* 2010. **40**: 2112–2118.

20 **Plantinga, M., Guilliams, M., Vanheerswynghels, M., Deswarte, K., Branco-Madeira, F., Toussaint, W., Vanhoutte, L. et al.**, Conventional and monocyte-derived CD11b(+) dendritic cells initiate and maintain T helper 2 cell-mediated immunity to house dust mite allergen. *Immunity*. 2013. **38**: 322–335.

21 **Bosteels, C., Neyt, K., Vanheerswynghels, M., van Helden, M. J., Sichien, D., Debeuf, N., De Prijck, S. et al.**, Inflammatory type 2 cDCs acquire features of cDC1s and macrophages to orchestrate immunity to respiratory virus infection. *Immunity*. 2020. **52**: 1039–1056.e1039.

22 **Misharin, A. V., Morales-Nebreda, L., Mutlu, G. M., Budinger, G. R. and Perlman, H.**, Flow cytometry analysis of macrophages and dendritic cell subsets in the mouse lung. *Am. J. Respir. Cell. Mol. Biol.* 2013. **49**: 503–510.

23 **Hussell, T. and Bell, T. J.**, Alveolar macrophages: plasticity in a tissue-specific context. *Nat. Rev. Immunol.* 2014. **14**: 81–93.

24 **Chakarov, S., Lim, H. Y., Tan, L., Lim, S. Y., See, P., Lum, J., Zhang, X. M. et al.**, Two distinct interstitial macrophage populations coexist across tissues in specific subtissular niches. *Science*. 2019. 363.

25 **Gibbings, S. L., Thomas, S. M., Atif, S. M., McCubbrey, A. L., Desch, A. N., Danhorn, T., Leach, S. M. et al.**, Three unique interstitial macrophages in the murine lung at steady state. *Am. J. Respir. Cell. Mol. Biol.* 2017. **57**: 66–76.

26 **Schyns, J., Bai, Q., Ruscitti, C., Radermecker, C., De Schepper, S., Chakarov, S., Farnir, F. et al.**, Non-classical tissue monocytes and two functionally distinct populations of interstitial macrophages populate the mouse lung. *Nat. Commun.* 2019. **10**: 3964.

27 **Wilensky, A., Mizraji, G., Tabib, Y., Sharawi, H. and Hovav, A. H.**, Analysis of leukocytes in oral mucosal tissues. *Methods Mol. Biol.* 2017. **1559**: 267–278.

28 **Bittner-Eddy, P. D., Fischer, L. A., Tu, A. A., Allman, D. A. and Costalonga, M.**, Discriminating between interstitial and circulating leukocytes in tissues of the murine oral mucosa avoiding nasal-associated lymphoid tissue contamination. *Front. Immunol.* 2017. **8**: 1398.

29 **Moutsopoulos, N. M. and Konkel, J. E.**, Tissue-specific immunity at the oral mucosal barrier. *Trends Immunol.* 2018. **39**: 276–287.

30 **Hovav, A. H.**, Dendritic cells of the oral mucosa. *Mucosal. Immunol.* 2014. **7**: 27–37.

31 **Hajishengallis, G.**, Periodontitis: from microbial immune subversion to systemic inflammation. *Nat. Rev. Immunol.* 2015. **15**: 30–44.

32 **Arizon, M., Nudel, I., Segev, H., Mizraji, G., Elnekave, M., Furmanov, K., Eli-Berchoer, L. et al.**, Langerhans cells down-regulate inflammation-driven alveolar bone loss. *Proc. Natl. Acad. Sci. U.S.A.* 2012. **109**: 7043–7048.

33 **Anders, H.-J., Wilkens, L., Schraml, B. and Marschner, J.**, One concept does not fit all: the immune system in different forms of acute kidney injury. *Nephrol. Dial. Transpl.* 2020. **36**: 29–38.

34 **Kurts, C., Ginhoux, F. and Panzer, U.**, Kidney dendritic cells: fundamental biology and functional roles in health and disease. Nature reviews. *Nephrology*. 2020. **128**: 1–17.

35 **Viehmann, S. F., Böhner, A. M. C., Kurts, C. and Brähler, S.**, The multifaceted role of the renal mononuclear phagocyte system. *Cell. Immunol.* 2018. **330**: 97–104.

36 **Munro, D. A. D. and Hughes, J.**, The origins and functions of tissue-resident macrophages in kidney development. *Frontiers in Physiology*. 2017. **8**: 275–313.

37 **Hochheiser, K., Heuser, C., Krause, T. A., Teteris, S., Ilias, A., Weisheit, C., Hoss, F. et al.**, Exclusive CX3CR1 dependence of kidney DCs impacts glomerulonephritis progression. *J. Clin. Invest.* 2013. **123**: 4242–4254.

38 **Watson, C. J. and Khaled, W. T.**, Mammary development in the embryo and adult: new insights into the journey of morphogenesis and commitment. *Development*. 2020. 147.

39 **Sun, X. and Ingman, W. V.**, Cytokine networks that mediate epithelial cell-macrophage crosstalk in the mammary gland: implications for development and cancer. *J Mammary Gland Biol Neoplasia*. 2014. **19**: 191–201.

40 **Chakrabarti, R., Celia-Terrassa, T., Kumar, S., Hang, X., Wei, Y., Choudhury, A., Hwang, J. et al.**, Notch ligand Dll1 mediates cross-talk between mammary stem cells and the macrophageal niche. *Science*. 2018. 360.

41 **Betts, C. B., Pennock, N. D., Caruso, B. P., Ruffell, B., Borges, V. F. and Schedin, P.**, Mucosal immunity in the female murine mammary gland. *J. Immunol.* 2018. **201**: 734–746.

42 **Dawson, C. A., Pal, B., Vaillant, F., Gandolfo, L. C., Liu, Z., Bleriot, C., Ginhoux, F. et al.**, Tissue-resident ductal macrophages survey the mammary epithelium and facilitate tissue remodelling. *Nat. Cell. Biol.* 2020. **22**: 546–558.

43 **Li, C. M., Shapiro, H., Tsiobikas, C., Selfors, L. M., Chen, H., Rosenbluth, J., Moore, K. et al.**, Aging-associated alterations in mammary epithelia and stroma revealed by single-cell RNA sequencing. *Cell. Rep.* 2020. **33**: 108566.

44 **Gao, H., Dong, Q., Chen, Y., Zhang, F., Wu, A., Shi, Y., Bandyopadhyay, A. et al.**, Murine mammary stem/progenitor cell isolation: Different method matters? *Springerplus*. 2016. **5**: 140.

45 **Chapman, P. B., Hauschild, A., Robert, C., Haanen, J. B., Ascierto, P., Larkin, J., Dummer, R. et al.**, Improved survival with vemurafenib in melanoma with BRAF V600E mutation. *N. Engl. J. Med.* 2011. **364**: 2507–2516.

46 **Luke, J. J., Flaherty, K. T., Ribas, A. and Long, G. V.**, Targeted agents and immunotherapies: optimizing outcomes in melanoma. Nature reviews. *Clin. Oncol.* 2017. **14**: 463–482.

47 **Pardoll, D. M.**, The blockade of immune checkpoints in cancer immunotherapy. *Nat. Rev. Cancer*. 2012. **12**: 252–264.

48 **Zitvogel, L., Pitt, J. M., Daillère, R., Smyth, M. J. and Kroemer, G.**, Mouse models in oncoimmunology. *Nat. Rev. Cancer*. 2016. **16**: 759–773.

49 **Oh, T., Fakurnejad, S., Sayegh, E. T., Clark, A. J., Ivan, M. E., Sun, M. Z., Safaee, M. et al.**, Immunocompetent murine models for the study of glioblastoma immunotherapy. *J. Transl. Med.* 2014. **12**: 107.

50 **Sanmamed, M. F., Chester, C., Melero, I. and Kohrt, H.**, Defining the optimal murine models to investigate immune checkpoint blockers and their combination with other immunotherapies. *Ann. Oncol.* 2016. **27**: 1190–1198.

51 **Herlyn, M. and Fukunaga-Kalabis, M.**, What is a good model for melanoma? *J. Invest. Dermatol.* 2010. **130**: 911–912.

52 **Fidler, I. J. and Nicolson, G. L.**, Organ selectivity for implantation survival and growth of B16 melanoma variant tumor lines. *J. Natl. Cancer Inst.* 1976. **57**: 1199–1202.

53 **Lugade, A. A., Moran, J. P., Gerber, S. A., Rose, R. C., Frelinger, J. G. and Lord, E. M.**, Local radiation therapy of B16 melanoma tumors increases the generation of tumor antigen-specific effector cells that traffic to the tumor. *J. Immunol.* 2005. **174**: 7516–7523.

54 **Becker, J. C., Houben, R., Schrama, D., Voigt, H., Ugurel, S. and Reisfeld, R. A.**, Mouse models for melanoma: a personal perspective. *Exp. Dermatol.* 2010. **19**: 157–164.

55 **Steitz, J., Brück, J., Steinbrink, K., Enk, A., Knop, J. and Tüting, T.**, Genetic immunization of mice with human tyrosinase-related protein 2: implications for the immunotherapy of melanoma. *Int. J. Cancer*. 2000. **86**: 89–94.

56 **Melnikova, V. O., Bolshakov, S. V., Walker, C. and Ananthaswamy, H. N.**, Genomic alterations in spontaneous and carcinogen-induced murine melanoma cell lines. *Oncogene*. 2004. **23**: 2347–2356.

57 **Jenkins, M. H., Steinberg, S. M., Alexander, M. P., Fisher, J. L., Ernstoff, M. S., Turk, M. J., Mullins, D. W. et al.**, Multiple murine BRaf(V600E) melanoma cell lines with sensitivity to PLX4032. *Pigment Cell Melanoma Res.* 2014. **27**: 495–501.

58 **Flaherty, K. T., Hodi, F. S. and Fisher, D. E.**, From genes to drugs: targeted strategies for melanoma. *Nat. Rev. Cancer*. 2012. **12**: 349–361.

59 **Knight, D. A., Ngiow, S. F., Li, M., Parmenter, T., Mok, S., Cass, A., Haynes, N. M. et al.**, Host immunity contributes to the anti-melanoma activity of BRAF inhibitors. *J. Clin. Invest.* 2013. **123**: 1371–1381.

60 **Koya, R. C., Mok, S., Otte, N., Blacketor, K. J., Comin-Anduix, B., Tumeh, P. C., Minasyan, A. et al.**, BRAF inhibitor vemurafenib improves the antitumor activity of adoptive cell immunotherapy. *Cancer Res.* 2012. **72**: 3928–3937.

61 **Meeth, K., Wang, J. X., Micevic, G., Damsky, W. and Bosenberg, M. W.**, The YUMM lines: a series of congenic mouse melanoma cell lines with defined genetic alterations. *Pigment Cell Melanoma Res.* 2016. **29**: 590–597.

62 **Guilliams, M., Dutertre, C.-A., Scott, C. L., McGovern, N., Sichien, D., Chakarov, S., Van Gassen, S. et al.**, Unsupervised high-dimensional analysis aligns dendritic cells across tissues and species. *Immunity*. 2016. **45**: 669–684.

63 **Conrad, C., Meller, S. and Gilliet, M.**, Plasmacytoid dendritic cells in the skin: to sense or not to sense nucleic acids. *Semin. Immunol.* 2009. **21**: 101–109.

64 **Baranska, A., Shawket, A., Jouve, M., Baratin, M., Malosse, C., Voluzan, O., Manh, T. P. V. et al.**, Unveiling skin macrophage dynamics explains both tattoo persistence and strenuous removal. *J. Exp. Med.* 2018. **215**: 1115–1133.

65 **Jakubzick, C., Gautier, E. L., Gibbings, S. L., Sojka, D. K., Schlitzer, A., Johnson, T. E., Ivanov, S. et al.**, Minimal differentiation of classical monocytes as they survey steady-state tissues and transport antigen to lymph nodes. *Immunity*. 2013. **39**: 599–610.

66 **Yona, S., Kim, K. W., Wolf, Y., Mildner, A., Varol, D., Breker, M., Strauss-Ayali, D. et al.**, Fate mapping reveals origins and dynamics of monocytes and tissue macrophages under homeostasis. *Immunity*. 2013. **38**: 79–91.

67 **Van Gassen, S., Callebaut, B., Van Helden, M. J., Lambrecht, B. N., Demeester, P., Dhaene, T. and Saeys, Y.**, FlowSOM: Using self-organizing maps for visualization and interpretation of cytometry data. *Cytom. Part A*. 2015. **87**: 636–645.

68 **Van Der Maaten, L. and Hinton, G.**, Visualizing data using t-SNE. *J. Mach. Learn. Res.* 2008. **9**: 2579–2605.

69 **McInnes, L., Healy, J. and Melville, J.**, UMAP: uniform manifold approximation and projection for dimension reduction. 2018.

70 **Coillard, A. and Segura, E.**, Antigen presentation by mouse monocyte-derived cells: Re-evaluating the concept of monocyte-derived dendritic cells. *Mol. Immunol.* 2021. **135**: 165–169.

71 **Biburger, M., Trenkwald, I. and Nimmerjahn, F.**, Three blocks are not enough—Blocking of the murine IgG receptor FcγRIV is crucial for proper characterization of cells by FACS analysis. *Eur. J. Immunol.* 2015. **45**: 2694–2697.

72 **Amon, L., Lehmann, C. H. K., Baranska, A., Schoen, J., Heger, L. and Dudziak, D.**, Transcriptional control of dendritic cell development and functions. *Int. Rev. Cell. Mol. Biol.* 2019. **349**: 55–151.

73 **Amon, L., Hatscher, L., Heger, L., Dudziak, D. and Lehmann, C. H. K.**, Harnessing the complete repertoire of conventional dendritic cell functions for cancer immunotherapy. *Pharmaceutics*. 2020. **12**: 663.

74 **Crozat, K., Tamoutounour, S., Vu Manh, T. P., Fossum, E., Luche, H., Ardouin, L., Guilliams, M. et al.**, Cutting edge: expression of XCR1 defines mouse lymphoid-tissue resident and migratory dendritic cells of the CD8α+ type. *J. Immunol.* 2011. **187**: 4411–4415.

75 **Watchmaker, P. B., Lahl, K., Lee, M., Baumjohann, D., Morton, J., Kim, S. J., Zeng, R. et al.**, Comparative transcriptional and functional profiling defines conserved programs of intestinal DC differentiation in humans and mice. *Nat. Immunol.* 2014. **15**: 98–108.

76 **Bonnardel, J., Da Silva, C., Wagner, C., Bonifay, R., Chasson, L., Masse, M., Pollet, E. et al.**, Distribution, location, and transcriptional profile of Peyer's patch conventional DC subsets at steady state and under TLR7 ligand stimulation. *Mucosal. Immunol.* 2017. **10**: 1412–1430.

77 **Lehmann, C. H. K., Baranska, A., Heidkamp, G. F., Heger, L., Neubert, K., Luhr, J. J., Hoffmann, A. et al.**, DC subset-specific induction of T cell responses upon antigen uptake via Fcgamma receptors in vivo. *J. Exp. Med.* 2017. **214**: 1509–1528.

78 **Nimmerjahn, F., Bruhns, P., Horiuchi, K. and Ravetch, J. V.**, FcgammaRIV: a novel FcR with distinct IgG subclass specificity. *Immunity*. 2005. **23**: 41–51.

79 **Miller, J. C., Brown, B. D., Shay, T., Gautier, E. L., Jojic, V., Cohain, A., Pandey, G. et al.**, Deciphering the transcriptional network of the dendritic cell lineage. *Nat. Immunol.* 2012. **13**: 888–899.

80 **Leach, S. M., Gibbings, S. L., Tewari, A. D., Atif, S. M., Vestal, B., Danhorn, T., Janssen, W. J. et al.**, Human and mouse transcriptome profiling identifies cross-species homology in pulmonary and lymph node mononuclear phagocytes. *Cell. Rep.* 2020. **33**: 108337.

81 **Gautier, E. L., Shay, T., Miller, J., Greter, M., Jakubzick, C., Ivanov, S., Helft, J. et al.**, Gene-expression profiles and transcriptional regulatory pathways that underlie the identity and diversity of mouse tissue macrophages. *Nat. Immunol.* 2012. **13**: 1118–1128.

82 **Scott, C. L., Bain, C. C., Wright, P. B., Sichien, D., Kotarsky, K., Persson, E. K., Luda, K. et al.**, CCR2(+)CD103(-) intestinal dendritic cells develop from DC-committed precursors and induce interleukin-17 production by T cells. *Mucosal. Immunol.* 2015. **8**: 327–339.

83 **Allard, B., Panariti, A. and Martin, J. G.**, Alveolar macrophages in the resolution of inflammation, tissue repair, and tolerance to infection. *Front. Immunol.* 2018. 9.

84 **Becher, B., Schlitzer, A., Chen, J., Mair, F., Sumatoh, H. R., Teng, K. W. W., Low, D. et al.**, High-dimensional analysis of the murine myeloid cell system. *Nat. Immunol.* 2014. **15**: 1181–1189.

85 **Merad, M., Sathe, P., Helft, J., Miller, J. and Mortha, A.**, The dendritic cell lineage: ontogeny and function of dendritic cells and their subsets in the steady state and the inflamed setting. *Annu. Rev. Immunol.* 2013. **31**: 563–604.

86 **Banchereau, J. and Steinman, R. M.**, Dendritic cells and the control of immunity. *Nature*. 1998. **392**: 245–252.

87 **Lyons-Cohen, M. R., Thomas, S. Y., Cook, D. N. and Nakano, H.**, Precision-cut mouse lung slices to visualize live pulmonary dendritic cells. *J. Vis. Exp.* 2017.

88 **Geurtsvankessel, C. H. and Lambrecht, B. N.**, Division of labor between dendritic cell subsets of the lung. *Mucosal Immunology*. 2008. **1**: 442–450.

89 **Edelson, B. T., Bradstreet, T. R., Hildner, K., Carrero, J. A., Frederick, K. E., Wumesh, K. C., Belizaire, R. et al.**, CD8α+ dendritic cells are an obligate cellular entry point for productive infection by listeria monocytogenes. *Immunity*. 2011. **35**: 236–248.

90 **Hildner, K., Edelson, B. T., Purtha, W. E., Diamond, M., Matsushita, H., Kohyama, M., Calderon, B. et al.**, Batf3 deficiency reveals a critical role for CD8α+ dendritic cells in cytotoxic T cell immunity. *Science*. 2008. **322**: 1097–1100.

91 **Dudziak, D., Kamphorst, A. O., Heidkamp, G. F., Buchholz, V. R., Trumpfheller, C., Yamazaki, S., Cheong, C. et al.**, Differential antigen processing by dendritic cell subsets in vivo. *Science*. 2007. **315**: 107–111.

92 **Schlitzer, A., McGovern, N., Teo, P., Zelante, T., Atarashi, K., Low, D., Ho, A. W. et al.**, IRF4 transcription factor-dependent CD11b+ dendritic cells in human and mouse control mucosal IL-17 cytokine responses. *Immunity*. 2013. **38**: 970–983.

93 **Tussiwand, R., Everts, B., Gary, N., Iwata, A., Bagaitkar, J., Wu, X., Wong, R. et al.**, Klf4 expression in conventional dendritic cells is required for T helper 2 cell responses. *Immunity*. 2015. **42**: 916–928.

94 **Lewis, K. L., Caton, M. L., Bogunovic, M., Greter, M., Grajkowska, L. T., Ng, D., Klinakis, A. et al.**, Notch2 receptor signaling controls functional differentiation of dendritic cells in the spleen and intestine. 2011. **35**: 780–791.

95 **Persson, E. K., Uronen-Hansson, H., Semmrich, M., Rivollier, A., Hägerbrand, K., Marsal, J., Gudjonsson, S. et al.**, IRF4 transcription-factor-dependent CD103(+)CD11b(+) dendritic cells drive mucosal T helper 17 cell differentiation. 2013. **38**: 958–969.

96 **Satpathy, A. T., Briseño, C. G., Lee, J. S., Ng, D., Manieri, N. A., KC, W., Wu, X. et al.**, Notch2-dependent classical dendritic cells orchestrate intestinal immunity to attaching-and-effacing bacterial pathogens. *Nat. Immunol.* 2013. **14**: 937–948.

97 **Brown, C. C., Gudjonson, H., Pritykin, Y., Deep, D., Lavallee, V. P., Mendoza, A., Fromme, R. et al.**, Transcriptional basis of mouse and human dendritic cell heterogeneity. *Cell*. 2019. **179**: 846–863.e824.

98 **Kumamoto, Y., Linehan, M., Weinstein, J. S., Laidlaw, B. J., Craft, J. E. and Iwasaki, A.**, CD301b$^+$ dermal dendritic cells drive T helper 2 cell-mediated immunity. 2013. **39**: 733–743.

99 **Becht, E., McInnes, L., Healy, J., Dutertre, C.-A., Kwok, I. W. H., Ng, L. G., Ginhoux, F. et al.**, Dimensionality reduction for visualizing single-cell data using UMAP. *Nat. Biotechnol.* 2019. **37**: 38–44.

100 **Lee, J., Boyce, S., Powers, J., Baer, C., Sassetti, C. M. and Behar, S. M.**, CD11cHi monocyte-derived macrophages are a major cellular compartment infected by Mycobacterium tuberculosis. *PLoS Pathog.* 2020. **16**: e1008621.

101 **Rauschmeier, R., Gustafsson, C., Reinhardt, A., N, A. G., Tortola, L., Cansever, D., Subramanian, S. et al.**, Bhlhe40 and Bhlhe41 transcription factors regulate alveolar macrophage self-renewal and identity. *EMBO J.* 2019. **38**: e101233.

102 **Auffray, C., Sieweke, M. H. and Geissmann, F.**, Blood monocytes: development, heterogeneity, and relationship with dendritic cells. *Annu. Rev. Immunol.* 2009. **27**: 669–692.

103 **Satpathy, A. T., KC, W., Albring, J. C., Edelson, B. T., Kretzer, N. M., Bhattacharya, D., Murphy, T. L. et al.**, Zbtb46 expression distinguishes classical dendritic cells and their committed progenitors from other immune lineages. *J. Exp. Med.* 2012. **209**: 1135–1152.

104 **Gao, Y., Nish, S. A., Jiang, R., Hou, L., Licona-Limón, P., Weinstein, J. S., Zhao, H. et al.**, Control of T helper 2 responses by transcription factor IRF4-dependent dendritic cells. 2013. **39**: 722–732.

105 **Ginhoux, F., Liu, K., Helft, J., Bogunovic, M., Greter, M., Hashimoto, D., Price, J. et al.**, The origin and development of nonlymphoid tissue CD103+ DCs. *J. Exp. Med.* 2009. **206**: 3115–3130.

106 **Fiedler, K. and Brunner, C.**, The role of transcription factors in the guidance of granulopoiesis. *Am. J. Blood Res.* 2012. **2**: 57–65.

107 **Steinman, R. M.**, Dendritic cells and the control of immunity: enhancing the efficiency of antigen presentation. *Mt. Sinai J. Med.* 2001. **68**: 160–166.

108 **Romani, N., Ratzinger, G., Pfaller, K., Salvenmoser, W., Stossel, H., Koch, F. and Stoitzner, P.**, Migration of dendritic cells into lymphatics-the Langerhans cell example: routes, regulation, and relevance. *Int. Rev. Cytol.* 2001. **207**: 237–270.

109 **Hovav, A. H.**, Mucosal and skin langerhans cells - nurture calls. *Trends Immunol.* 2018. **39**: 788–800.

110 **Capucha, T., Koren, N., Nassar, M., Heyman, O., Nir, T., Levy, M., Zilberman-Schapira, G. et al.**, Sequential BMP7/TGF-beta1 signaling and microbiota instruct mucosal Langerhans cell differentiation. *J. Exp. Med.* 2018. **215**: 481–500.

111 **Capucha, T., Mizraji, G., Segev, H., Blecher-Gonen, R., Winter, D., Khalaileh, A., Tabib, Y. et al.**, Distinct murine mucosal langerhans cell subsets develop from pre-dendritic cells and monocytes. *Immunity*. 2015. **43**: 369–381.

112 **Guilliams, M., Ginhoux, F., Jakubzick, C., Naik, S. H., Onai, N., Schraml, B. U., Segura, E. et al.**, Dendritic cells, monocytes and macrophages: a unified nomenclature based on ontogeny. *Nat. Rev. Immunol.* 2014. **14**: 571–578.

113 **Schraml, B. U., van, B. J., Zelenay, S., Whitney, P. G., Filby, A., Acton, S. E., Rogers, N. C. et al.**, Genetic tracing via DNGR-1 expression history defines dendritic cells as a hematopoietic lineage. *Cell*. 2013. **154**: 843–858.

114 **Salei, N., Rambichler, S., Salvermoser, J., Papaioannou, N. E., Schuchert, R., Pakalniškytė, D., Li, N. et al.**, The kidney contains ontogenetically distinct dendritic cell and macrophage subtypes throughout development that differ in their inflammatory properties. *J. Am. Soc. Nephrol.* 2020. **31**: 257–278.

115 **Summers, K. M., Bush, S. J. and Hume, D. A.**, Network analysis of transcriptomic diversity amongst resident tissue macrophages and dendritic cells in the mouse mononuclear phagocyte system. *Plos Biol.* 2020. **18**: e3000859.

116 **Lever, J. M., Yang, Z., Boddu, R., Adedoyin, O. O., Guo, L., Joseph, R., Traylor, A. M. et al.**, Parabiosis reveals leukocyte dynamics in the kidney. *Lab. Invest.* 2017. **98**: 391–402.

117 **Lever, J. M., Hull, T. D., Boddu, R., Pepin, M. E., Black, L. M., Adedoyin, O. O., Yang, Z. et al.**, Resident macrophages reprogram toward a developmental state after acute kidney injury. *JCI Insight*. 2019. **4**: 833.

118 **Gottschalk, C. and Kurts, C.**, The debate about dendritic cells and macrophages in the kidney. *Front. Immunol.* 2015. **6**: 435.

119 **Ide, S., Yahara, Y., Kobayashi, Y., Strausser, S. A., Ide, K., Watwe, A., Xu-Vanpala, S. et al.**, Yolk-sac-derived macrophages progressively expand in the mouse kidney with age. *eLife*. 2020. **9**: 929.

120 **Salei, N., Ji, X., Pakalniškytė, D., Kuentzel, V., Rambichler, S., Li, N., Moser, M. et al.**, Selective depletion of a CD64-expressing phagocyte subset mediates protection against toxic kidney injury and failure. *Proc. Natl. Acad. Sci. U.S.A.* 2021. 118. https://doi.org/10.1073/pnas.2022311118.

121 **Brähler, S., Zinselmeyer, B. H., Raju, S., Nitschke, M., Suleiman, H., Saunders, B. T., Johnson, M. W. et al.**, Opposing roles of dendritic cell subsets in experimental GN. *J. Am. Soc. Nephrol.* 2018. **29**: 138–154.

122 **Evers, B. D. G., Engel, D. R., Böhner, A. M. C., Tittel, A. P., Krause, T. A., Heuser, C., Garbi, N. et al.**, CD103+ kidney dendritic cells protect against crescentic GN by maintaining IL-10-producing regulatory T cells. *Journal of the American Society of Nephrology : JASN*. 2016. **27**: 3368–3382.

123 **Hitchcock, J. R., Hughes, K., Harris, O. B. and Watson, C. J.**, Dynamic architectural interplay between leucocytes and mammary epithelial cells. *FEBS J.* 2020. **287**(2): 250–266.

124 **Stewart, T. A., Hughes, K., Hume, D. A. and Davis, F. M.**, Developmental stage-specific distribution of macrophages in mouse mammary gland. *Front. Cell. Dev. Biol.* 2019. **7**: 250.

125 **Steinman, R. M.**, Decisions about dendritic cells: past, present, and future. *Annu. Rev. Immunol.* 2012. **30**: 1–22.

126 **Steinman, R. M. and Hemmi, H.**, Dendritic cells: translating innate to adaptive immunity. *Curr. Top. Microbiol. Immunol.* 2006. **311**: 17–58.

127 **Böttcher, J. P. and Reis e Sousa, C.**, The role of type 1 conventional dendritic cells in cancer immunity. *Trends Cancer*. 2018. **4**: 784–792.

128 **Guilliams, M., Henri, S., Tamoutounour, S., Ardouin, L., Schwartz-Cornil, I., Dalod, M. and Malissen, B.**, From skin dendritic cells to a simplified classification of human and mouse dendritic cell subsets. *Eur. J. Immunol.* 2010. **40**: 2089–2094.

129 **Durai, V. and Murphy, K. M.**, Functions of murine dendritic cells. *Immunity*. 2016. **45**: 719–736.

130 **Murphy, T. L., Grajales-Reyes, G. E., Wu, X., Tussiwand, R., Briseño, C. G., Iwata, A., Kretzer, N. M. et al.**, Transcriptional control of dendritic cell development. *Annu. Rev. Immunol.* 2016. **34**: 93–119.

131 **Bachem, A., Hartung, E., Güttler, S., Mora, A., Zhou, X., Hegemann, A., Plantinga, M. et al.**, Expression of XCR1 characterizes the Batf3-dependent lineage of dendritic cells capable of antigen cross-presentation. *Front. Immunol.* 2012. **3**: 214.

132 **Broz, M. L., Binnewies, M., Boldajipour, B., Nelson, A. E., Pollack, J. L., Erle, D. J., Barczak, A. et al.**, Dissecting the tumor myeloid compartment reveals rare activating antigen-presenting cells critical for T cell immunity. *Cancer Cell.* 2014. **26**: 638–652.

133 **Salmon, H., Idoyaga, J., Rahman, A., Leboeuf, M., Remark, R., Jordan, S., Casanova-Acebes, M. et al.**, Expansion and activation of CD103(+) dendritic cell progenitors at the tumor site enhances tumor responses to therapeutic PD-L1 and BRAF inhibition. *Immunity*. 2016. **44**: 924–938.

134 **Spranger, S., Dai, D., Horton, B. and Gajewski, T. F.**, Tumor-residing Batf3 dendritic cells are required for effector T cell trafficking and adoptive T cell therapy. *Cancer Cell.* 2017. **31**: 711–723.e714.

135 **Malissen, B., Tamoutounour, S. and Henri, S.**, The origins and functions of dendritic cells and macrophages in the skin. *Nat. Rev. Immunol.* 2014. **14**: 417–428.

136 **Wade, C. G., Rhyne, R. H., Jr., Woodruff, W. H., Bloch, D. P. and Bartholomew, J. C.**, Spectra of cells in flow cytometry using a vidicon detector. *J Histochem. Cytochem.* 1979. **27**: 1049–1052.

137 **Gauci, M. R., Vesey, G., Narai, J., Veal, D., Williams, K. L. and Piper, J. A.**, Observation of single-cell fluorescence spectra in laser flow cytometry. *Cytometry*. 1996. **25**: 388–393.

138 **Nolan, J. P. and Condello, D.**, Spectral flow cytometry. Curr Protoc Cytom 2013. Chapter 1: Unit1.27.

139 **Chen, D. S. and Mellman, I.**, Oncology meets immunology: the cancer-immunity cycle. *Immunity*. 2013. **39**: 1–10.

140 **Hornsteiner, F., Sykora, M. M., Tripp, C. H., Sopper, S. and Stoitzner, P.**, Mouse dendritic cells and other myeloid subtypes in healthy lymph nodes and skin: 26-Color flow cytometry panel for immune phenotyping. *Eur. J. Immunol.* 2022. https://doi.org/10.1002/eji.202250004

Abbreviations: **ANR**: Agence Nationale de la Recherche · **APC**: Antigen-Presenting Cells · **BALF**: Bronchoalveolar Lavage Fluid · **Col IV**: Collagenase IV · **cDC**: conventional DC · **DC**: Dendritic Cells · **DNAse I**: Deoxyribonuclease I · **DFG**: Deutsche Forschungsgemeinschaft · **DAPI**: Dissolve 4´,6-diamidino-2´-phenylindole dihydrochlorid · **DTT**: Ditihiothreitol · **DN cDC**: Double negative conventional DC · **DMEM**: Dulbecco's Modified Eagle Medium · **Eos**: Eosinophils · **EDTA**: Ethylenediaminetetraacetic acid · **FcγRs**: Fc gamma receptors · **FCS**: Fetal Bovine Serum · **FMO**: Fluorescence Minus One Control · **FZI**: Forschungszentrum Immuntherapie · **G418**: Geneticin 418 · **HBSS**: Hank's balanced salt solution · **IZKF**: Interdisziplinäres Zentrum für klinische Forschung · **IEL**: Intraepithelial Lymphocytes · **IMDM**: Iscove's Modified Dulbecco's Media · **LPC**: Lamina Propria Cells · **LC**: Langerhans Cells · **LT**: Lymphoid Tissue · **mPh**: Macrophages · **MG**: Mammary gland · **MLN**: Mesenteric Lymph Nodes · **moDC**: Monocyte derived DC · **NALT**: Nasal-Associated Lymphoid Tissue · **PBS**: Phosphate Buffered Saline · **pDC**: plasmacytoid DC · **Treg**: regulatory T cells · **RPMI**: Roswell Park Memorial Institute · **SI**: Small Intestine · **s.c.**: Subcutaneously · **TF**: Transcription Factors · **TAM**: Tumor-Associated Macrophages · **UMAP**: Uniform-Manifold Approximation and Projection

Full correspondence: Dr. Hans Christian Probst and Prof. Patrizia Stoitzner
e-mail: hcprobst@uni-mainz.de; patrizia.stoitzner@i-med.ac.at

Received: 17/1/2022
Revised: 24/8/2022
Accepted: 25/8/2022